National Library of Canada
Acquisitions and Bibliographic Services Branch
395 Wellington Street
Ottawa, Ontario
K1A 0N4

Bibliothèque nationale du Canada
Direction des acquisitions et des services bibliographiques
395, rue Wellington
Ottawa (Ontario)
K1A 0N4

Your file Votre référence

Our file Notre référence

NOTICE

The quality of this microform is heavily dependent upon the quality of the original thesis submitted for microfilming. Every effort has been made to ensure the highest quality of reproduction possible.

If pages are missing, contact the university which granted the degree.

Some pages may have indistinct print especially if the original pages were typed with a poor typewriter ribbon or if the university sent us an inferior photocopy.

AVIS

La qualité de cette microforme dépend grandement de la qualité de la thèse soumise au microfilmage. Nous avons tout fait pour assurer une qualité supérieure de reproduction.

S'il manque des pages, veuillez communiquer avec l'université qui a conféré le grade.

La qualité d'impression de certaines pages peut laisser à désirer, surtout si les pages originales ont été dactylographiées à l'aide d'un ruban usé ou si l'université nous a fait parvenir une photocopie de qualité inférieure.

Canada

Structural Analysis of Rectangular Bolted Flanged Connections for Pressure Vessels

Lihua Xue

A Thesis

in

The Department

of

Mechanical Engineering

Presented in Partial Fulfillment of the Requirements
for the Degree of Master of Science at
Concordia University
Montreal, Quebec, Canada

September 1992

ISBN 0-315-97643-8

Canada

ABSTRACT

Structural Analysis of Rectangular Bolted
Flanged Connections for Pressure Vessels

Lihua Xue

The ASME Boiler and Pressure Vessel Code contains rules for non-circular pressure vessels of unreinforced and reinforced construction. These rules cover the sides, reinforcing ribs, and end plates of such vessels. For bolted flanged connections of such non-circular pressure vessels, which are employed extensively in industry, however, no design rules are presently included in the Code.

In this dissertation, the modeling and analysis of rectangular bolted flanged connections employed in pressure vessels by using the finite element method are presented. The results are compared with experimental values from strain gauge measurements on test pressure vessels and with analysis data derived by two approximate methods presently used by pressure vessel designers. The relative advantages and limitations of each method are discussed in terms of results obtained.

Two types of rectangular bolted flanged connections are analysed, one on a thick walled unreinforced pressure vessel, the other on a rib-reinforced thin walled pressure vessel. Three types of gaskets are considered for each of the flanged connections; O-gasket, strip gasket

and full face gasket.

A modified structural model meshing scheme is proposed to fully make use of the limited space of the pre-wave front matrix used in the frontal method of the ANSYS program. The best possible numerical results that can be offered by the program employed are then obtained.

The parameter analysis of the rectangular bolted flanged connections is also carried out via the convenient finite element method. The influence of design parameters of the bolted flanged connections on their stiffness and strength characteristics and the design guidelines are thus established. The analysis results show that the rectangular flanged structure with strip gasket is very sensitive to the bolt preload value.

Based upon comparison of the results by using the approximate methods, the experimental work, and the finite element analysis, it is concluded that a good correlation between the results from the three different approaches has been observed. The analytic approximate methods yield results on the conservative side. The finite element analysis gives a complete picture of mechanical behavior of the flange structures, and design guide lines without costly experiments.

ACKNOWLEDGEMENTS

The author wishes to express her sincere appreciation to her thesis supervisor, Dr. A. E Blach, for initiating the study topic, providing continued support and guidance throughout the course of this research.

Thanks are due to the colleagues, faculty and staff at the Mechanical Engineering Department, Computer Centre, and Composite Material Research Centre of the Concordia University, for their assistance and time.

The financial support provided by the assistantships and fellowships funded by the NSERC grants and the Department of Mechanical Engineering is gratefully acknowledged.

Finally, the author wishes to thank her family members for their encouragement and understanding, specially her husband, Hong Su, for his help and valuable discussions concerning the thesis work.

TABLE OF CONTENTS

TABLE OF CONTENTS (Continued) Page

TABLE OF CONTENTS (Continued) Page

LIST OF FIGURES

LIST OF FIGURES (Continued)

LIST OF FIGURES (Continued)

LIST OF TABLES

NOMENCLATURE

a	length of rectangular shape (m)
A	outside diameter (m)
b	width of rectangular shape (m) width of gasket (m)
b_r	space between reinforcing ribs (m)
b_x	space between bolts in x direction (m)
b_y	space between bolts in y direction (m)
B	equivalent inside diameter (m)
[B]	strain matrix
c	Code constant circle diameter bolt (m)
d	bolt hole diameter (m)
[D]	element elasticity matrix
E	Young's modulus of elasticity (Pa)
E_G	modulus of elasticity of gasket (Pa)
g	hub thickness (m)
h_D	moment arm for hydrostatic end force (m)
h_G	moment arm for gasket force (m)
h_T	moment arm for hydrostatic force under gasket (m)
H_D	hydrostatic end force (N)
H_G	gasket compression force (N)
H_T	hydrostatic force under gasket (N)
[J]	Jacobian matrix
K	ratio of the outside to inside diameter
[k]	element stiffness matrix

NOMENCLATURE (Continued)

ℓ	dimension length (m)
ℓ_1, ℓ_2	dimension length (m)
l_{fx}	length of flange in x direction (m)
l_{fy}	width of flange in y direction (m)
l_{fr}	distance between flange and rib (m)
l_r	width of reinforcing rib (m)
l_{vx}	length of vessel in x direction (m)
l_{vy}	width of vessel in y direction (m)
l_{vz}	height of vessel in z direction (m)
m	gasket constant
M_A	corner moment (N·m)
M_B	bending moment (N·m)
M_o	external flange moment (N·m)
M_o	external flange bending moment (N·m)
n	wave front size
N	shape function of the element
P	internal pressure (Pa)
{q}	element displacement vector
S	elastic section modulus (m^3)
S_u	section modulus of a rectangular section (m^3)
t	thickness (m)
t_b	thickness of bottom plate (m)
t_f	thickness of flange (m)
t_G	gasket thickness (m)

NOMENCLATURE (Continued)

t_r	thickness of reinforcing rib (m)
t_v	thickness of vessel (m)
u	displacement function of element (m) coordinate displacement (m)
u_i	displacement of the ith node (m)
v	coordinate displacement (m)
w	coordinate displacement (m)
W	bolt load on flange (N)
x	global coordinate (m)
x_i	global coordinate value of node i (m)
y	global coordinate (m) gasket constant
y_i	global coordinate value of node i (m)
Y	flange parameter of the ASME Code
z	global coordinate (m)
z_i	global coordinate value of node i (m)
Z	Code design factor for rectangular flange
α	gasket compression coefficient
β	stress factor
ε	strain
$\{\varepsilon\}$	strain vector
ζ_i	local coordinate value of node i
η_i	local coordinate value of node i
ν	Poison ratio of flange material
ν_G	Poison ratio of gasket material

NOMENCLATURE (Continued)

ξ_i	local coordinate value of node i
σ	stress (Pa)
σ_b	bending stress (Pa)
σ_f	frame bending stress (Pa)
σ_T	flange stress (Pa)
$\{\sigma\}$	stress vector
ω	uniformly distributed loading (Pa)
$[\cdot]^{-1}$	inverse matrix of $[\cdot]$
$[\cdot]^T$	transposed matrix of $[\cdot]$

CHAPTER 1

INTRODUCTION AND LITERATURE SURVEY

1.1 General

Bolted flanged connections are widely employed in pressure containing apparatus, such as pressure vessels and piping. The availability of bolted flanged connections provides a convenient means of joining together the various pieces of equipment which make up plants in our modern chemical and process industries. Bolted flanges, therefore, constitute a very important part of all pressure containing apparatus.

Most of the flanges used are of circular shape, such as used in pressure vessels and piping systems, due to their favorable geometrical configuration to retain pressure. They are available in a variety of pressure classes and facing types. There are, however, many applications in which circular pressure containers or conduits cannot be used for various reasons and non-circular pressure containers or conduits are applied. The inlet nozzles on cyclones, for example, are usually of rectangular shape as are the wood chip chutes on pulp digesters; the headers on steam boilers are normally square; and the inlet and outlet headers of air cooled heat exchangers are rectangular. For such non-circular cross-sections, flanges are often required, be it for access or for connection to other equipment.

The bolted flanged connections are part of pressure containing

systems. The analysis and design of bolted flanged connections are governed by various pressure vessel codes and standards established in the industrialized countries over the world. In north America, for example, the ASME Boiler and Pressure Vessel Code [1] is used. The ASME code contains extensive rules for the design of pressure vessels and pressure vessel components, including rules for non-circular pressure vessels, However, there are, no rules at present for analysis and design of non-circular bolted flanged connections.

To investigate the best design for these non-circular bolted flanged connections, a large number of parametric variation and analyses have to be carried out. This work normally involves evaluation of the mechanical behavior of non-circular flanges, such as the deflection and stress distribution, under bolt-up and pressurized working conditions. The evaluation of the bolted flanged connection structures can, in general, be realized by employing approaches based on either existing codes and standards, modified analytical approximation methods, numerical computation methods such as finite element technique, or experiment validations.

This dissertation presents the analysis of rectangular bolted flanged connections used in pressure vessels by using the finite element method. Several structural models with various boundary conditions, with or without reinforcement, are established. Bolted flanged connections with full and strip gaskets, as well as without gaskets are considered in the modeling and analysis. Deformation and stress profiles of rectangular flange connection structures are

computed using the finite element method. The numerical results are compared with data from strain gauge measurements on rectangular pressure vessels to show consistence and validity of the analysis results. The relative advantages and limitations of the finite element numerical method, the two design methods presented in chapter 4,are discussed and compared with the results of experimental work.

The parameter analysis of the rectangular bolted flanged connections, in terms of deflection and stress distribution of the structure, is also carried out via the convenient finite element method. The influence of design parameters of the bolted flanges on their strength and stiffness characteristics and design guidelines are established. A modified structure meshing scheme is proposed in the finite element modeling to fully make use of the limited space of the pre-wave front matrix, used in the frontal method of the ANSYS program [2], in order to obtain the best numerical results that can be offered within the limitations of the program used.

1.2 Literature Review

Technical publications contain a large number of bolted flanged connection design papers, covering a wide variety of investigations concerning the analysis of such connections, using different approaches. There are also several extensive literature reviews on non-circular bolted flanged connections available. A brief description of the relevant literature is presented here.

As early as 1890's there were some pioneer literature publications on flange design by Bach [3] and Westphal [4]. Bach's work [3] discussed deflections and stresses of plates of various shapes; this formed the basis for the 'Bach-Method' in flange design which was used for many years. Westphal [4] first analyzed stresses in loose flanges and in straight hub flanges, based on the theory of elasticity. The analysis showed that the flange thickness can be reduced, if the influence of a hub is included in the strength calculations.

The theory of elasticity has been extensively employed in analysis and design of bolted flanged connections. Waters and Taylor [5] developed an analytical method, based on the theory of elasticity, for ring and hub flanges with straight hubs. The deflection results calculated were compared with test results to demonstrate good agreement.

Based on the theory of beam on elastic foundation, Timoshenko [6] proposed a simplified method for the analysis of bending of circular rings. The maximum circumferential stresses for ring flanges and longitudinal stresses for hub flanges can be calculated by using this method.

Holmberg and Axelson [7] presented an analysis of stresses in circular plates and rings, with applications to rigidly attached flat plates and flanges, considering the loading at bolt force points as well as gasket compression.

The original method of Waters [5], however, could not be used to solve the problem of tapered hub welding neck flanges which became popular and are now employed in pressure vessels and piping systems for higher pressures and temperatures. To overcome the limitations, an elastic analysis by Waters et al. [8] [9], based on the theory of a beam on an elastic foundation and the deflection of flat circular plates was proposed in 1937. This elastic analysis forms the basis of most of the flange design methods used in industrial countries, such as the flange design rules of the ASME Boiler and Pressure Vessel Code [1].

The experimental determination of stresses is a very reliable method for the verification of the results of structural analysis of elements of pressure contain apparatus [10]. Experimental date provide a base for many important empiric formulas employed in engineering practice. Experimental techniques also provides engineers with a unique means in development and validation of various theoretical, analytical and numerical methods. The major limitations of experimental stress anaysis lie in relatively high costs, time consuming work, and sometimes limited accuracy, depending on test method and equipment employed.

Thum [11] was the first to employ strain gage measurement to obtain stress distributions in hub flanges. He compared the measured results to those calculated based on the theoretical and analytical methods proposed by Timoshenko,[5] Waters,[8] [9] and others. Based

on the comparison of experimental data with analytical values, Thum proposed an improved design method for flange design.

Andreosso and Flesch [12] employed photoelastic methods as well as strain gauge measurements to verify a simplified method in bolted flange design. Stresses were measured at elevated tempretures and compared with those of the simplified method and with the finite element method. It has been shown that all the results obtained agree very well and the simplified method can also be used to calculate the variation in loads over a period of time, depending on thermal and pressure loadings. Mckenzie et al [13] also used a two-dimensional photoelastic test method to measure and analyse the stress and strain distribution in steam turbine flanges. The photoelastic test method proved to be very useful in the design of flanges.

The paper by Spaas and Latzko [14] presented both experimental and theoretical investigations aimed at quantifying the thermal transient effects for light-water nuclear pressure vessel flanges. The experiments were performed on the 1:4 scale model of the reactor pressure vessel for the Dodewaadrd I unit (a 50 MWa BWR). Four studs were equipped with 4 strain gauges each attached in the longitudinal direction. The cross sections of the vessel and head flanges were equipped with a total of 74 strain gauges and 70 Chromel-Alumel thermocouples.

Boissent and Lachat [15] also used strain gauge measurements in flange design and analysis. The flange was forged in a single piece. It consisted of a cylinder, a cone of linearly varying thickness (taper hub) and a flange plate with twelve bolt holes. The cylinder was welded on to a sphere. The strain gauges were located inside and on the outside surface of the flange. The authors calculated the stress and deflection by the finite element method, on one hand assuming the geometry and loading to be axisymmetric, and on the other hand treating the flange as a three dimensional problem. The theoretical results were confirmed by experiment results. The relative difference in the strain results on the two meridians between the two methods was found to be about 20 percent.

The development of computers with high speed and large storage space, and the advancement of efficient numerical technique have introduced new tools in engineering design and analysis. The finite element method as a powerful computational numeric technique [16] provides a very useful means in structural and continuum mechanics, as well as in design of pressure containing apparatus.

Mckenzie et al [13] employed a finite element plane stress program, which was developed by the English Electric Whetstone Company, to analyse flange structures. The program uses triangular elements and can solve a plane-stress problem. The flanges are rectangular with metal-to-metal contact over the full flange faces. The structure consists of a split cylinders, i.e., two semi-circular halves bolted together along longitudinal (axial) flanges. Flanges

with different parameters, such as flange depth, flange width, bolt location, and so on, were analysed. The calculated stress distributions made by the finite element program were compared with the experimentally (photoelastically) determined distributions. It was shown that there is good agreement between experiment and calculation when the depth of the flange exceeds the width, and the bolt load acts within the inner half of the flange face.

Irons [17] developed a frontal solution program that assembles and solves symmetric positive definite equations using only limited computer working space, which is very much desirable in finite element applications. The technique is more involved than the standard band matrix algorithms, but it is more efficient in the important case when two or three dimensional elements employed have other than corner nodes. The frontal solution technique is now widely used in many finite element programs.

Gould and Mikic [18] employed the finite element method to investigate the contact areas in bolted joints, and compared the calculated data with that of experiment results. It was found that the contact areas are smaller that suggested by previous publications.

Nerli and Bertoni [19] used the finite element method to calculate the deformation of flange rings due to the influence of bolt loadings and compared the computed results with that of experiment. Their experimental apparatus provided for four (4) types of tests, including the simulation of the real conditions of operation in the

presence of internal pressure, and of use with only tightening of the bolts, as well as application of the load on the bolts with the model constrained at the level of the stiffened tank. It was found that the results derived from the finite element method are very close to the experimental values.

The standard flange design method used in the ASME Boiler and Pressure Vessel Code [1] was established principally based on work by Waters et al [8] [9], aided by a large number of contributions from engineers and scientists over several decades. This standard code method has served as a valuable design procedure and has been adopted by many boiler and pressure vessel codes all over the world.

The ASME Code contains extensive rules for the design of pressure vessels and pressure vessel components, including rules for non-circular pressure vessels of unreinforced and reinforced construction. These rules are given in Section VIII, Division 1, Appendix 13, which covers the sides, reinforcing ribs, and end plates of such vessels. There are, however, no design rules for non-circular bolted flanged connections presently included in the ASME Code.

Two extensive literature searches of bolted flanged connection publications were conducted by Cassidy and Kim [20], and Blach and Bazergui [21], respectively. The literature searches indicate that very little has been published on the subject of the non-circular bolted flanged connections. The only type of non-circular bolted flanged connection which has received some attention seems to be the

flanged joint in split steam turbine housings. This type of bolted flanged connection, important for steam turbine housings is, however, not representative of the majority of non-circular flanges used.

Blach [22] recently presented a paper on non-circular bolted flanged connections, in which two approximation design methods were discussed. One of the approximation methods is based on an equivalent circular flange and then uses all code formulas for the circular flanges. The other method is called the frame bending flange design method. The equivalent circular flange method has a limitation of length-to-width ratio of 1.5, and is applicable only for unreinforced non-circular pressure vessels where the frame bending stresses are fully absorbed by the pressure vessel side plates. The second method employs a combination of frame analysis for the ability of the flange to retain its rectangular shape, and of bending of a long rectangular flange section in a plane perpendicular to the frame. This method can be used for large length to width ratio, and also for reinforced pressure vessel. The frame bending stresses can be found from structural analysis.

1.3 Scope of The Thesis

The objective of this thesis is to model and analyse rectangular bolted flanged connections used in pressure vessels, using the finite

element method with three dimensional elements, and to compare the computed results with those obtained by experiments and with calculated values using the approximate design methods.

Chapter 2 deals with the finite element modeling of the rectangular bolted flanged connections under investigation. Models for three contact cases of the flanges are developed. and an improved meshing scheme is proposed in the modeling. Due to symmetry only one quarter of the vessels needs to be modeled, boundary and bolt preloading conditions are selected accordingly.

In Chapter 3, the results of the finite element analysis of the models are presented in terms of deflection and stress profiles. The results of different cases are compared with each other and discussed with respect to the strength and stiffness characteristics of the flanges. A parameter study was also conducted for the unreinforced and reinforced pressure vessels.

Chapter 4 presents a comparison of the results using the finite element method with experimental results and the result of calculations using the approximate methods. The relative merits and limitations of the different methods are discussed.

Finally, conclusion and highlights of the investigation, and recommendations for the future work are presented in Chapter 5.

CHAPTER 2

DEVELOPMENT OF RECTANGULAR FLANGED STRUCTURAL MODELS FOR FINITE ELEMENT ANALYSIS

2.1 General

In order to design a noncircular bolted flange optimally in terms of structural strength and material saving, stress distribution and deflection profiles of the flanged structure are the most important information needed. It is often impossible to do a complete stress analysis of the noncircular flange only by using classical analytical methods. An experimental determination of stresses, though costly and time consuming, can only get surface stresses (through measuring surface strains) at several limited points on a flange. The amplitude and location of the critical stresses can only be estimated. The finite element analysis, on the other hand, provides a powerful means in the evaluation of complicated bolted flanges by deriving complete information of stresses as well as a deflection distribution within the whole structure. The first step in the finite element analysis is to generate a model in terms of nodes and elements of the structure.

In this chapter, two types of rectangular bolted flanges are modeled for the finite element analysis. One is welded to a thick wall pressure vessel the other to a rib-reinforced thin wall pressure vessel. Three types of flange gaskets are considered; O-ring gasket, strip-gasket and full face gasket. The procedure used to generate a finite element model of the flange structure is presented.

A quadrant of the bolted flanged structural model is developed by taking advantage of the symmetry of the rectangular structure. The finite element program ANSYS is employed as the tool for the flanged structural analysis. The metallic vessel-flange structure and nonmetallic gaskets are all modeled by using three dimensional isoparametric elements with different material properties. In order to use the limited size of wave front matrix and save CPU time, an improved model meshing scheme is utilized to reorder the sequence of model elements based on the properties of the wave front method. The loading conditions due to preloading of bolts and pressurization of on the vessel, the proper boundary conditions, and the material properties of flanges and gaskets are also discussed in this chapter.

2.2 Description of the Rectangular Flanged Structures

Flanges constitute a very important part of all pressure containing apparatus. While most flanges are circular rectangular flanges are often required in industrial equipment and on apparatus having non-circular cross section.

A representative rectangular flanged connection structure, bolted together with different types of gaskets, is illustrated in Figure 2.1. The bolted flange structure was designed and constructed for the purpose of structural evaluation by using experimental techniques, to be verified by approximate analytical methods and finite element analysis. Three kinds of flange gaskets are considered in the finite element modeling and analysis, that is O-ring gasket, strip-gasket and full face gasket.

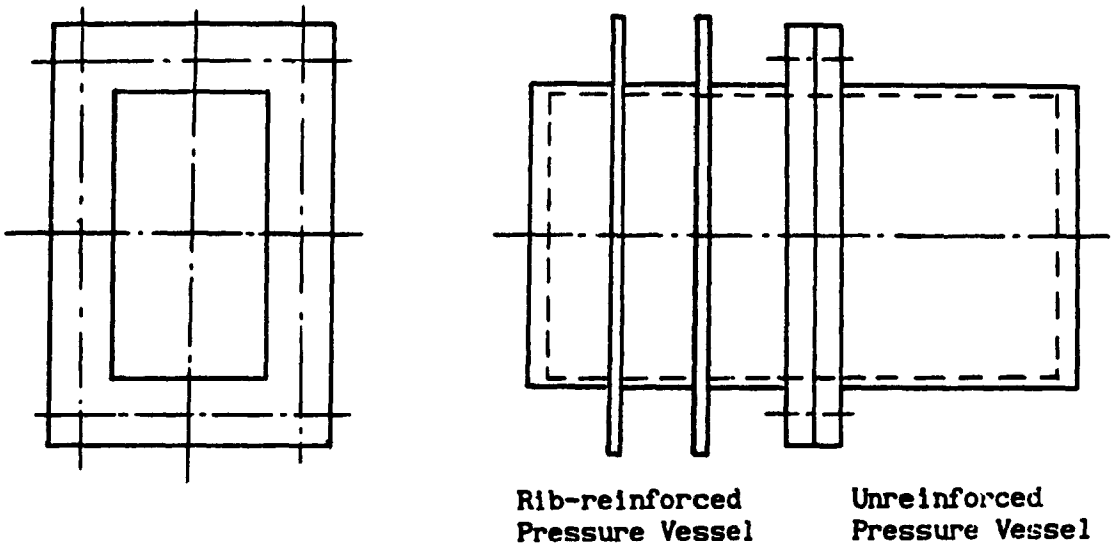

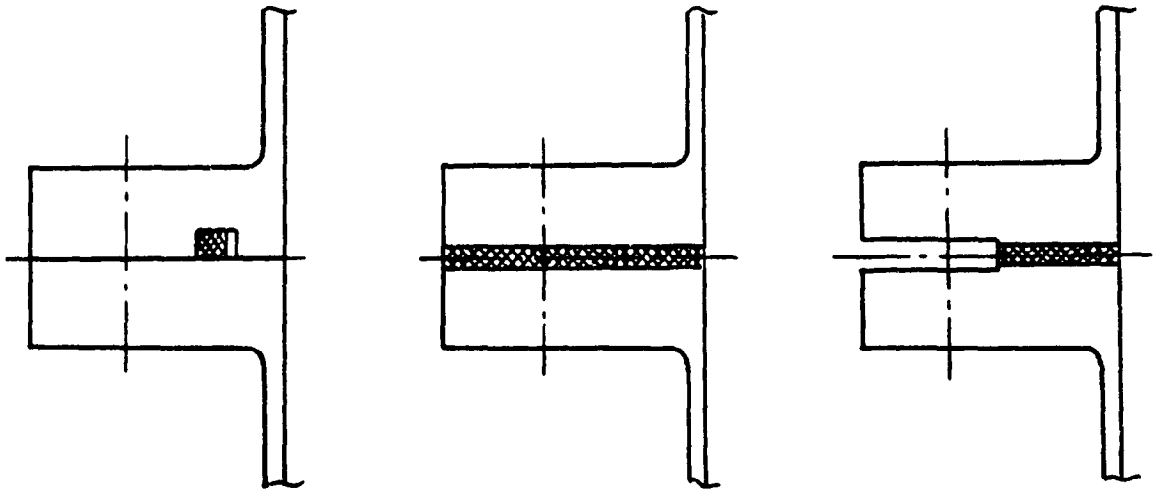

Figure 2.1 A Rectangular Bolted Flanged Connection

The representative structural set-up consists of two types of pressure vessels, bolted together. One part is a thick walled section, the other is rib-reinforced, as presented in Figures 2.2 and 2.3, respectively. The opposite ends of the flanges are rectangular flat plates. The longitudinal dimensions of the two pressure vessel sections are chosen based on elastic theory so that flange deflection and stresses are not influenced by the deflection of the flat ends.

The basic data and dimensions of the two bolted flanged pressure vessels, which are used for testing, modeling and analysis, are summarized in Tables 2.1 and 2.2, respectively.

A parameter variations in the bolted flange structure is also carried out to determine the sensitivity of mechanical characteristics of the flange to design parameters, by taking advantage of flexibility of the computer numerical technique. The parameter variations in the finite element model include the thickness of flanges, the thickness of vessel shells, and the size and spacing of reinforcing ribs.

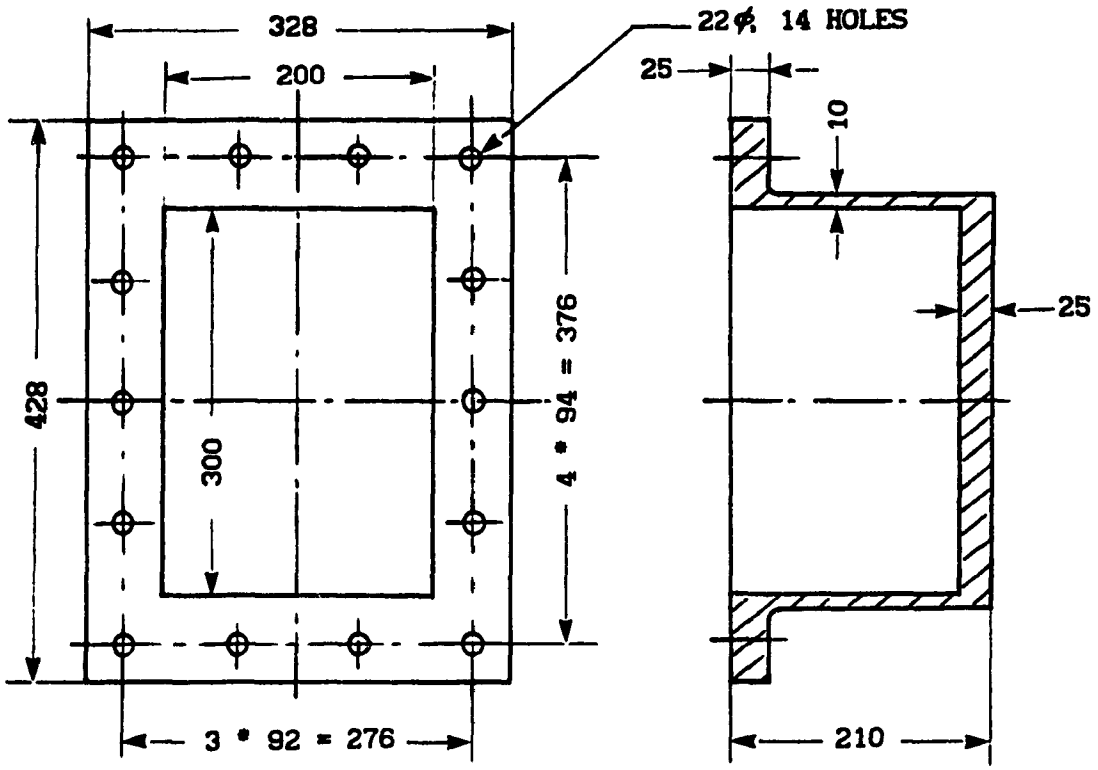

Figure 2.2 Thick Wall Pressure Vessel

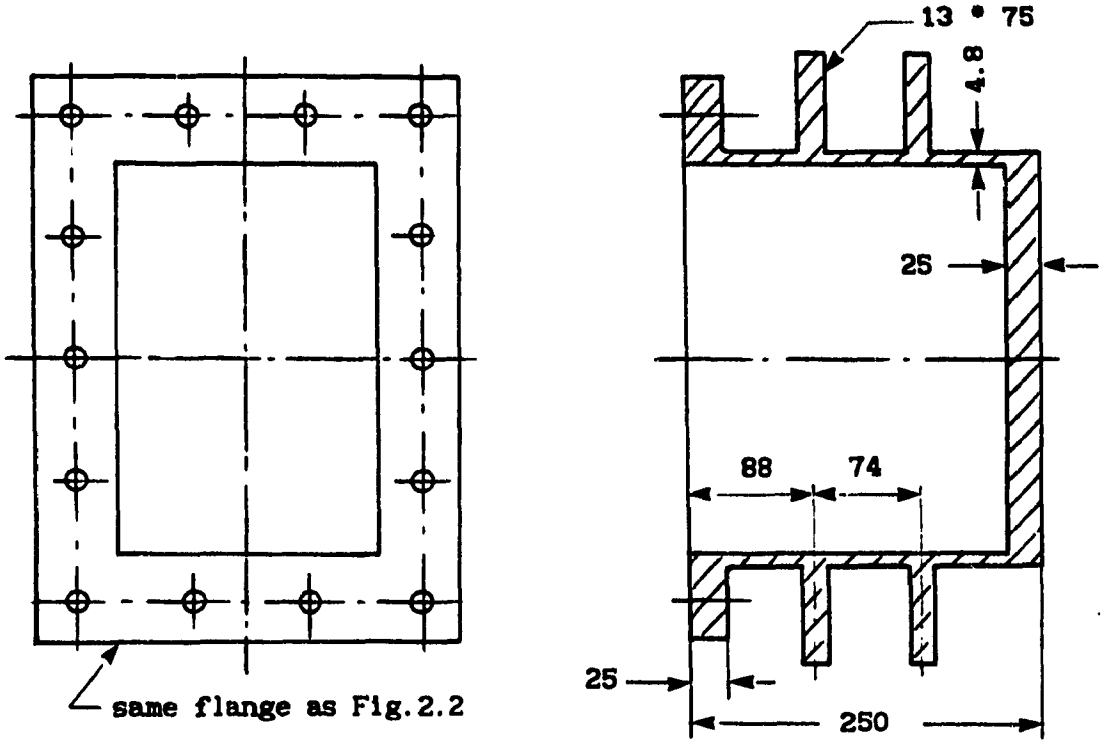

Figure 2.3 Reinforced Pressure Vessel

TABLE 2.1

Dimensional Parameters of
Flange Structure on thick Walled Vessel

SYMBOL	DESCRIPTION	VALUE
l_{fx}	Length of flange in x direction	428 mm (16.85 in)
l_{fy}	Width of flange in y direction	328 mm (12.9 in)
l_{vx}	Length of vessel in x direction	300 mm (11.8 in)
l_{vy}	Width of vessel in y direction	200 mm (7.87 in)
l_{vz}	Height of vessel in z direction	200 mm (7.87 in)
t_f	Thickness of rectangular flange	25 mm (.984 in)
t_v	Thickness of rectangular vessel	10 mm (.394 in)
t_b	Thickness of bottom plate	25 mm (.984 in)
b_x	Space between bolts in x direction	94 mm (3.7 in)
b_y	Space between bolts in y direction	92 mm (3.62 in)

TABLE 2.2

Dimensional Parameters of Flanged Structure on Rib-Reinforced Vessel

SYMBOL	DESCRIPTION	VALUE
l_{fx}	Length of flange in x direction	428 mm (16.85 in)
l_{fy}	Width of flange in y direction	328 mm (12.9 in)
l_{vx}	Length of vessel in x direction	300 mm (11.8 in)
l_{vy}	Width of vessel in y direction	200 mm (7.87 in)
l_{vz}	Height of vessel in z direction	250 mm (9.84 in)
t_f	Thickness of rectangular flange	25 mm (.984 in)
t_v	Thickness of rectangular vessel	4.8 mm (.189 in)
t_b	Thickness of bottom plate	25 mm (.984 in)
b_x	Space between bolts in x direction	94 mm (3.7 in)
b_y	Space between bolts in y direction	92 mm (3.62 in)
l_r	Width of reinforcing rib	75 mm (7.87 in)
t_r	Thickness of reinforcing rib	13 mm (.512 in)
b_r	Space between reinforcing ribs	74 mm (2.913 in)
l_{fr}	Distance between flange and rib	88 mm (3.465 in)

2.3 The ANSYS Finite Element Program

The ANSYS software is a large scale general purpose finite element program which has capabilities for linear and non-linear static and dynamic analysis. It can handle small and large displacements, as well as solve problems involving elastic, plastic creep, and swelling effects. It utilizes the matrix displacement method for the analysis and the wave front method for matrix reduction and solution. Over a hundred linear and non-linear elements are available in its library for modeling purposes.

There are basically three phases involved in the finite element solution. Figure 2.4 shows a flow chart of the analysis methodology for any type of problem. The pre-processing is generally carried out using the Prep7 module either interactively or by inputting the model data from CAD finite element modeling pre-processor. User interaction in this module is done by using a command language specific to this module. Any one of the different analysis options can be specified in this module before the model is sent for analysis. After the analysis stage, there are a number of post-processors available within ANSYS for the plotting and sorting of the data. Post1 is the post-processor in which results are normally transformed into various coordinate systems. Stress contour plots as well as displaced shape plots can be generated within this post-processor.

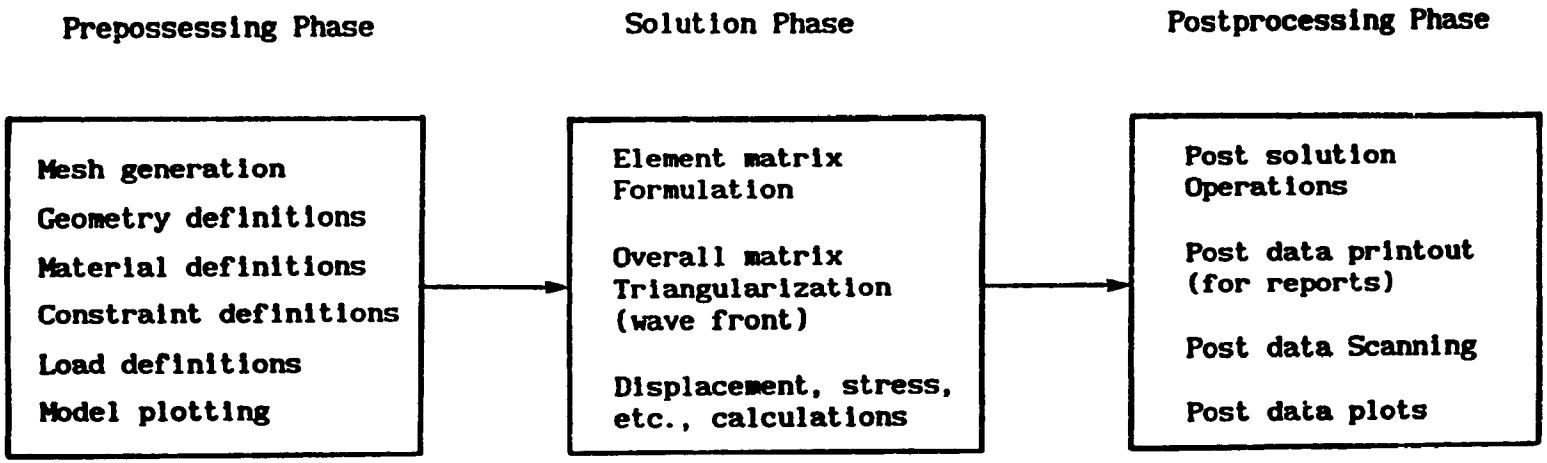

Figure 2.4 Typical Phases of an ANSYS Analysis

2.3.1 3-D Isoparametric Elements

In the analysis of complicated structures, isoparametric elements are widely and successfully employed. For an isoparametric element, the displacement function and the coordinate expression have not only the same shape function, but also the same interpolation formula. The advantages of using isoparametric elements, as compared with ordinary elements such as the Lagrange element [28], can be summarized as follows:

1. The use of isoparametric elements can guarantee the compatibility of displacements between adjacent elements, in both local and global coordinate systems, since the geometry of the edges of an element will vary in the same way as the displacement function;
2. The use of isoparametric elements allows any arbitrary geometry to be closely approximated, thereby minimizing any error associated with modeling of the geometry and without resorting to the use of a fine mesh along the boundaries;
3. The commonly used isoparametric elements, up to the cubic element, have no internal nodes and are therefore more efficient from the computational point of view.

The accuracy of the element stiffness matrix and the computation analysis of complicated structures can thus be improved by employing isoparametric elements. In this work, a three dimensional isoparametric solid element is used in the modeling and analysis of mechanical behaviors of the rectangular flange under bolt-preload and pressure conditions.

For a 3-D isoparametric element of a hexahedron with eight node, as shown in Figure 2.5, the stiffness matrix of the element can be derived through either a total potential energy or a virtual work approach [16]. The general form of the element stiffness matrix can be expressed as:

$$[\ k\ ] = \int_V [\ B_i\ ]^T [\ D\ ] [\ B_i\ ]\ dV \qquad (2.1)$$

where $[\ B_i\ ]$ is the strain matrix and $[\ D\ ]$ is the elasticity matrix. The stiffness matrix of the hexahedron isoparametric element is presented in Appendix A.

2.3.2 Wave Front Procedure

The ANSYS program employs an in-core wave front procedure for the finite element assembly and solution of the simultaneous linear equations. The number of equations which are active after any element has been processed during the solution procedure is called the wave front at that node point [17]. For most structure analysis problems the stiffness matrices are very sparse. The wave front procedure, therefore, takes advantage of this property in reducing the requirement on computer working space and CPU time.

Compared with bandwidth solution procedure, it has been shown [28] that the wave front method is never less efficient. For the majority of cases the wave front procedure is often much more efficient, especially for problems in which elements with midside nodes are used. The operations of a wave front solver can be split up

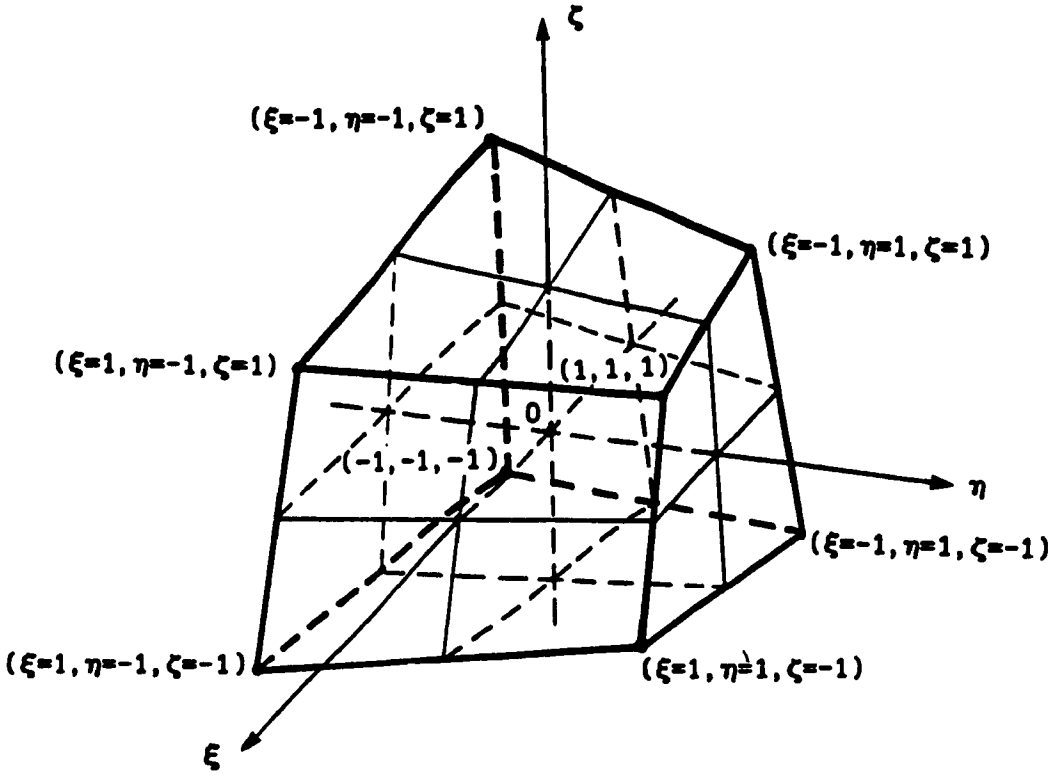

Figure 2.5 3-D Isoparametric Element of a Hexahedron with Eight Nodes

into the following three logical parts:

1) prefront;

2) reduction and pre-constraints;

3) back substitution and post-constraints.

A brief flow diagram of the wave front procedure is illustrated in Figure 2.6. In a wave front method nodes of all elements are scanned to determine which element is the last to use each node. When the total system of equations is assembled from the element matrices, the equations corresponding to a node which occurs for the last time are algebraically solved in terms of the remaining unknowns and eliminated from the assembled matrix in memory. The maximum number of equations of the working matrix is the size of maximum wave front width required.

The wave front method places a restriction on the problem definition that the allowable size of the wave front depends upon the amount of core storage available for a given problem. Moreover, the computer time required for the solution procedure is proportional to the square of the mean wave front size. Therefore, it is advantageous to be able to minimize the wave front size for a given problem.

It can be shown from Figure 2.6 that the maximum wave front size required is determined by the sequence in which the elements are arranged for a specific problem. In other word, the ordering of the elements is crucial to minimize the size of the wave front.

To reduce the maximum wave front size, the elements must be

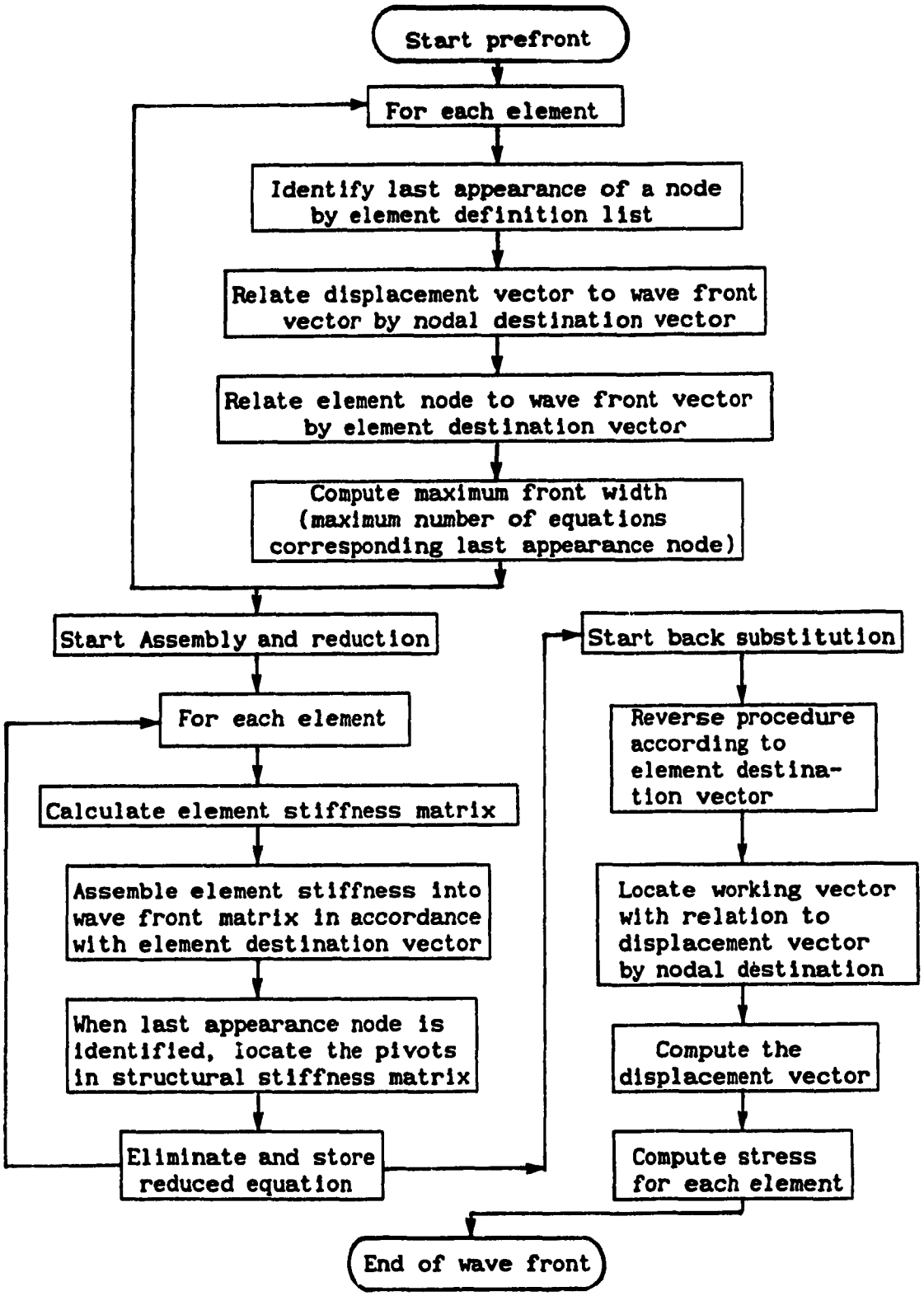

Figure 2.6 Flow Diagram of Wave Front Procedure

ordered for the assembly and solution so that the element for which each node is mentioned first is as close in sequence to the element for which it is mentioned last. In geometric terms, the elements should be ordered so that the wave front sweeps through the model continuously from one end to the other in the direction which has the largest number of nodes. In this way, equations will be processed and then deleted from the structural matrix as soon as possible after they are assembled.

2.4 Development of Analytical Models

Two basic types of rectangular bolted flange connections for pressure vessels are modeled for finite element analysis. One is an unreinforced pressure vessels with heavy side wall which can resist internal pressure without excessive deformations. The other is a rib-reinforced vessels in which relatively thin rectangular panels are reinforced with frames or ribs to carry the force due to internal pressure. Both vessel are bolted together as shown in Figure 2.1. The finite element models are developed using the same concept, one thick walled unreinforced vessel bolted to a thin wall rib-reinforced vessel.

Properties of the structure and the finite element program are employed to develop a proper analysis model in terms of working space and CPU time. The structural symmetry of the rectangular flanges is used in finite element modeling. The generation of nodes and elements is established by utilizing the properties of the wave front method.

2.4.1 Structural Symmetry and Analytical Model

It is easy to see that the rectangular bolted flanged structure is symmetric about its center, as shown in Figures 2.2 and 2.3. For a symmetric loading condition, such as bolt preloading on the flanges and internal pressure loading on the wall, the deflection and stress of the linear system will be also symmetric about the same center. In order to save computer working space and time, only one quarter of the bolted flanged vessel structure, therefore, need to be considered in the modeling.

A three dimensional thick shell structure as one quarter of the bolted flange-shell region, as well as the coordinate system, is shown in Figure 2.7.

2.4.2 Nodes and Elements Generation

The initial work with a coarse mesh model of 35 elements is shown in Figure 2.8. The purpose to use the simple model is two fold: one is to check ANSYS software package to see if it yields reasonably accurate results; the other is to establish a baseline of results for further comparison with other schemes and methods corresponding to the same rectangular structure under the same bolt-up and pressure loading conditions.

It has been found that the model of 35 elements is too coarse to yield a smooth result profile and can not simulate gaskets between the flanges either. A model of 157 elements with an extra layer of elements representing the gasket is then generated as shown in Figure

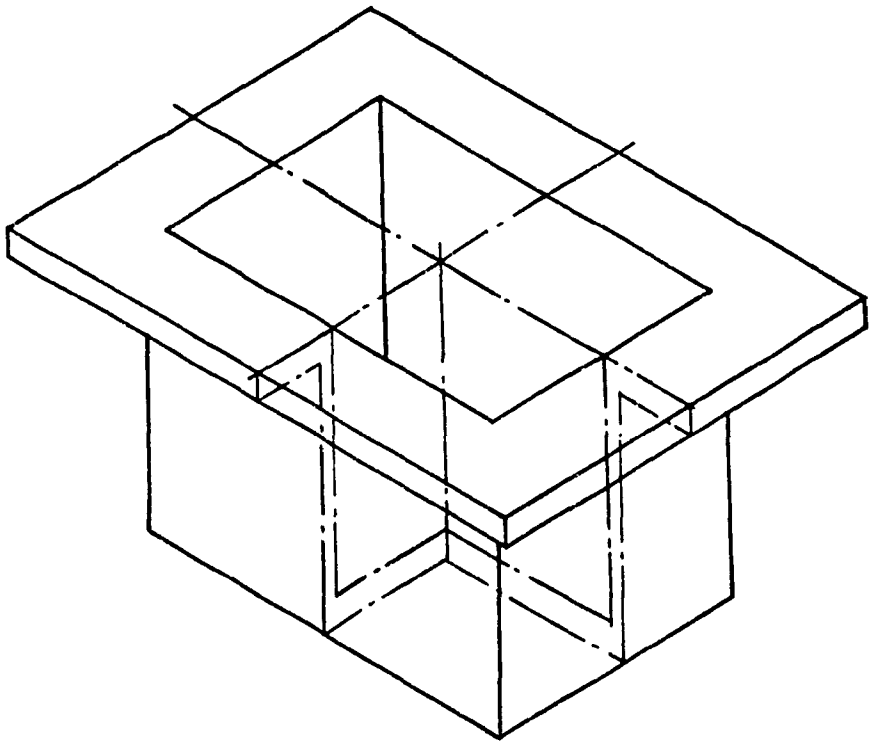

Figure 2.7 One Quarter of Rectangular Flange

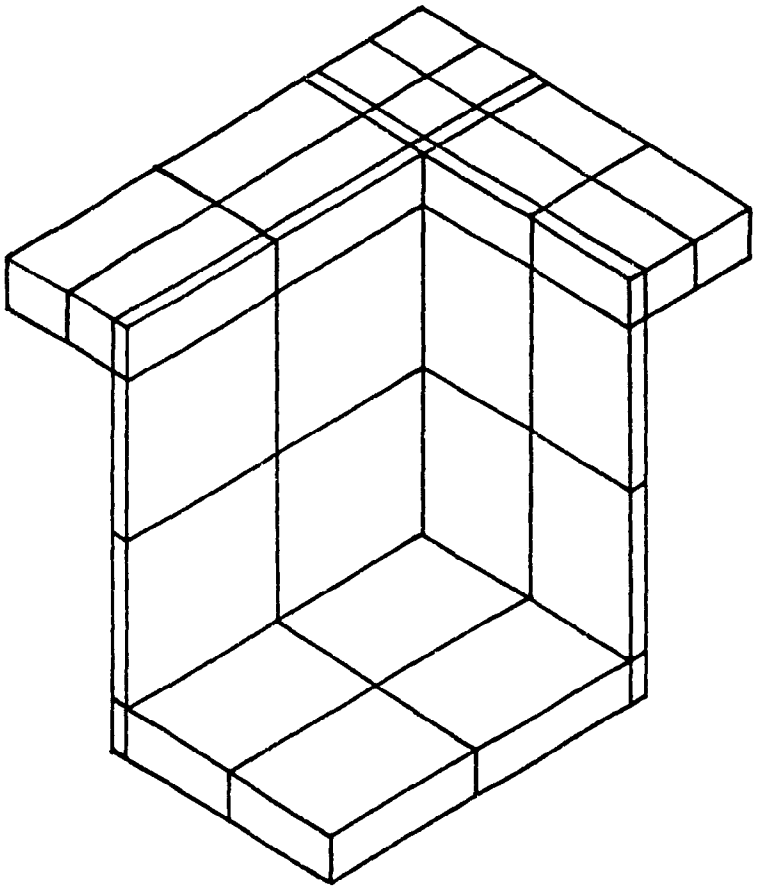

Figure 2.8 Simple Finite Element Mesh Configuration

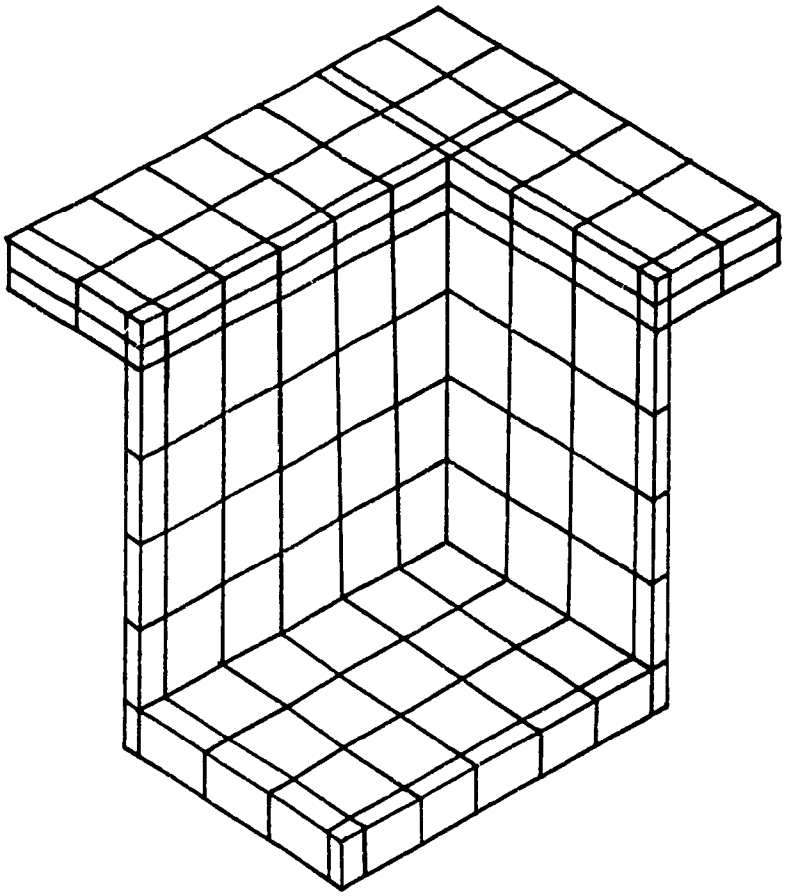

Figure 2.9 157 Elements Configuration

2.9. This model yields a reasonably accurate displacement profile. But it does not permit to simulate the uneven bolt-up pressure exerted onto the flange-gasket assembly, nor the stiffening ribs of a reinforced pressure vessel.

In order to properly simulate the various gasket configurations and the flange-bolt interaction, more elaborate meshed models with up to 550 elements were used subsequently. The final number of elements used in a model differ for different types of gaskets simulated, and configurations of pressure vessels investigated: unreinforced thick walled vessel or rib-reinforced thin walled vessel.

As the size of a model is increased, the major challenge to the structural modeling is the limit of the maximum size of wave front matrix provided with respect to the software and computer. The limiting pre-wave front matrix in the ANSYS package in the VAX 8530 at Concordia University was 200x200. With limited maximum wave front size, the elements and nodes of a model should be generated with respect to certain a scheme, as discussed in section 2.3.2, such that the best possible (finest) mesh can be used within these limitations and thus improved results can be obtained.

The improved models of the bolted flange structure in Figures 2.2 and 2.3 are modeled based on the "one sweep" scheme presented in section 2.3.2. The maximum wave front size required for the model is n= 189, which satisfied the limits of n=200 available for the program.

2.4.3 Finite Element Model of the Flanged Structure

The quadrant finite element models of two types of the rectangular bolted flanged structures are shown Figures 2.10 and 2.11, respectively. The thick wall flange model, as shown in Figure 2.10, is modeled with 973 nodes and 550 3-D isoparameter elements. The flange thickness is 25mm and the shell thickness is 10mm. The finite element model of the reinforced flange structure, as shown in Figure 2.11, has 1004 nodes and 540 elements. The flange thickness is also 25mm; however, the shell thickness is only 4.8mm. The rib size of dimension is 75mm X 13mm. The distance between the ribs is 56mm. The thickness of the bottom plate is 25mm (1 in) for both flange structures.

2.4.4 Analytic Models of the Gaskets

In order to analyse the deformation and stress of bolted flange connection structures more realistically, the gaskets should be included in the computation models. The finite element method has the advantage of dealing with different materials in one model. In the computation models used, two types of gaskets are considered in the assembly of the bolted flanged connections, namely full face and strip gaskets, as shown in Figures.2.12 and 2.13.

The gasket is the heart of a bolted joint. It is essentially an elasto-plastic material which is softer than that of the flange faces. Under the application of a bolt load, the gasket deforms and fills up irregularities on the flange face. In this condition, the gasket is considered to be seated. When pressure is introduced in the pressure vessel, and the flanges separate by a small amount at the gasket

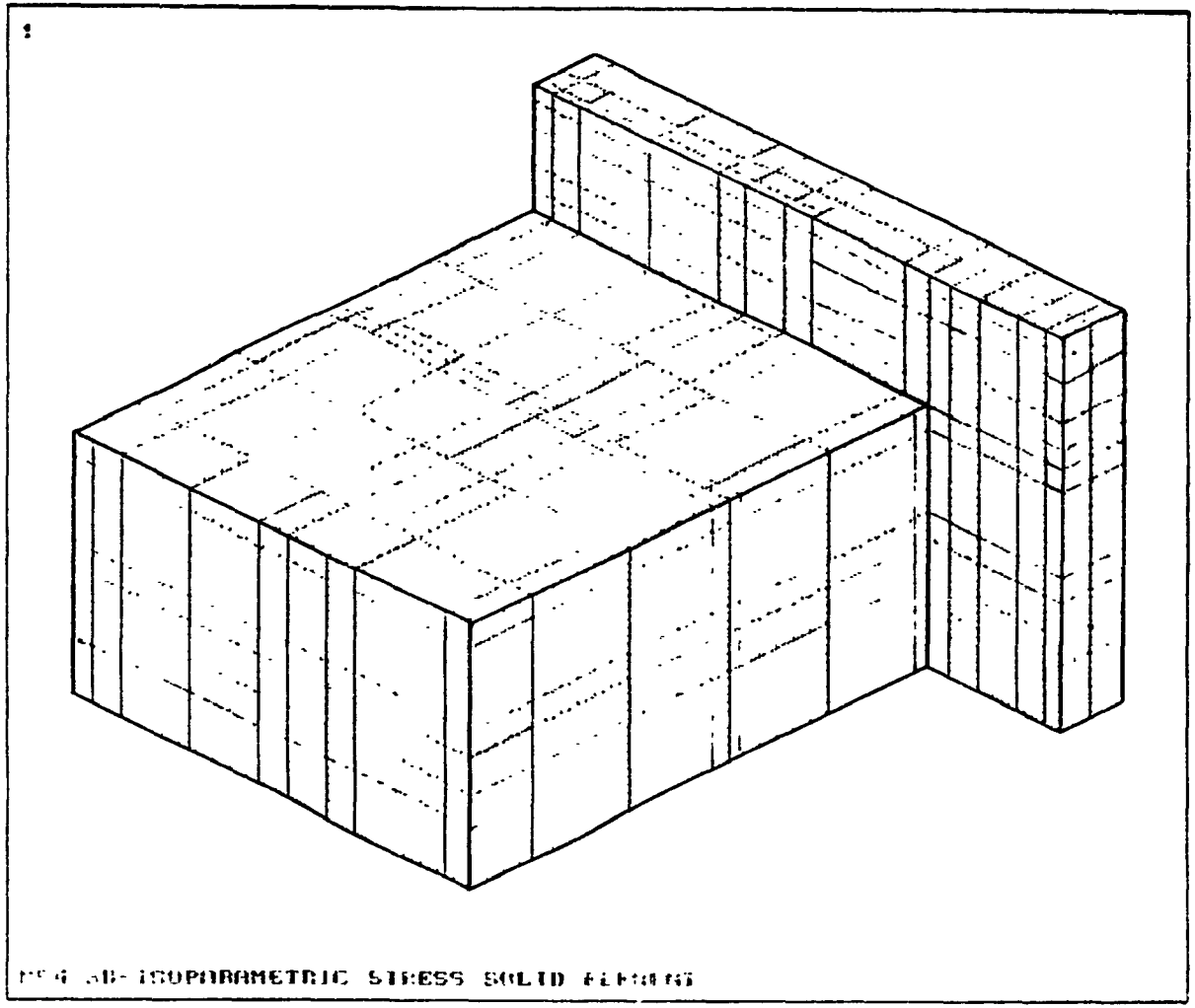

Figure 2.10 Finite Element Model of Thick Walled Vessel Flange with 550 Elements and 973 Nodes

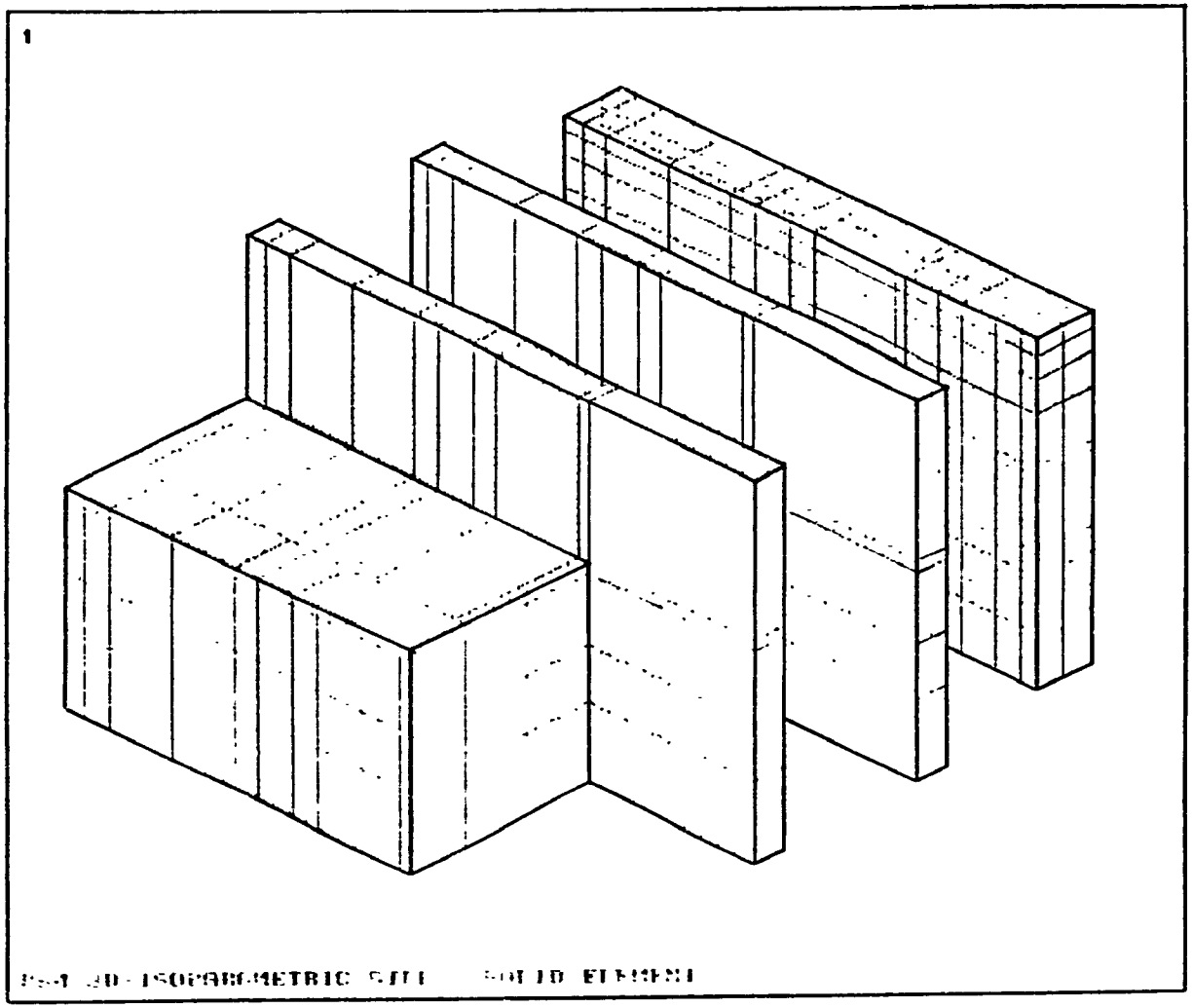

Figure 2.11 Finite Element Model of Rib-reinforced Flange with 540 Elements and 1004 Nodes

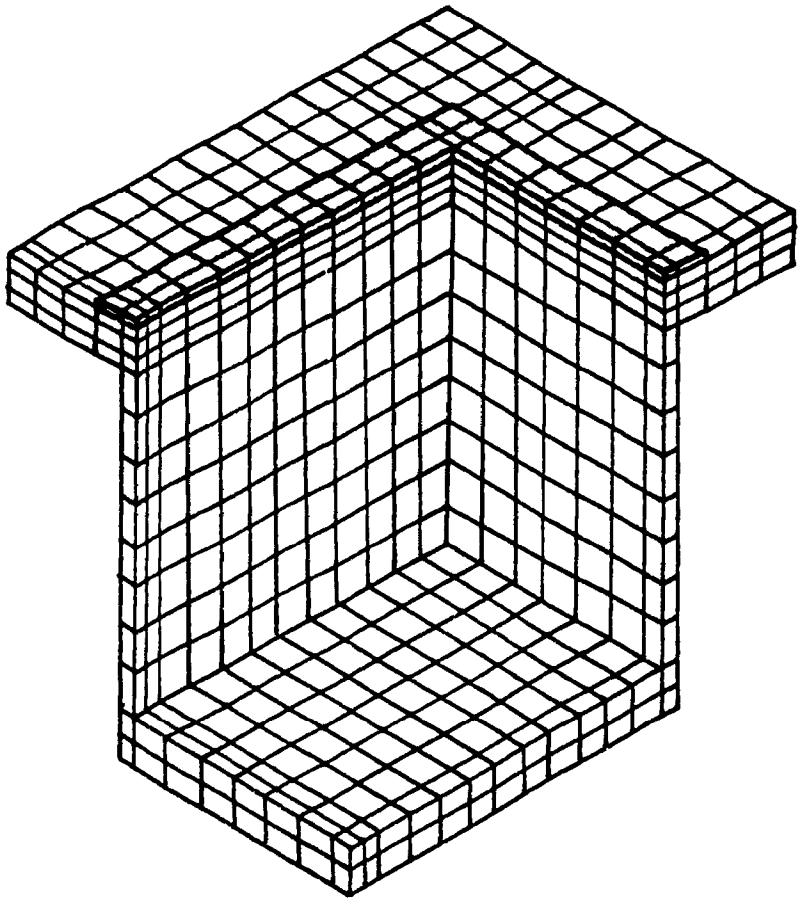

Figure 2.12 Flange-Shell Structure with Strip Gasket

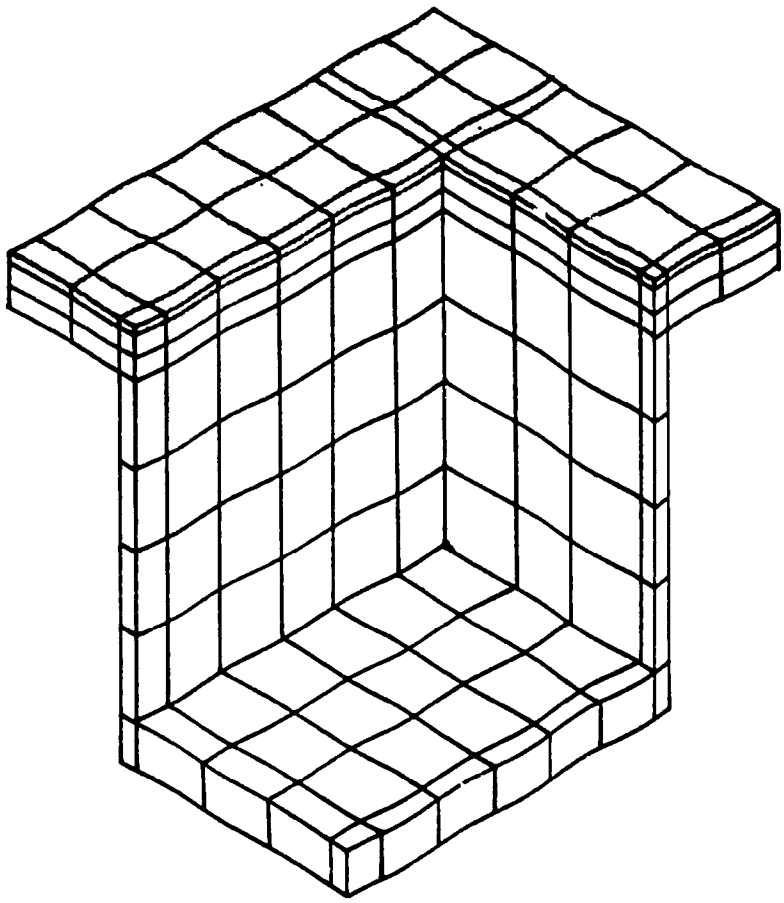

Figure 2.13 Flange-Shell Structure with Full Face Gasket

location, the gasket should possess enough resilience to maintain sufficient residual surface pressure in order to keep the joint from leaking.

The deformation of gasket material with respect to loading is essentially nonlinear. After large deformation due to applying the bolt preloading, however, the deflection of the gasket with respect to internal pressure is relatively small. With the presence of the bolt preloading, the mechanical properties of the gasket material is approximated to be linear in modeling and analysis.

2.5 Other Modeling Considerations

The input parameters for the finite element models are established based on the experimental setup for the two rectangular flanged pressure vessels. The boundary and loading conditions corresponding to the quadrant flanged structural models, and the materials employed are discussed in this section.

2.5.1 Boundary Conditions

The boundary conditions consist of the constraints at the symmetric planes, and the constraints on the interface surfaces of flanges or gaskets according to the type of flanged connection simulated. For a quadrant flanged model, as illustrated in Figure 2.7, all nodal displacements on the central plane XOZ in Y direction should be fixed. The nodal displacements on the central plan YOZ in X direction, in the same way, are constrained.

The constraints on the interface plane of the flange or gasket are established according to the construction of different type of gasket used by the flanged assemblies. The degree of freedom of nodal points which are perpendicular to the interface plane of the flanged connection are all constrained.

2.5.2 Preload and Pressure

The bolts employed in the flanged connection are 3/4-16 UNF with a nominal diameter 19.05 mm (.75 in), made of SA-193-B7, low alloy steel. A total of fourteen (14) bolts are used in the connection. The preloading bolt forces used in the analysis are calculated based on the preloading stress of the tension bolts and the tightening torques on the bolts. Two different bolt forces are used in the computation, namely, 62.3 KN (14000 lbf) and 89.0 KN (20000 lbf).

The bolt force is assumed to be evenly distributed within the washer covered area, along the bolt line in the analytical models. The bolt force is then apportioned to the individual nodes in the vicinity of the actual location of each bolt in the assembly.

The pressure applied within the bolted flanged apparatus is set to be 2070 kPa (300 psi) for the testing, which was also used for all analytical model analyses. The pressure loading is applied on all the inner surfaces of the structural model.

2.5.3 Material Properties

The material of the flange, vessel and reinforcing ribs is made of steel SA-516-70. The gasket must be strong enough to withstand the

bolt pre-load without crushing or extruding out. The gasket selected is made of compressed asbestos.

The mechanical properties of the flange structure and the gasket are listed in Table 2.3.

TABLE 2.3

Material Properties of Flanged Structure

SYMBOL	DESCRIPTION	VALUE
E_f	Modulus of elasticity of flanged structure	2.0×10^{11} Pa (29×10^{6} psi)
ν_f	Poison ratio of flanged structure	0.3
E_g	Modulus of elasticity of gasket material	5.5×10^{7} Pa (7.9×10^{3} psi)
ν_g	Poison ratio of gasket material	0.32

2.6 Summary

Finite element models of rectangular flange structures are developed in this chapter. Two types of rectangular bolted flanged connections are illustrated. The structural features and modeling procedures are presented. The analysis program, 3-D isoparametric element and wave front technique used for the finite element modeling are discussed. A brief discussion on the gaskets behavior, the loading types and materials, is also given. The detailed analysis of the bolted flange structural models will be discussed in the following chapters.

CHAPTER 3

FINITE ELEMENT ANALYSIS OF RECTANGULAR BOLTED FLANGED STRUCTURES

3.1 General

The different structural models of the rectangular bolted flanged connections, developed and presented in chapter 2, are numerically analyzed in this chapter by employing the finite element method. The mechanical behaviors of the bolted flanged structures are evaluated and presented in terms of the structural displacement profiles and stress distributions, under the specified loading conditions.

For bolted flanged structures, a pre-tension of the bolts should be required such that a compression stress in the gasket in between the flanges be generated and remain compressive under the operating pressure loading in order to ensure a proper sealing. The pre-tension in bolts is set-up by application of a preloading torque [39]. The deflections and stresses of a bolted flanged connection structure are, therefore, the results of the combined loading due to bolt pre-loading and operating pressure loading. In the finite element analysis, two types of loading conditions are considered in order to identify the contribution of each loading to the deflection and stress of the bolted structure, that is (1) preloading condition and (2) working condition (combined preloading and pressure loading).

The two types of rectangular bolted flanged structures, that is the thick wall and the reinforced thin wall flanged structures, are

analyzed for the strip-gasket and full face gasket connections. The maximum deflections and stresses due to various models and loadings are identified. The computed results are discussed and compared with respect to different structural models and loading conditions.

A parametric study of the bolted flanged structures is also carried out to show the relative sensitivity of the design parameters on structure strength and stiffness characteristics. The parameters considered in the study include the flange thickness, vessel wall thickness, bolt preloading force and reinforcing rib size.

3.2 Structural Behaviour Under the Preload of Tension Bolts

Bolt pre-tension in flanged connections is required to pre-stress the gasket for proper sealing. A pre-loading torque is usually applied to a bolt to perform the bolt pre-tensioning. The flanged connection structures under bolt pre-loading will yield certain deflection and stress profiles. The pre-load defelections and stresses for certain flanged structures, for example, strip gasket flanges (as will be shown later), are sometimes significant as compared with those due to operating pressure.

3.2.1 O-ring Gasket Flanged Connection

In an O-ring gasket flanged assembly, as shown in Figure 2.1 (a), an O-ring groove is usually machined into one of the flanges and the O-ring gasket forms a seal against leakage. The two bolted flanges are actually in contact with each other over the width of the flat faces. This kind of bolted flange connection is often utilized in case of low

pressure vessels. In the finite element model the O-ring gasketed flanged structure is therefore modelled as metal to metal connection at the flange interface. The flange face is constrained from moving from the bolted region to the flange edges in the Z direction.

Two different values of preload bolt forces are applied for each model, one is 62.3 KN (14000 lbf) and the other 89.0 KN (20000 lbf) per bolt, the same as used for experimental tests.

A deflection profile for bolt force of 62.3 KN, in the YOZ plane at X=0 where the maximum deflections and stresses are identified, is shown in Figure 3.1 (a). The maximum displacement of the flanged structure in the Y direction is 0.0038 mm at node 21 of the flange model, while the maximum displacement in the Z direction is -0.0063 mm at node 27, where the bolt force is applied. Figure 3.1 (b) shows the deflection profile of the flange when the bolt force changed to 89.0 KN. The maximum displacement in the Y direction is 0.0054 mm also at node 21. In the Z direction the maximum displacement is 0.009 mm at node 27 of the flange model.

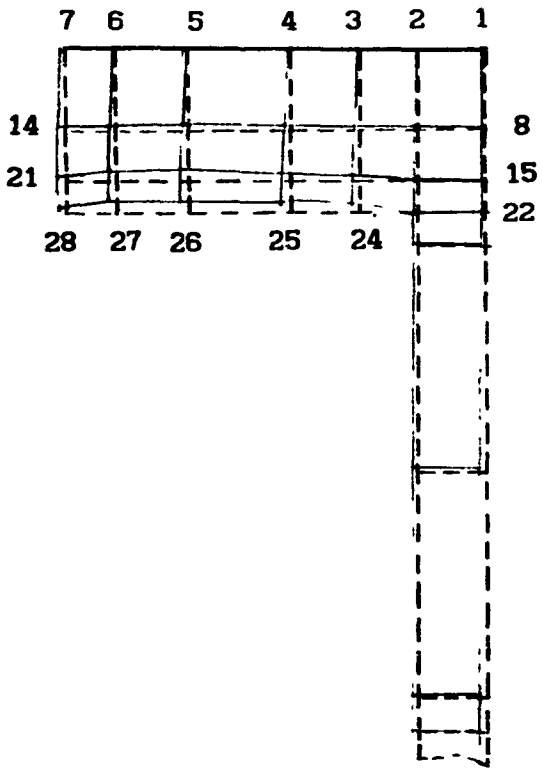

(a) Bolt Preload F_1= 62.3 KN

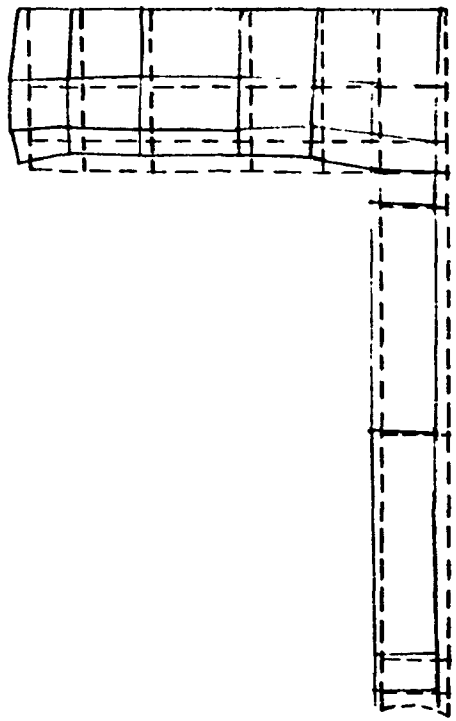

(b) Bolt Preload F_2= 89.0 KN

Figure 3.1 Deflection of Bolted Flanged Connection with O-ring Gasket due to Bolt Preload Alone

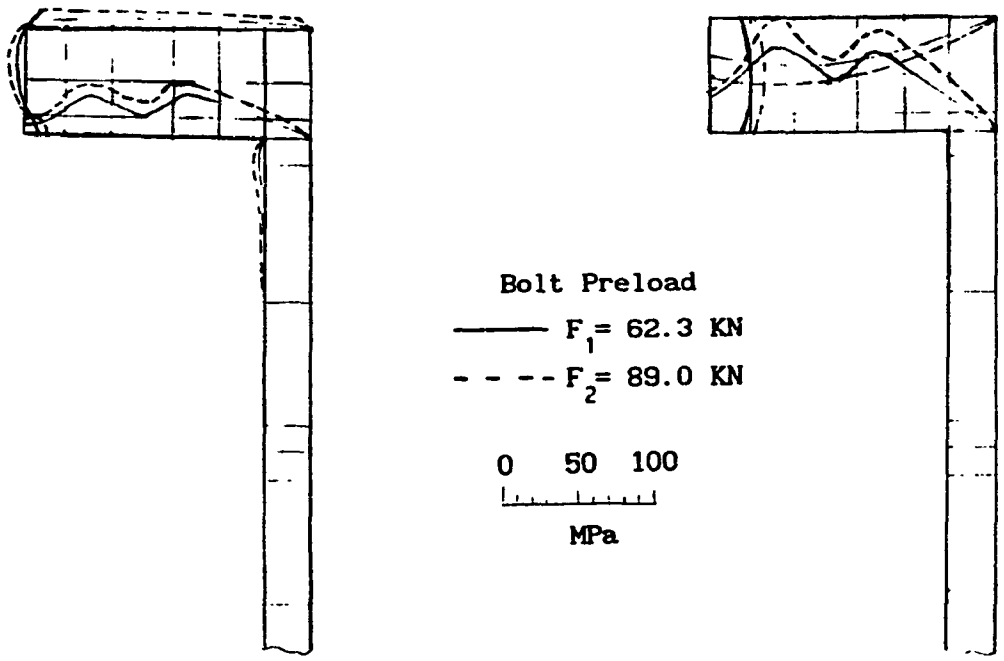

(a) Tangential Stress σ_x

(b) Longitudinal Stress σ_z

Figure 3.2 Stress Profile of Bolted Flanged Connection with O-ring Gasket due to Bolt Preload Alone

The stress profile for the bolt force of 62.3 KN is shown in Figure 3.2. The maximum tangential stress σ_{xmax} is -22 MPa, while the maximum longitudinal stress σ_{zmax} is -55 MPa. The maximum stresses corresponding to bolt force of 89.0 KN are σ_{xmax}= -32 MPa and σ_{zmax} = -78 MPa at the same locations as for the 62.3 KN blt force.

The deflections and stresses results of the O-ring gasket flanged structure under the preload bolt force only are summarized in the Tables 3.1 and 3.2, respectively.

TABLE 3.1

Summary of Deflections of Bolted Flanged Connection
With O-ring Gasket Due to Bolt Preload Alone

mm

direction	Y			Z		
node #	21	24	27	21	24	27
F1	0.0038 *	0.0025	0.0028	-0.0024	-0.0054	-0.0063 *
F2	0.0054 *	0.0036	0.004	-0.0034	-0.0077	-0.009 *

F_1 = 62.3 KN.

F_2 = 89.0 KN.

* denotes the maximum value

TABLE 3.2

Stress Summary of Bolted Flanged Connection With O-ring Gasket Due to Bolt Preload Alone

MPa

element #		15	17	18	19
F1	σ_x	- 22.2	- 22.2	13.1	2.28
	σ_z	- 51.4	- 54.8	32.3	3.37
F2	σ_x	- 31.7	- 31.7	18.7	3.26
	σ_z	- 73.5	- 78.3	46	4.8

F_1 = 62.3 KN

F_2 = 89.0 KN

σ_x = tangential stress

σ_z = longitudinal stress

It can be seen from the analysis results that for the O-ring gasketed flanged connection with flat faces, the major displacements and stresses due to the preload bolt force are all around the bolt areas. There are only insignificant displacements and stresses along the vessel shells.

3.2.2 Full Face Gasket Flanged Connection

This type of flange structure is also called a flat-face flange. In the finite element model the gasket is modelled as a layer with a different modulus of elasticity from that of the flange. The top gasket face in Z direction is fixed, while the bottom face of the gasket is connected with the whole face of the flange. Both thick wall and reinforced thin wall structures are analyzed for the bolt preloading of condition.

The deflection profiles in the YOZ plane at X=0 for the thick

wall structure, for bolt forces of 62.3 KN and 89.0 KN, are presented in Figures 3.3 (a) and (b), respectively. For the bolt force of 62.3 KN the gasket has the maximum displacement of 0.032 mm at node 7 in the Y direction. The maximum displacement of the flange in the Y direction is 0.017 mm at node 38. The maximum displacement in Z direction is -0.061 mm at node 21. For a bolt force of 89.0 KN, the maximum displacement values of the same structure model are proportionally increased and with the same profile, as summarized in Table 3.3.

Figure 3.4 shows the stress profile of the thick wall structure with full face gasket under bolt pre-load alone. For a bolt force of 62.3 KN, the maximum gasket stresses are σ_{xmax} = -5.92 MPa and σ_{zmax} = -14.98 MPa. The maximum flange stresses are σ_{xmax} = -54.6 MPa and σ_{zmax} = -60.2 MPa. When a bolt force of 89.0 KN is applied, the stress level is also increased proportionally as shown in Figure 3.4 and Table 3.4.

The deflection profiles of the reinforced thin wall structure under the bolt forces of 62.3 KN and 89.0 KN are shown in Figures 3.5 (a) and (b). It can be seen that the maximum gasket displacements occur all at node 7. The maximum displacement of the flange in the Y direction is at node 31 and in the Z direction at node 21, as summarized in Table 3.3. The stress distributions of the reinforced thin wall flanged structure due to bolt pre-load alone are shown in Figure 3.6 and the maximum stresses are listed in Table 3.4.

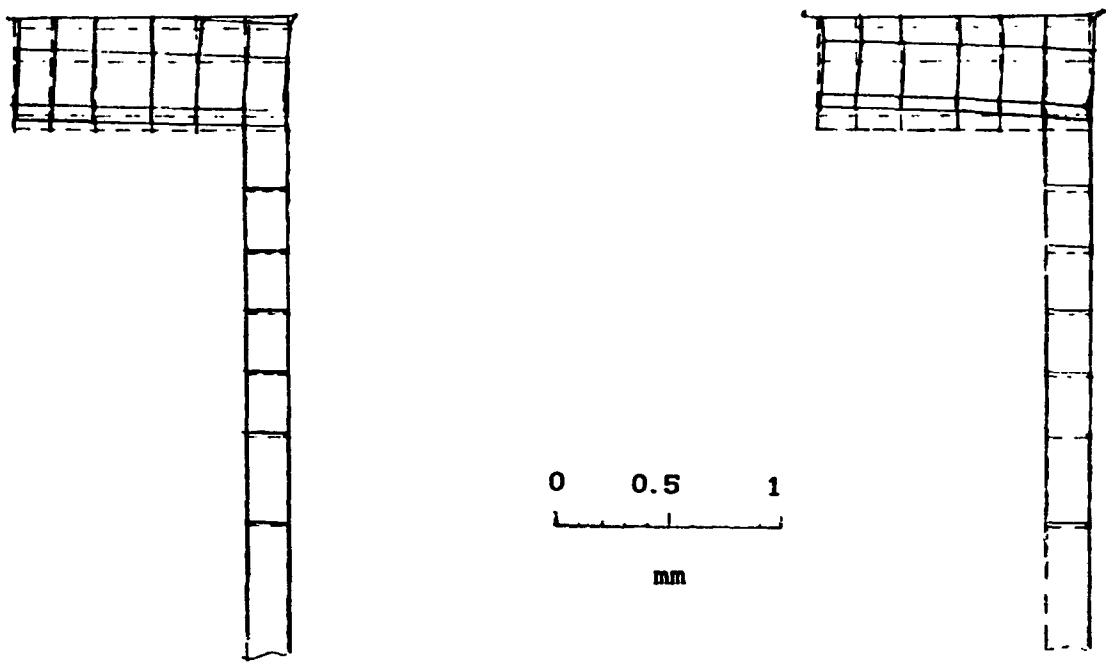

(a) Bolt Preload F_1= 62.3 KN

(b) Bolt Preload F_2= 89.0 KN

Figure 3.3 Deflection of Bolted Flanged Connection on Thick Walled Vessel with Full Face Gasket due to Bolt Preload Alone

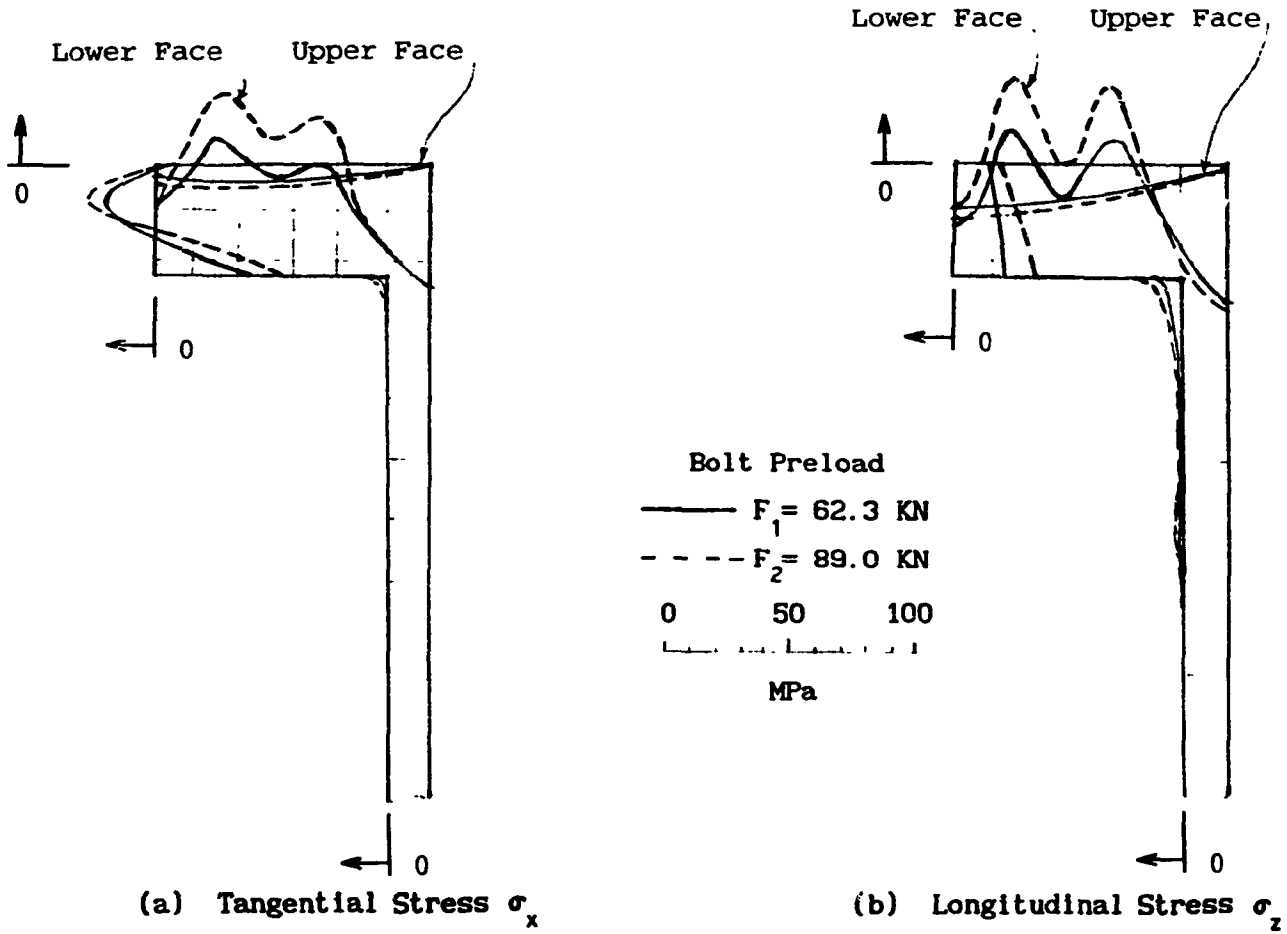

(a) Tangential Stress σ_x

(b) Longitudinal Stress σ_z

Figure 3.4 Stress profile of Bolted Flanged Connection on Thick Walled Vessel with Full Face Gasket due to Bolt Preload Alone

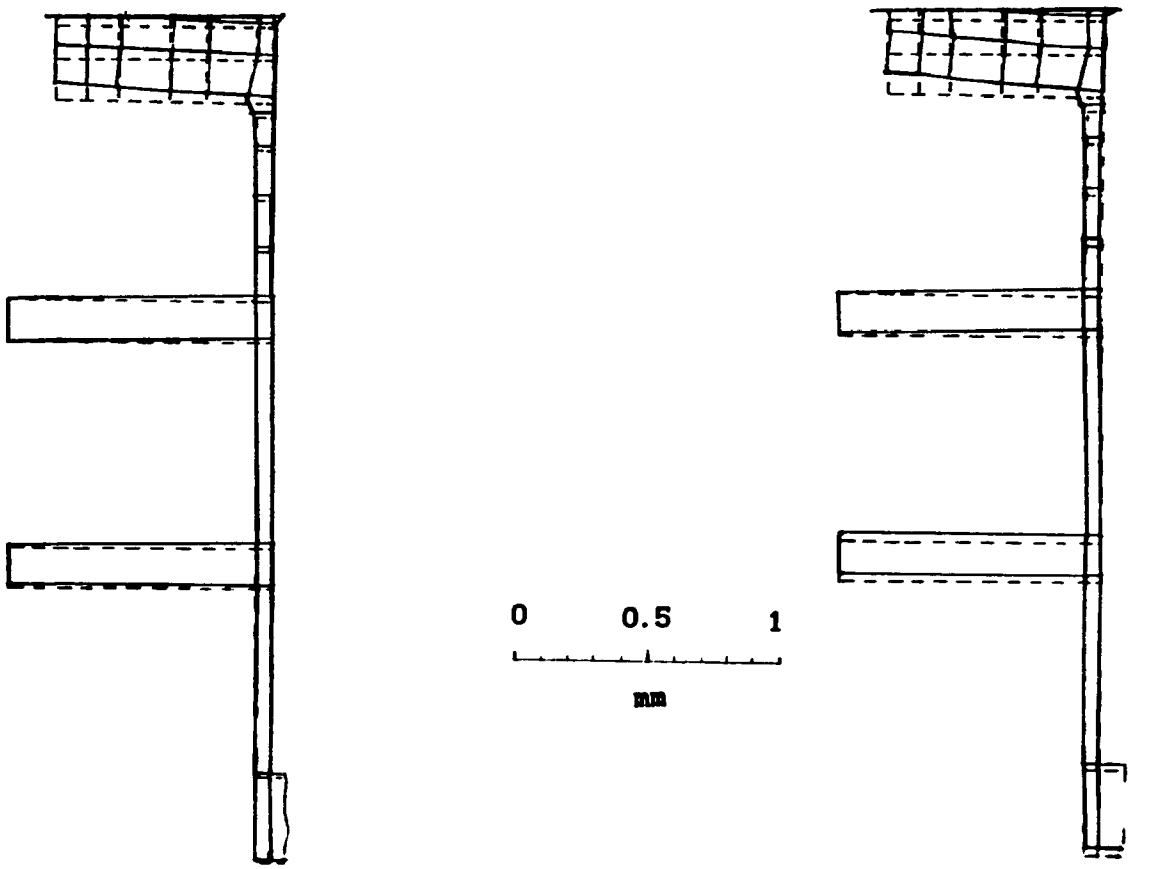

(a) Bolt Preload F_1= 62.3 KN

(b) Bolt Preload F_2= 89.0 KN

Figure 3.5 Deflection of Bolted Flanged Connection on Rib-reinforced Thin Walled Vessel with Full Face Gasket due to Bolt Preload Alone

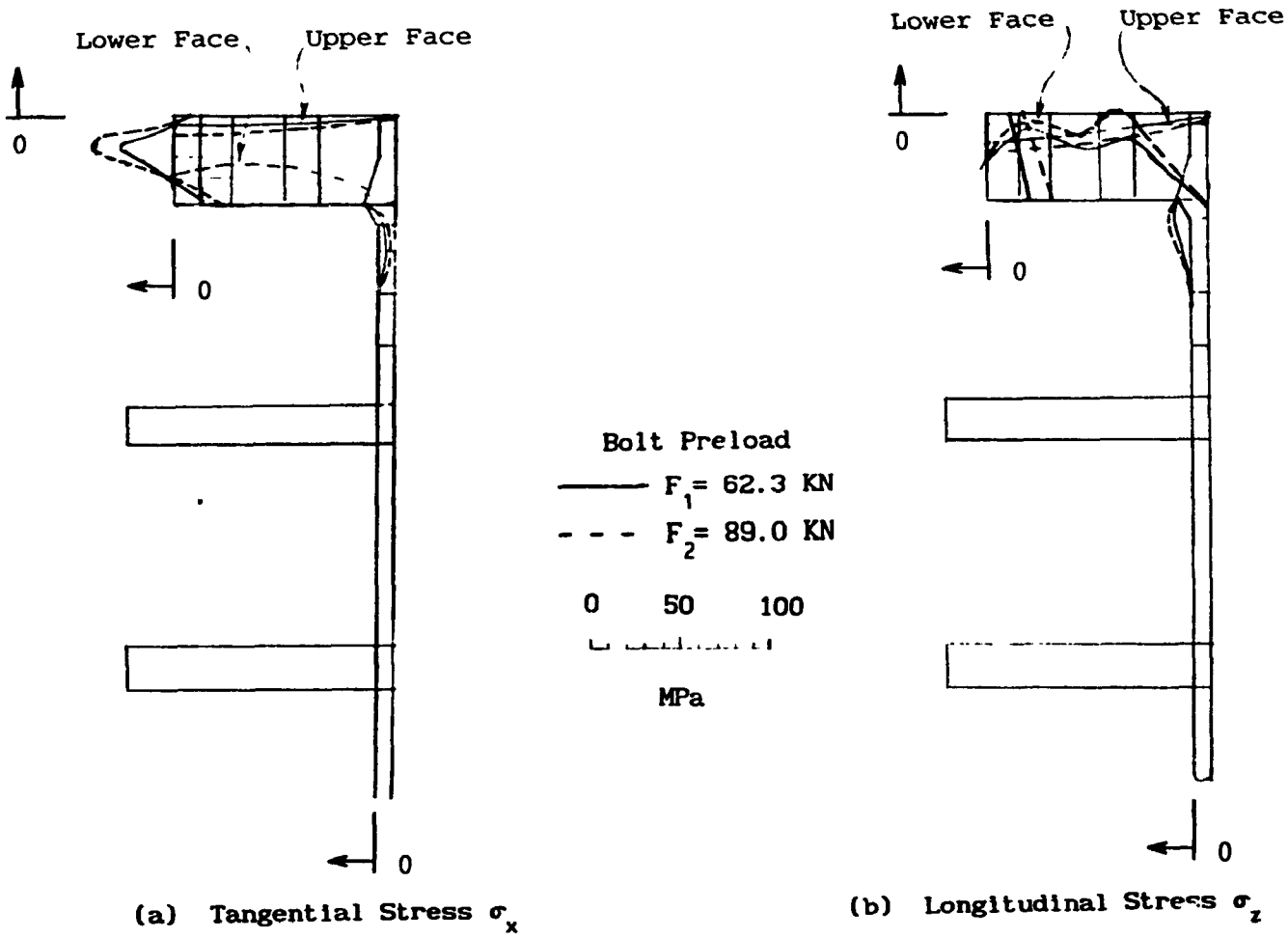

(a) Tangential Stress σ_x

(b) Longitudinal Stress σ_z

Figure 3.6 Stress Profiles of Bolted Flanged Connection on Rib-reinforced Thin Walled Vessel with Full Face Gasket due to Bolt Preload Alone

TABLE 3.3

Maximum Deflections of Bolted Flanged Connection With Full Face Gasket due to Bolt Preload Alone

mm

		thick wall model		reinforced shell model	
location		gasket	flange	gasket	flange
F_1	δ_y	0.032		0.0346	
	δ_z		- 0.061		- 0.0614
F_2	δ_y	0.0456		0.0495	
	δ_z		- 0.0865		- 0.0877

F_1 = 62.3 KN

F_2 = 89.0 KN

δ_y = deflection in Y direction

δ_z = deflection in Z direction

TABLE 3.4

Maximum Stresses in Bolted Flanged Connection With Full Face Gasket Due to Bolt Preload Alone

MPa

		thick wall model		reinforced shell model	
location		gasket	flange	gasket	flange
F_1	σ_x	- 6.27	- 54.6	- 6.33	- 16.96
	σ_z	- 14.55	- 60.19	- 14.7	- 35.76
F_2	σ_x	- 8.46	- 78	- 8.57	- 24.23
	σ_z	- 21.4	- 85.98	- 21.68	- 51.1

F_1 = 62.3 KN

F_2 = 89.0 KN

σ_x = tangential sresses

σ_z = longitudinal stresses

It is clear that the displacements and stresses of the full face gasketed flanged structure due to bolt force alone are similar to that of the O-ring gasket. The large displacements and high stresses are found in the flange, in vicinity of the bolts, only insignificant values are found in the vessel shells.

A comparison of the results of the structures with metal to metal interface (O-ring gasket) and full face gasket shows that the deflections of the gasket due to bolt force is significant because of the relatively low value of modulus of elasticity of the gasket. The gasket therefore introduces an additional displacement to the whole flange structure in the Z direction.

3.2.3 Strip Gasket Flanged Connection

The rectangular bolted flanged connections assembled with a strip gasket, as shown in Figure 2.1 (c), is analyzed for bolt preload alone. In the finite element model, the strip gasket is modelled by using elements with a different modulus of elasticity from that of the flange. Only the top face of the strip gasket is fixed in the Z direction. Both thick wall and reinforced thin wall structures are evaluated. The bolt force employed is 44.4 KN.

The deflection profile of the thick wall structure in the YOZ plane at X=0, due to bolt preload alone, is shown in Figure 3.7 (a), while the deflection of the reinforced thin wall structure is shown in Figure 3.7 (b). The maximum values of deflections for both structures are listed in Table 3.5. In contrast to the flat-face cases, it can be seen that the deflections in the vessel shells for both structures are larger than those of gaskets and flanges.

The stress profiles of the strip gasket flanged connections for thick and reinforced thin wall structures are illustrated in Figures 3.8 and 3.9, respectively. The maximum stress values at different locations are summarized in Table 3.6. The results show that the maximum stress values, due to bolt preload alone, are no longer in the gasket as compared with those of the O-ring gasket and full face gasket cases. For the thick wall structure the maximum tangential stress is found in the flange (-71.5 MPa). The maximum longitudinal

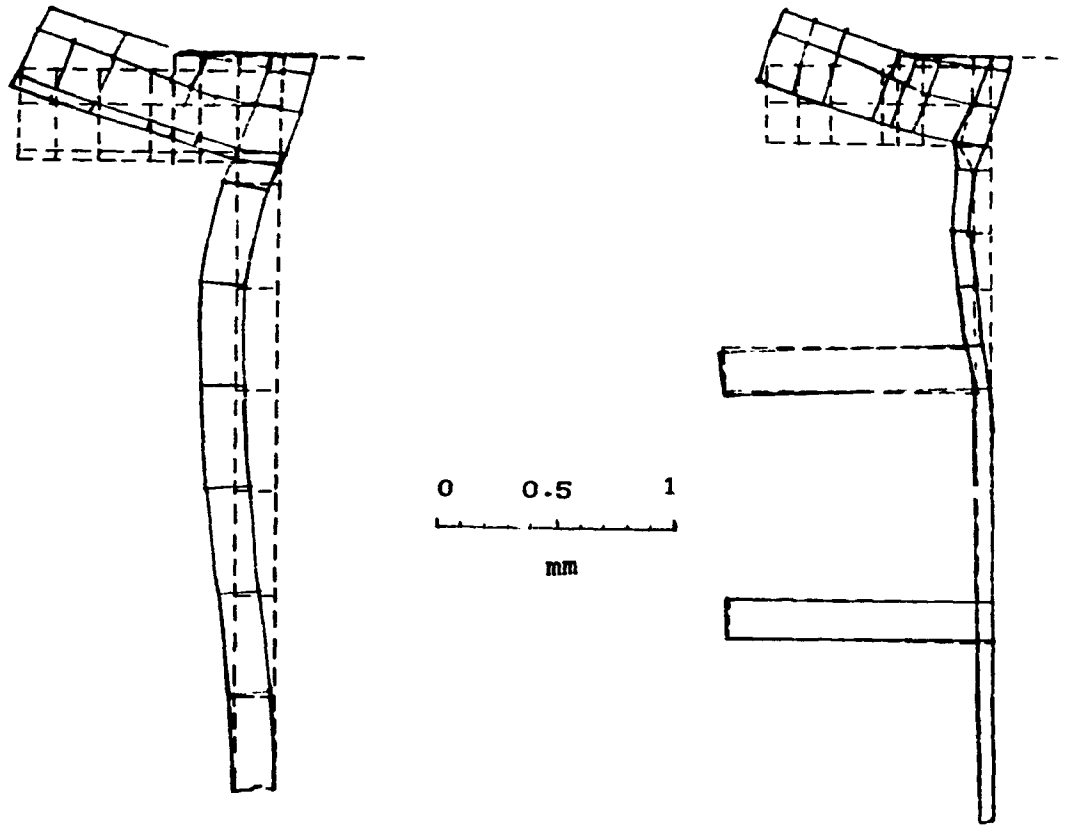

(a) Thick Wall Structure

(b) Reinforced Thin Wall Structure

Figure 3.7 Deflection of Bolted Flanged Connection with Strip Gasket due to Bolt Preload Alone

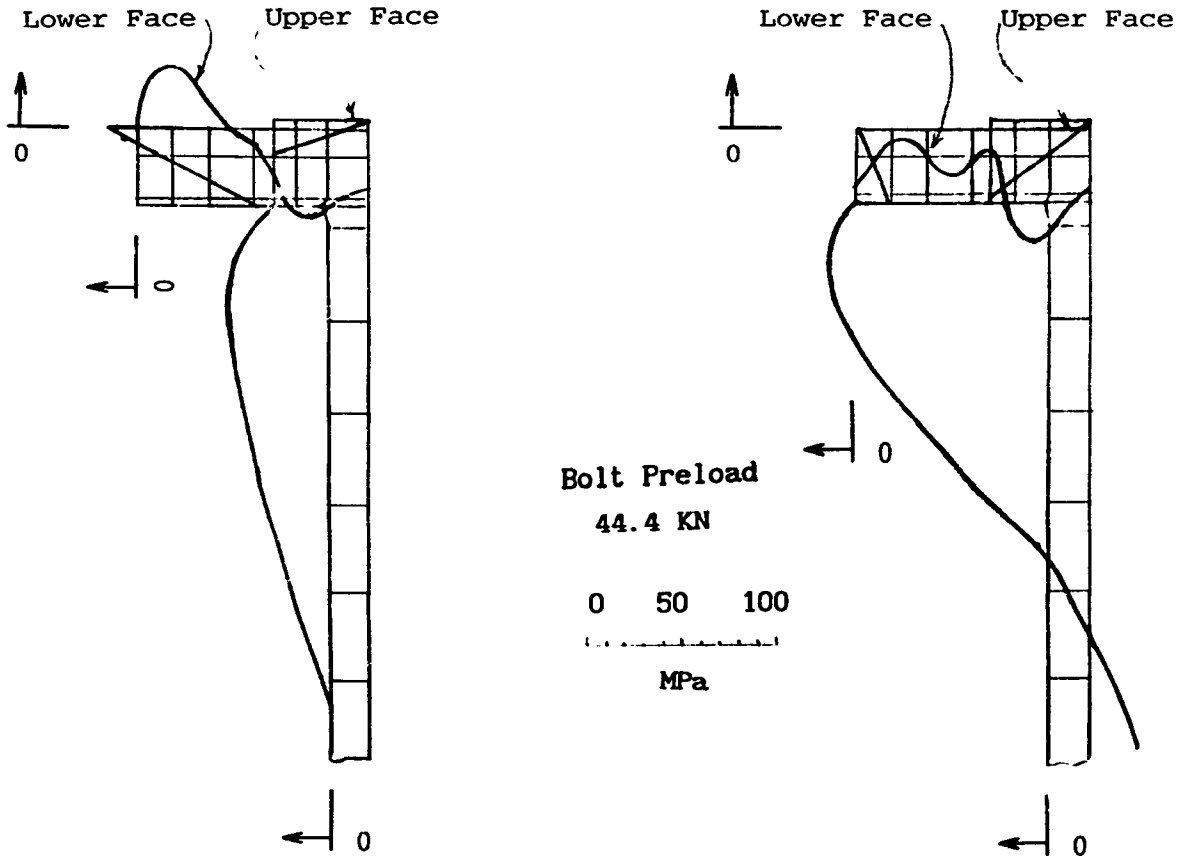

(a) Tangential Stress σ_x

(b) Longitudinal Stress σ_z

Figure 3.8 Stress Profiles of Flanges on Thick Walled Vessel with Strip Gasket due to bolt preload alone

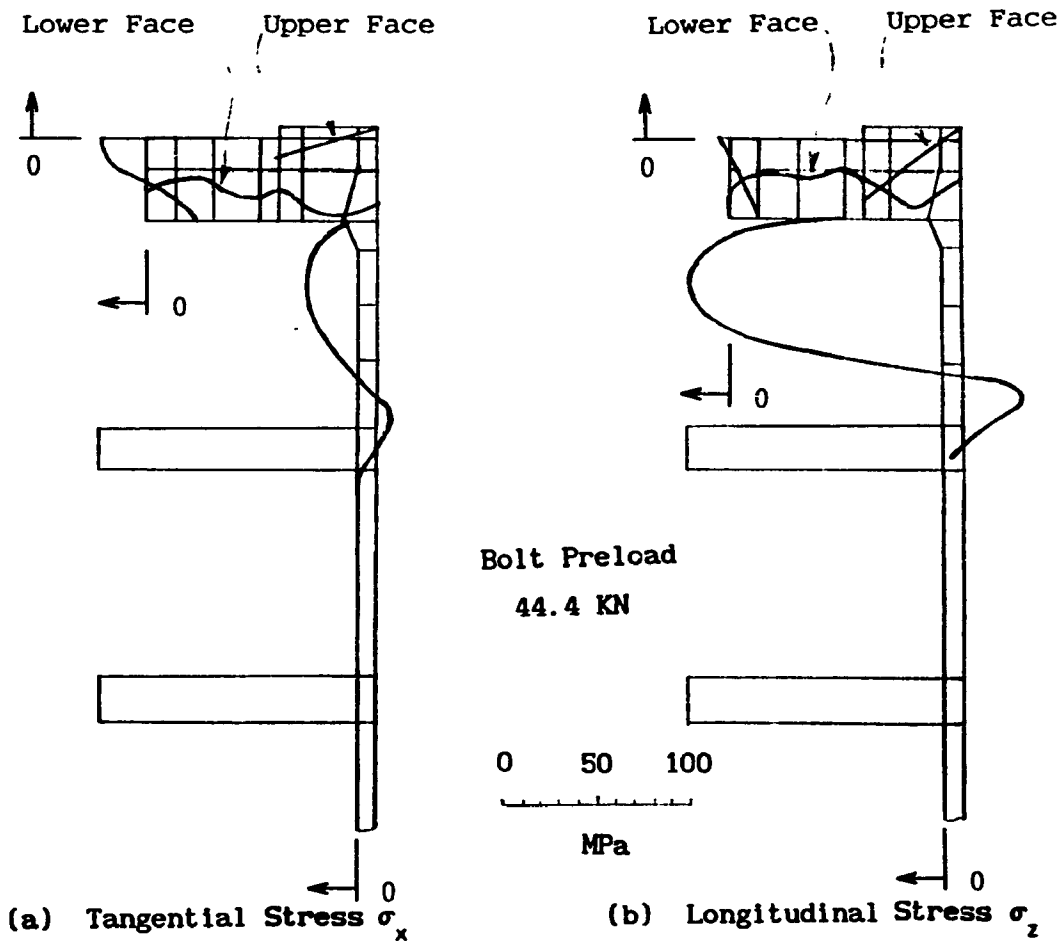

Figure 3.9 Stress Profiles of Flanges on Rib-reinforced Vessel with Strip Gasket due to Bolt Preload Alone

stress of 113 MPa is located in the shell, while for the reinforced thin wall structure both maximum tangential and longitudinal stresses are all located in the vessel shell, valued as 21.2 and 130 MPa respectively.

TABLE 3.5

Maximum Deflections of Bolted Flanged Connection
With Strip Gasket deu*p+25Xto Bolt Preload Alone

mm

	Thick wall model		Reinforced shell model	
location	gasket	flange	gasket	flange
δ max	- 0.142	- 0.339	- 0.088	- 0.256

TABEL 3.6

Summary of Stresses of Bolted Flanged Connection
With Strip Gasket deu to Bolt Preload Alone

MPa

location		gasket	flange	bolt circle	shell
thick wall model	σ_x	- 15.74	- 70.7	- 71.48	44.1
	σ_z	- 40.21	- 15.8	- 34.65	113.16
reinforced wall model	σ_x	- 12.3	- 18.2	- 20.3	21.2
	σ_z	- 31.5	- 7.53	- 14.7	130.7

σ_x = tangential stress

σ = longitudinal stress

It is obvious that the bolt preload on the strip gasket flange connection generates a bending moment in the flange which in turn yields a large deflection and high stresses in the rectangular vessel shell. The stresses in the vessel shell are larger than those in flange and gasket. It is also observed that the structure with a strip gasket may needs a tapered section in order to reduce high stress on the flange and in the hub.

The parametric study of bolt force influence on the rectangular flanged structure with strip gasket will be discussed in section 3.4.4.

3.3 Mechanical Behavior of Rectangular Flanges Under Working Condition

The working condition applied to the rectangular bolted flanged vessel structure is the combined loading due to both bolt preload and internal pressure in the vessel. The pressure value utilized in the analysis is the same as the one used in the tests, namely 2,070 KPa (300 psi).

In this section, for the purpose of easy comparison, the stiffness characteristics of the structure, under the combined working loadings, are first discussed in terms of deflections using various gaskets. The strength properties of the structures, presented as stress profiles of all the bolted flanged connections, will then be compared and discussed after the stiffness properties.

3.3.1 Flange Structure Deflections

Under working conditions, the 3.2 mm thick gasket is compressed due to the bolt forces applied on the two flanges. The flange thus has a displacement along the bolt force direction due to the deformation of the gasket. The rectangular bolted flanged vessels also have additional deflections due to flange bending moment and frame bending caused by pressure effect.

In the following sections, the stiffness characteristics of the rectangular bolted flanged connection, under working loadings, are evaluated for three types of gaskets.

3.3.1.1 O-ring Gasket Flanged Connection

The displacement profiles of the O-ring gasket flanged connection under combined working loading conditions in the YOZ plane at X=0, are shown in Figures 3.10 (a) and (b), for an internal pressure is of 2,070 MPa (300 psi). Figure 3.10 (a) is for a bolt preload of 62.3 KN (14000 lb), and (b) for a bolt preload of 89.0 KN (20000 lb). Table 3.7 summarizes the deflection results of the analysis model.

As compared with the results of bolt preload only, shown in Figure 3.1, it is easy to see that the internal pressure dominates the structural deflection, while the influence of the bolt preload is limited. The rectangular vessel shell with the O-ring gasket in the flanged connection yields a large deflection produced by the bending moment due to the internal pressure.

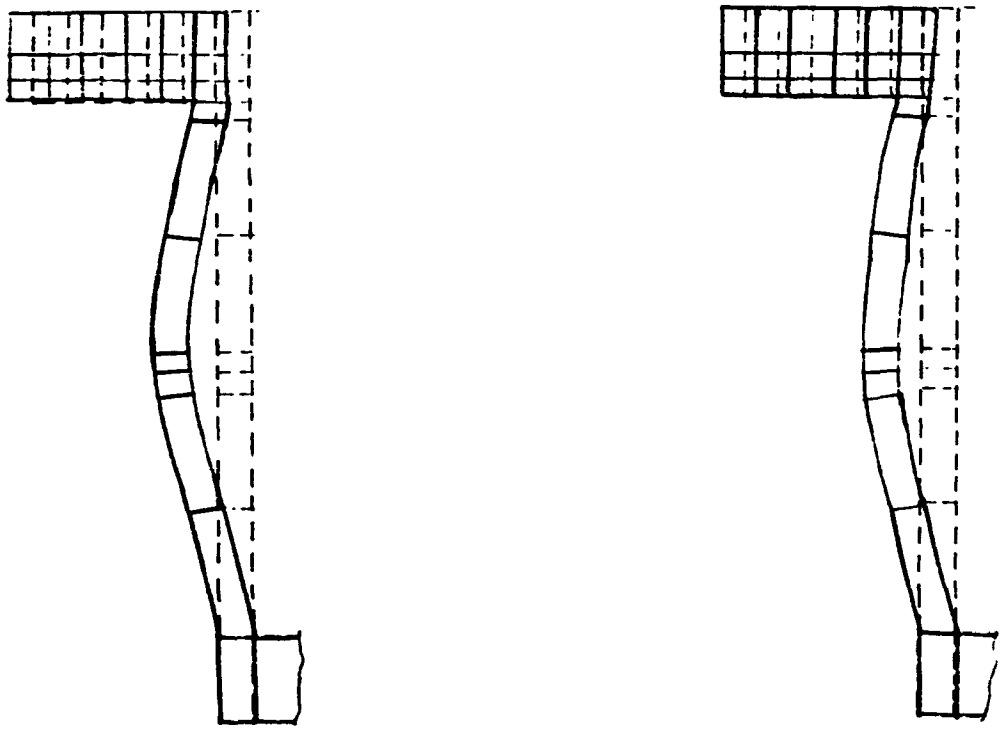

(a) Pressure and Preload F_1

(b) Pressure and Preload F_2

Figure 3.10 Deflections of Bolted Flanged Connections with O-ring Gaskets under Working Condition

moment due to the internal pressure.

TABLE 3.7

Summary of Deflections of Bolted Flanged Connection
With O-ring Gasket Under Working Condition

mm

direction	Y			Z		
node #	22	33	40	22	33	40
F_1	0.133	0.276*	0.13	0.019	0.013	0.0453*
F_2	0.134	0.277*	0.13	0.018	0.012	0.0447*

F_1 = 62.3 KN

F_2 = 89.0 KN

* denotes the maximum value

3.3.1.2 Full Face Gasket Flanged Connection

The deflections of the thick wall vessel structure with a full facegasket flanged connection under working loading conditions are shown in Figures 3.11 (a) and (b), for different bolt preload values. It can be seen that the internal pressure again dominates the structural deflection as similar to the case of the O-ring gasket.

Figures 3.12 (a) and (b) show the displacement profiles of the rib-reinforced thin wall vessel structure with full face gasket flanged connection under working condition. As compared with the case of bolt preload alone in Figure 3.5, it is observed that the internal pressure has a dominant influence on the structural deflection. The large deflection is induced in the vessel wall between the flange and

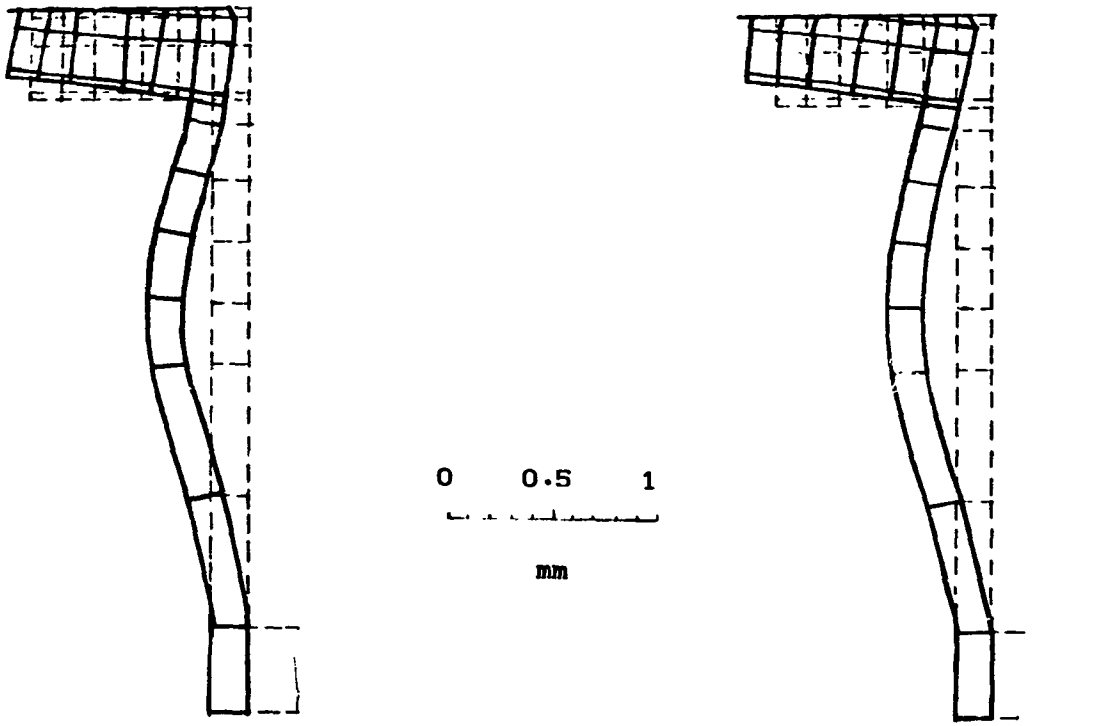

(a) Pressure and preload F_1

(b) Pressure and preload F_2

Figure 3.11 Deflections of Thick Walled Vessel Flanges with Full Face Gasket under Working Condition

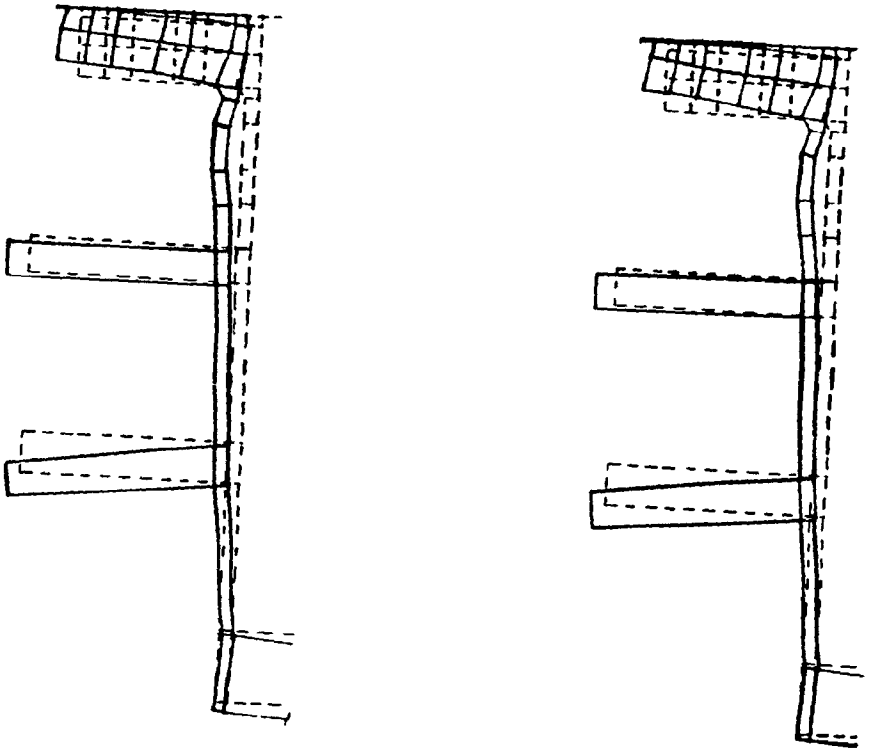

(a) Pressure and Preload F_1

(b) Pressure and Preload F_2

Figure 3.12 Deflections of Rib-reinforced Vessel Flanges with Full Face Gasket under Working Condition

wall model, is relatively small, due to the effects of rib reinforcement.

The maximum deflections of the model with full face gasket connection are summarized in Table 3.8.

TABLE 3.8

Maximum Deflection of Bolted Flanged Connection
With Full Gasket Under Working Condition

mm

	thick wall model		reinforced shell model	
location	gasket	flange	gasket	flange
F1	0.154	0.313	0.117	0.135
F2	0.168	0.32	0.132	0.14

F_1 = 62.3 KN

F_2 = 89.0 KN

3.3.1.3 Strip Gasket Flanged Connection

The deflection profile of the thick wall vessel structure with a strip gasket connection is shown in Figure 3.13 (a), under working conditions with a bolt preload of 44.4 KN and an internal pressure of 2,070 KPa. Figure 3.13 (b) illustrates the deformation of the reinforced vessel structure with a strip gasketand the same oprating, and bolt preload condition. The maximum deflections of both structures are summarized in Table 3.9.

As compared with the results of the strip gasket due to the bolt

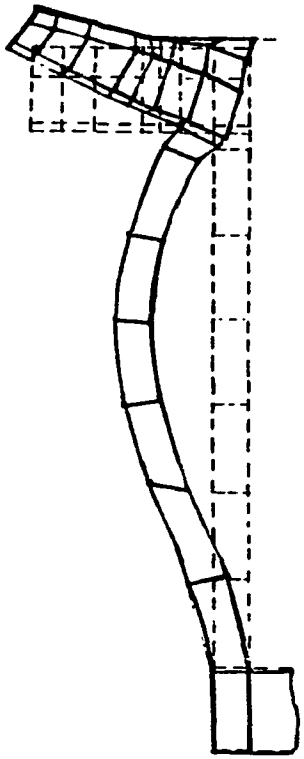

(a) Thick Wall Structure

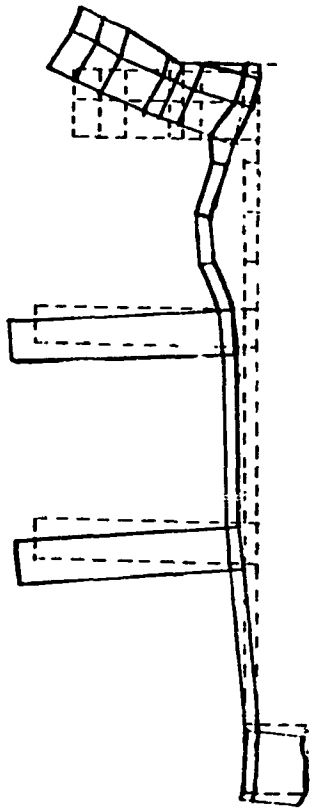

(b) Reinforced Thin Wall Structure

Figure 3.13 Deflections of Bolted Flanged Connections with Strip Gaskets under Working Condition

preload alone in Figures 3.7+25X(a) and (b), it can be seen that the bolt preload dominates the deflections in the gasket and in the flange, while the deflection on the rectangular vessel wall are influenced by both bolt preload and internal pressure, this is different from the cases of the O-ring gasket and the full face gasket flanged connections.

TABLE 3.9

Maximum Deflection of Bolted Flanged Connection
With Strip Gasket Under Working Condition

mm

The structure with thick wall			The structure with reinforced shell	
location	gasket	flange	gasket	flange
δ max	- 0.0573	0.45	- 0.045	- 0.2985

3.3.2 Flange Stresses

The strength of rectangular flanged connections and vessels, under working conditions, is evaluated in terms of stress distributions of the structures. In the same way as for deflection analysis, the stress results are organized with respect to the different types of gaskets used.

3.3.2.1 O-ring Gasket Flanged Connection

The distributions of tangential stress, σ_x , of the rectangular flanged vessel structure with O-ring gasket connection are illustrated in Figure 3.14 (a) and (b), for bolt preloads of 62.3 KN and 89.0 KN respectively. The internal pressure applied is of 2,070 KPa. The stress profiles are shown in the YOZ plane at X=0 where the maximum stress values are identified. Figures 3.14 (b) shows the longitudinal stress profile σ_z , of the O-ring gasket flanged connection. Table 3.10 summarizes the stress results of the O-ring gasket structure under the working loadings.

A comparison of the stress results with those due to bolt preload alone in Figure 3.2 reveals that the internal pressure dominates both, tangential and longitudinal stress values, in the same way as in the deflection results. The highest stress level is 171.9 MPa (24.9 ksi), on the rectangular vessel wall along the longitudinal direction.

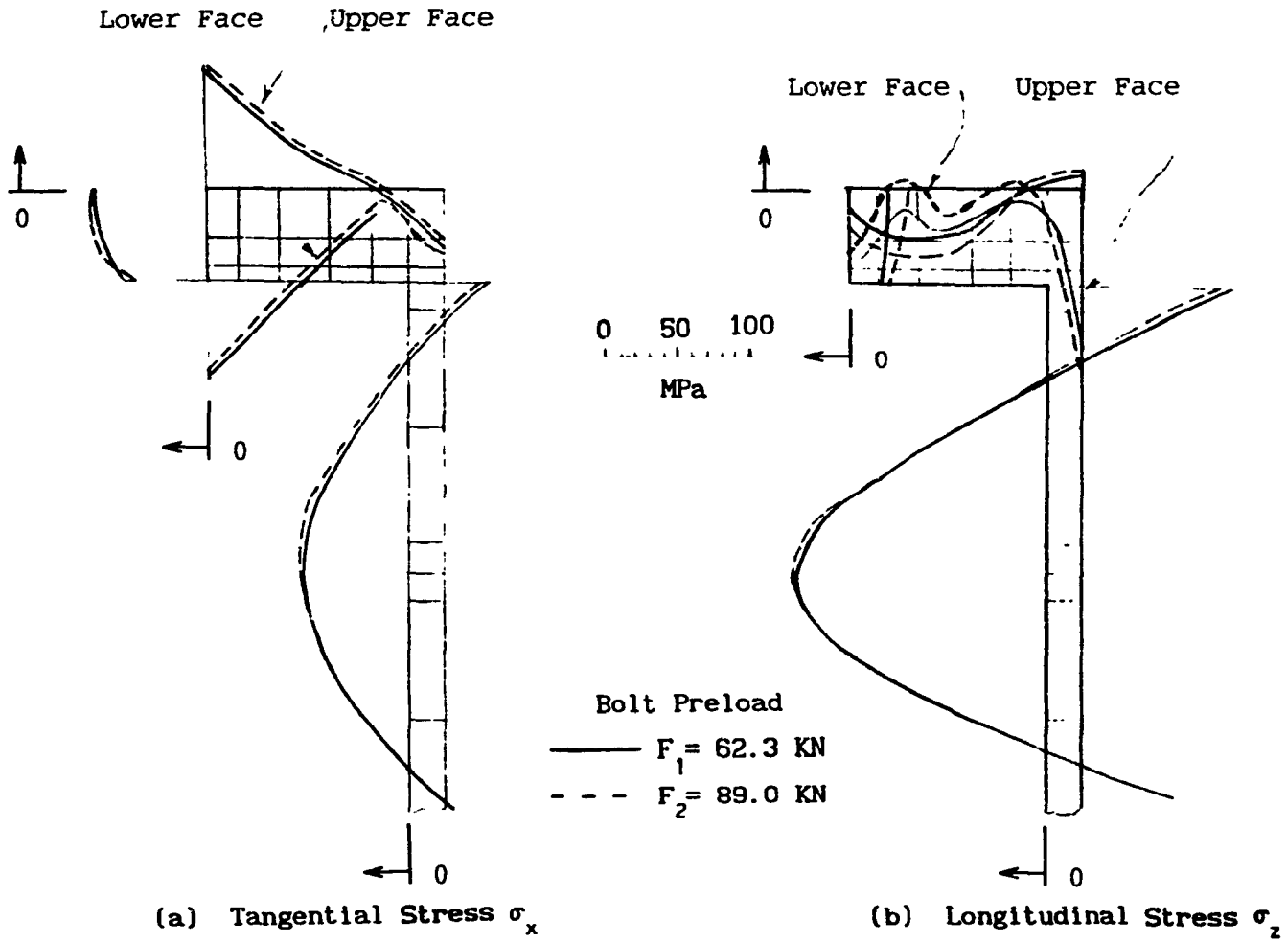

Figure 3.14 Stress of Bolted Flanged Connections with O-ring Gasket under Working Condition

TABLE 3.10

Stress Summary of Bolted Flanged Connection With O-ring Gasket Under Working Condition

MPa

element #		6	12	19	22
F_1	σ_x	75.3	72.5	- 56.4	74.5
	σ_z	- 29	- 25.5	- 130.3	171.9
F_2	σ_x	78.6	74.4	- 55.5	74.7
	σ_z	- 40	- 36.2	- 129	171.9

F_1 = 62.3 KN

F_2 = 89.0 KN

σ_x = tangential stress

σ_z = longitudinal stress

3.3.2.2 Full face Gasket Flanged Connection

The tangential stress profiles σ_x, for the full face gasket flanged structure with thick vessel wall are presented in Figure 3.15 (a) for both bolt preload values, while Figure 3.15 (b) shows the longitudinal stress profiles σ_z. The stress profiles for the reinforced thin wall vessel with full face gasket are shown in Figures 3.16 (a) and (b), for tangential stresses σ_x and longitudinal stresses σ_z, respectively. A summary of the stress analysis results is presented in Table 3.11.

As can be seen from the stress results, the internal pressure dominates the maximum stress levels of the flanged structure. The gasket stresses are, however, mainly dependent on the bolt preload. It also shows that the maximum stress is of 99.3 MPa (14.4 ksi) occurs on the thick vessel wall along the longitudinal center line. In

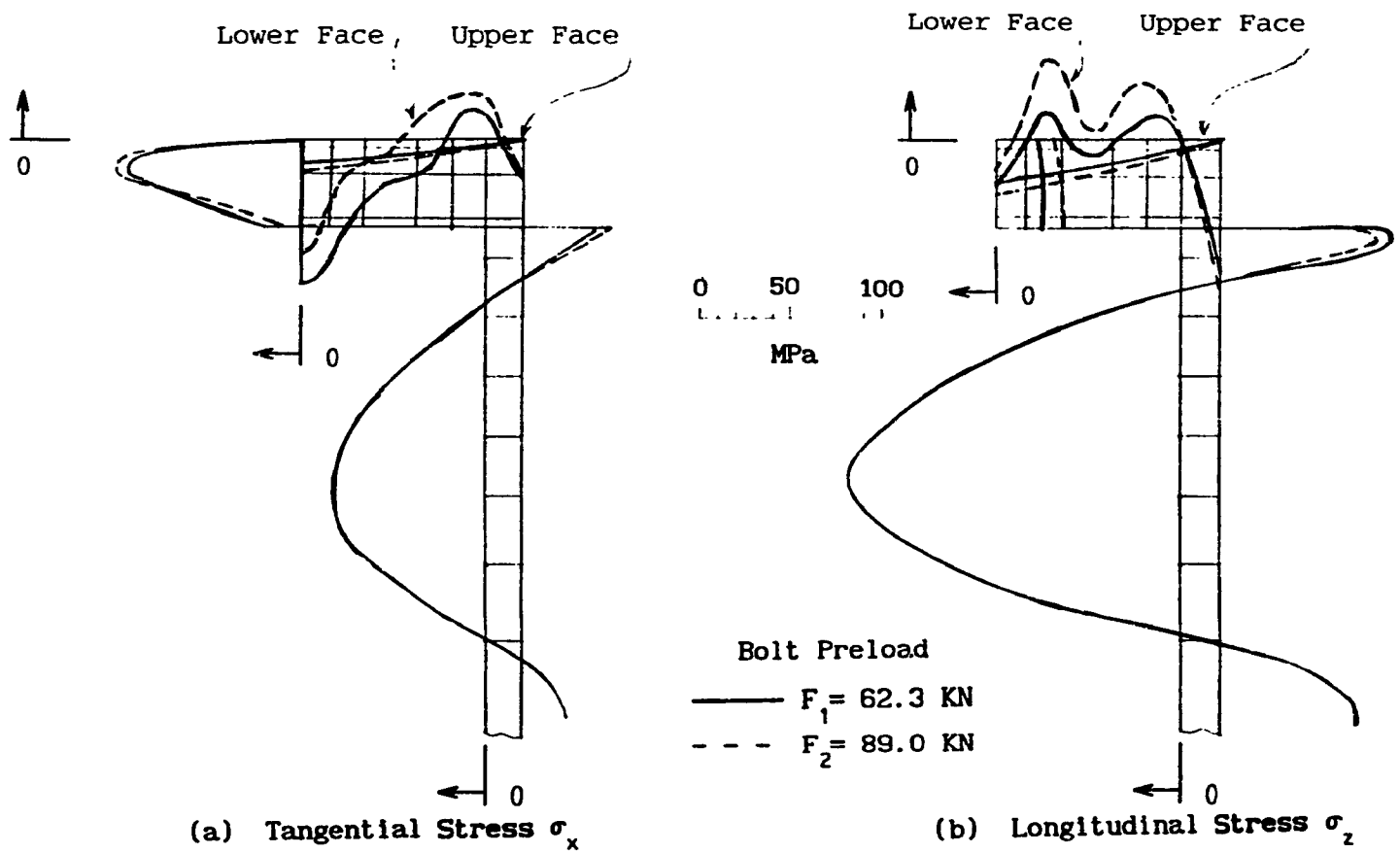

Figure 3.15 Stress of Bolted Flange on Thick Walled Vessel with Full Face Gasket under Working Condition

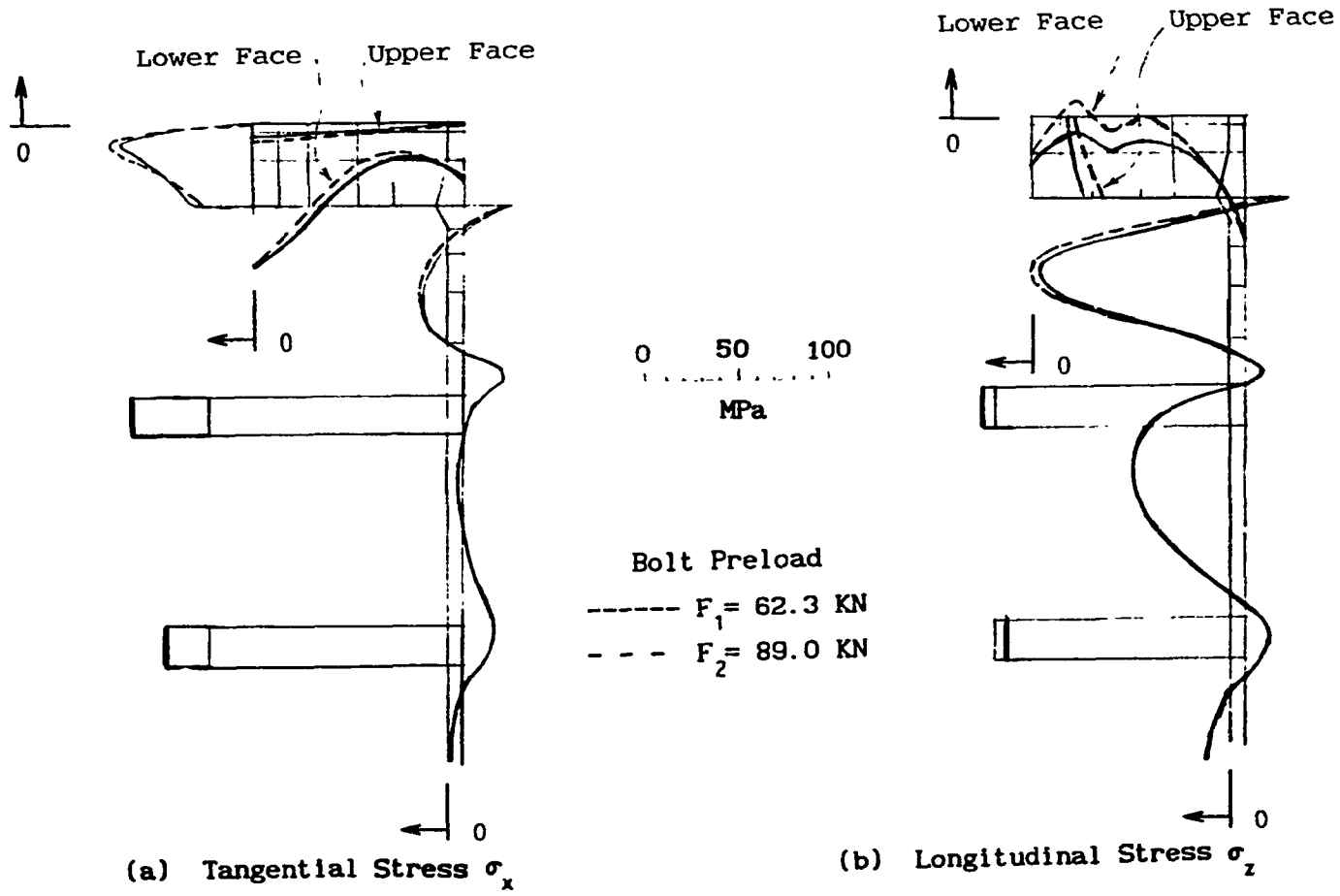

Figure 3.16 Stress of Bolted Flange on Rib-reinforced Walled Vessel with Full Face Gasket under Working Condition

reinforced thin wall structure, however, the corresponding maximum stress value reducesto 76.8 MPa (11.1 ksi).

TABLE 3.11

Stress Summary of Bolted Flanged Connection With Full Face Gasket Under Working Condition

MPa

		thick wall model		reinforced shell model	
location		gasket	flange	gasket	flange
F_1	σ_x	- 7.85	89.8	- 7.03	66.3
	σ_z	- 20.2	- 22.3	- 18	- 20.1
F_2	σ_x	- 10.4	99.3	- 9.6	76.8
	σ_z	- 26.6	- 29.85	- 24.5	- 27.6

F_1 = 62.3 KN

F_2 = 89.0 KN

σ_x = tangential stress

σ_z = longitudinal stress

3.3.2.3 Strip Gasket Flanged Connection

The profiles of tangential σ_x and longitudinal σ_z stresses, for the flanged thick wall vessel structure with strip gasket are shown in Figures 3.17 (a) and (b), respectively. The bolt preload used is of 44.4 KN, while the internal pressure applied is of 2,070 KPa. The stress profiles are shown in the YOZ plane at X=0, where the maximum stress values are identified. Figures 3.18 (a) and (b) illustrate the stress profiles for the reinforced thin vessel wall structure with strip gasket connections. Table 3.12 summarizes the

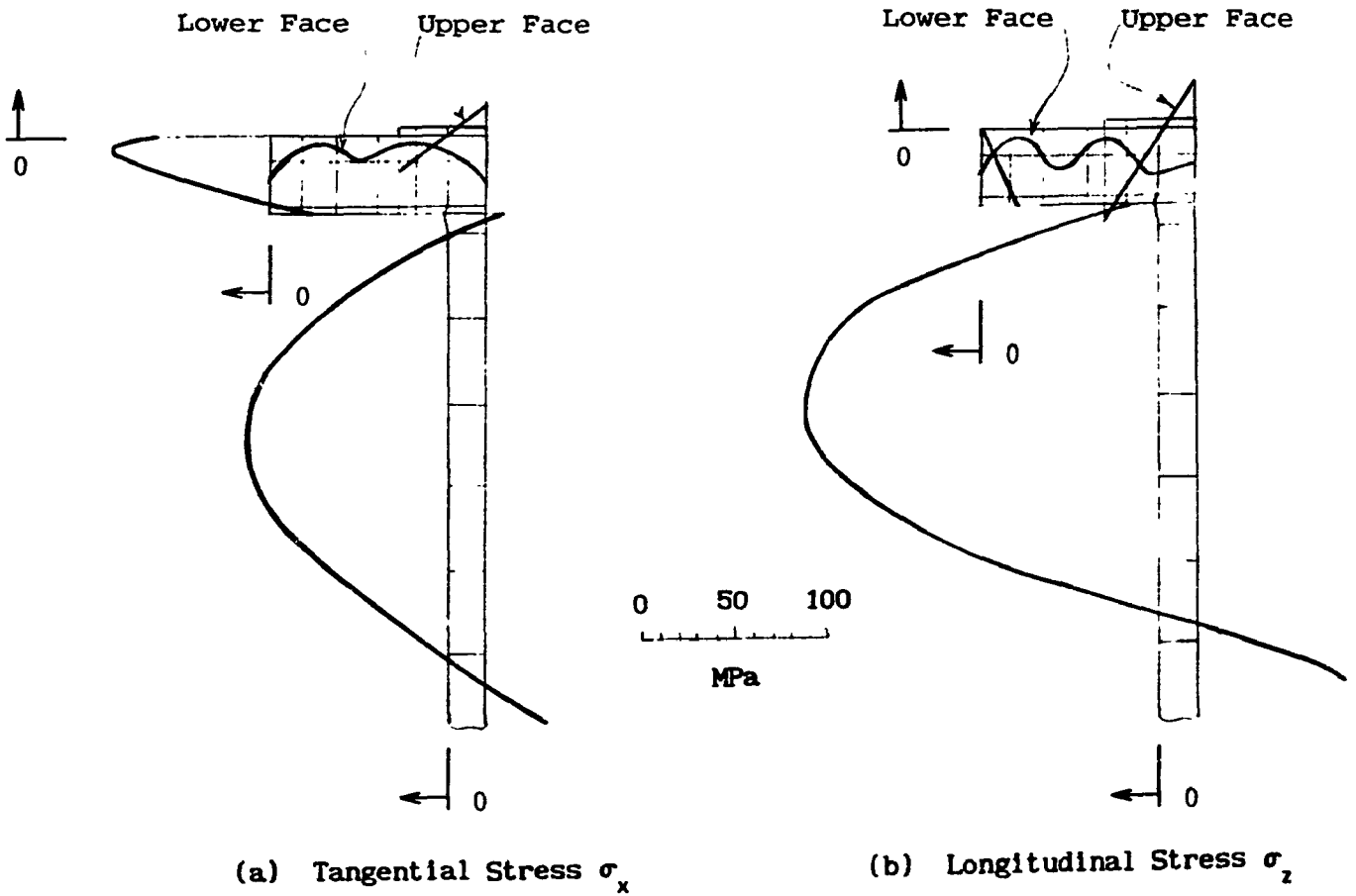

(a) Tangential Stress σ_x

(b) Longitudinal Stress σ_z

Figure 3.17 Stress of Bolted Flange on Thick Walled Vessel with Strip Gasket under Working Condition

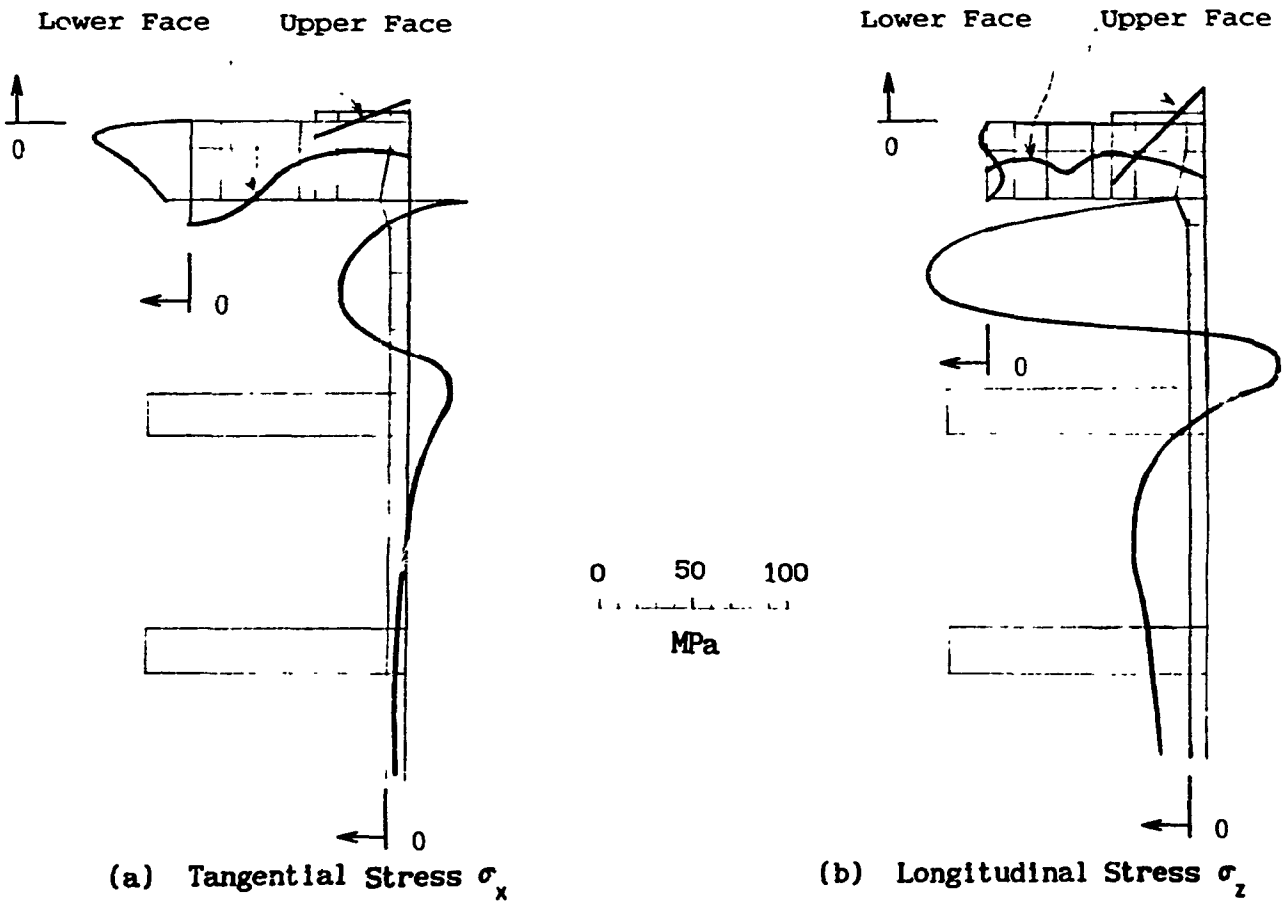

Figure 3.18 Stress of Bolted Flange on Rib-reinforced Vessel with Strip Gasket under Working Condition

stress results for the strip gasket flanged structure under the working conditions.

A comparison of the stress results of the two structural models with strip gasket shows that the maximum tangential stress σ_x of the thick wall vessel is of 107.8 MPa (15.6 kpsi). For the rib reinforced thin wall vessel, this stress reduces to 28.6 MPa (4.15 kpsi), shifting the maximum tangential stress value of 54.7 MPa (7.9 kpsi) to the flange instead. For the longitudinal stress, the location of the maximum stress levels for both vessels is similaras can be seen in Table 3.12.

As further comparison with stress results due to bolt preload alone, as shown in Figures 3.8, 3.9, and Table 3.6, it can be observed that the bolt preload has a strong influence on the longitudinal stress σ_z for the rectangular strip gasket vessel structure. For the thick wall case the maximum stress σ_z in the vessel wall due to the combined working loading is 191.9 MPa (27.8 kpsi); while the bolt preload alone contributes the stress of 113.2 MPa (16.4 kpsi). For the reinforced thin wall case, the bolt preload contribution to the stress level is 130.7 MPa (18.9 kpsi) out of the maximum stress of 185.9 MPa (26.9 kpsi) under the working loadings, which is up to 70% of the maximum longitudinal stress.

TABEL 3.12

Stress Result Summary of Bolted Flanged Connection
With Strip Gasket Under Working Condition

MPa

location		gasket	flange	bolt line	shell
thick wall model	σ_x	- 17	84.57	- 39.8	107.8
	σ_z	- 43.3	- 30	- 35.76	191.9
reinforced wall model	σ_x	- 12.3	54.7	- 18.9	28.6
	σ_z	- 31.45	- 1.86	- 18.3	185.9

σ_x = tangential stress

σ_z = longitudinal stress

3.4 Parametric Analysis of Flanges

A preliminary parametric study of the rectangular bolted flanged structures is presented in this section. The relative sensitivity of the design parameters with respect to the structural properties is briefly discussed. The parameters considered in this study include the flange thickness, vessel wall thickness, bolt preload, and rib reinforcement parameters.

3.4.1 Flange Thickness Influence

The influence of the flange thickness values on maximum stresses of the rectangular bolted connections is analyzed for both thick wall and reinforced thin wall structures. The full face and strip gasket connections are employed in the finite element models. The sizes of

the flange thickness are varied with reference to the values used for experiment (as discussed in Chapter 4), which are from 13 mm to 25 mm.

3.4.1.1 Structures With Full Gasket

The maximum stresses in the thick wall vessel structure with full face gasket due to the variation in flange thickness are shown in Figure 3.19. Both maximum tangential σ_x and longitudinal σ_z stresses are found to be in the vessel walls. When the flange thickness is decreased both σ_x and σ_z stresses are increased. Figure 3.20 illustrates the changes of maximum stresses in the reinforced thin wall structure with respect to changes in flange thickness. It can be seen that the maximum longitudinal stress in the vessel structure is comparatively more sensitive to the reduction of the flange thickness. When the flange thickness value is further reduced the stress on the flange will become the maximum value.

3.4.1.2 Structures With Strip Gasket

The maximum stresses in rectangular bolted flanged vessels employing a strip gasket with variation in flange thickness are shown in Figure 3.21 for thick wall, and in Figure 3.22 for reinforced thin wall vessels, respectively. It can be observed that the maximum stresses will decrease when the flange thickness is increased; while the changes in maximum longitudinal stress σ_z are relatively unaffected.

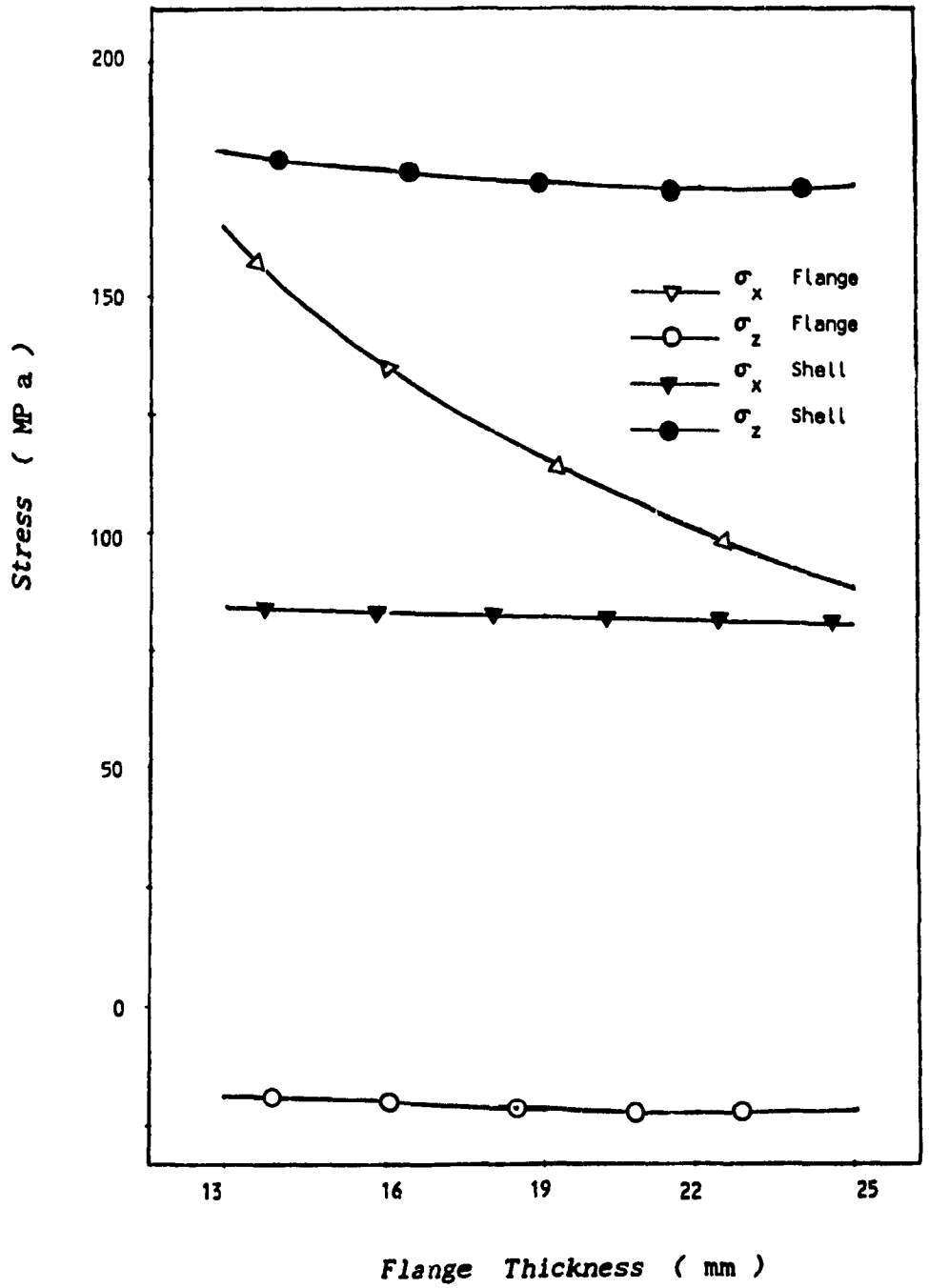

Figure 3.19 Maximum Stress of Bolted Flange on Thick Walled Vessel with Full Face Gasket due to Flange Thickness Variation

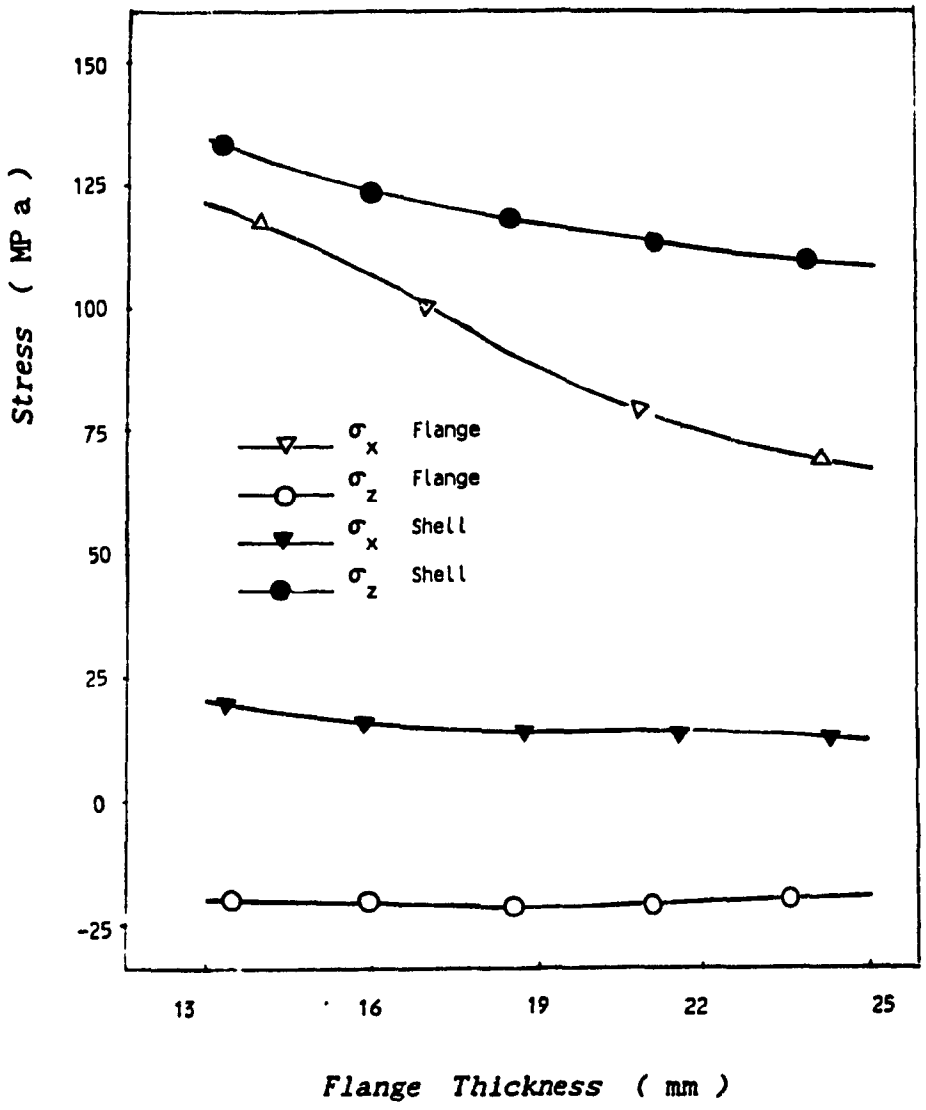

Figure 3.20 Maximum Stress of Bolted Flange on Rib-reinforced Vessel with Full Face Gasket due to Flange Thickness Variation

In a comparison of the results in Figures 3.21 and 3.22 for the strip gasket and in Figures 3.19 and 3.20 for full face gasket, it can be seen that the maximum stress of the vessel with strip gasket is much more sensitive to flange thickness changes. In other words, the maximum stress level is strongly related to the type of gasketemployed. The vessel structure with strip gasket will yields a larger stress value than other types of gasket when subjected the same loading conditions.

3.4.2 Vessel Wall Thickness Influence

The change of maximum stresses in the thick wall vessel structure with full face gasket due to the variation in vessel wall thickness is illustrated in Figure 3.23. It is shown that both tangential σ_x and longitudinal σ_z maximum stresses are increased as the wall thickness is reduced. Especially when the thickness value is less than 10 mm the rate of change in stress increase in the vessel shell is very much significant. On the other hand the maximum stress in the flange is much less sensitive to shell thickness change than that of the vessel wall stress.

Figure 3.24 shows the influence of the wall thickness on the maximum stresses in the reinforced thin wall structure. It is clear that the tendency of the change in stresses is almost the same as that of the thick wall case. A too thin vessel wall will yield a stress level greater than the allowable stress value of the material, which, if the yield strength of the material is exceeded, will then lead to

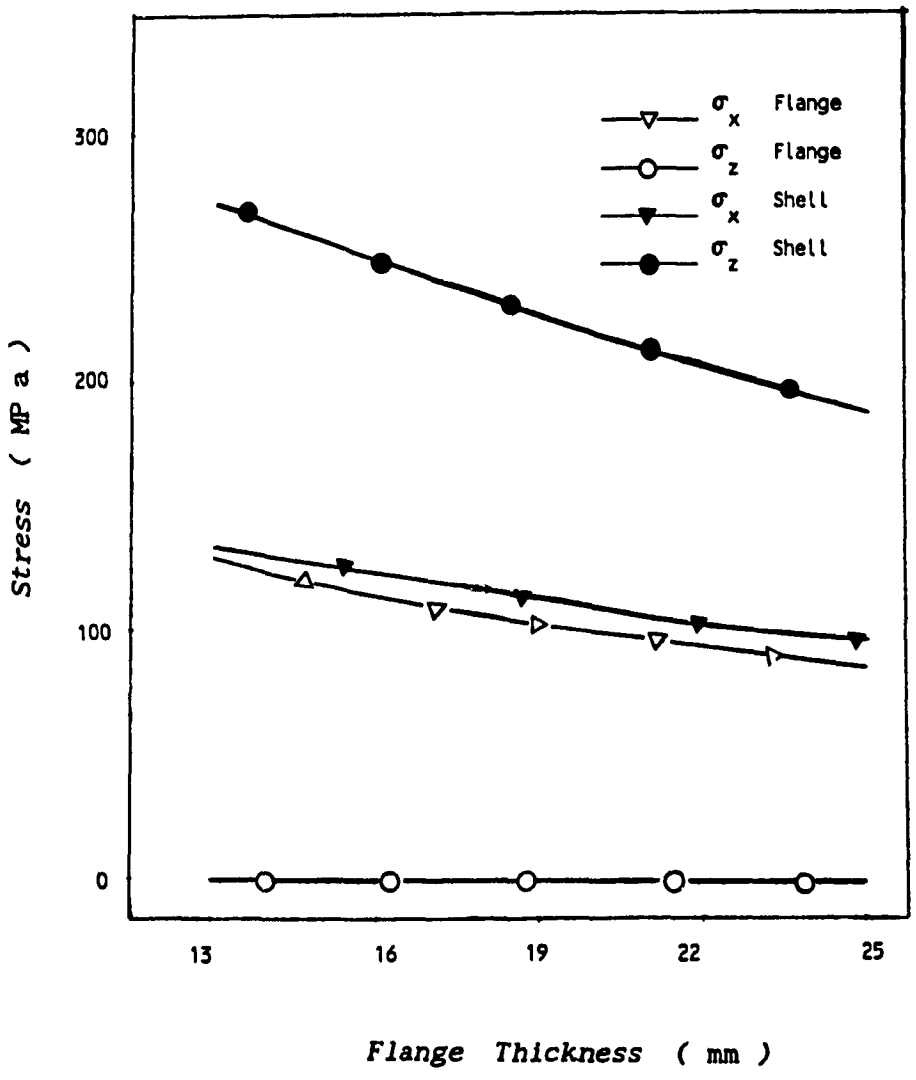

Figure 3.21 Maximum Stress of Bolted Flange on Thick Walled Vessel with Strip Gasket due to Flange Thickness Variation

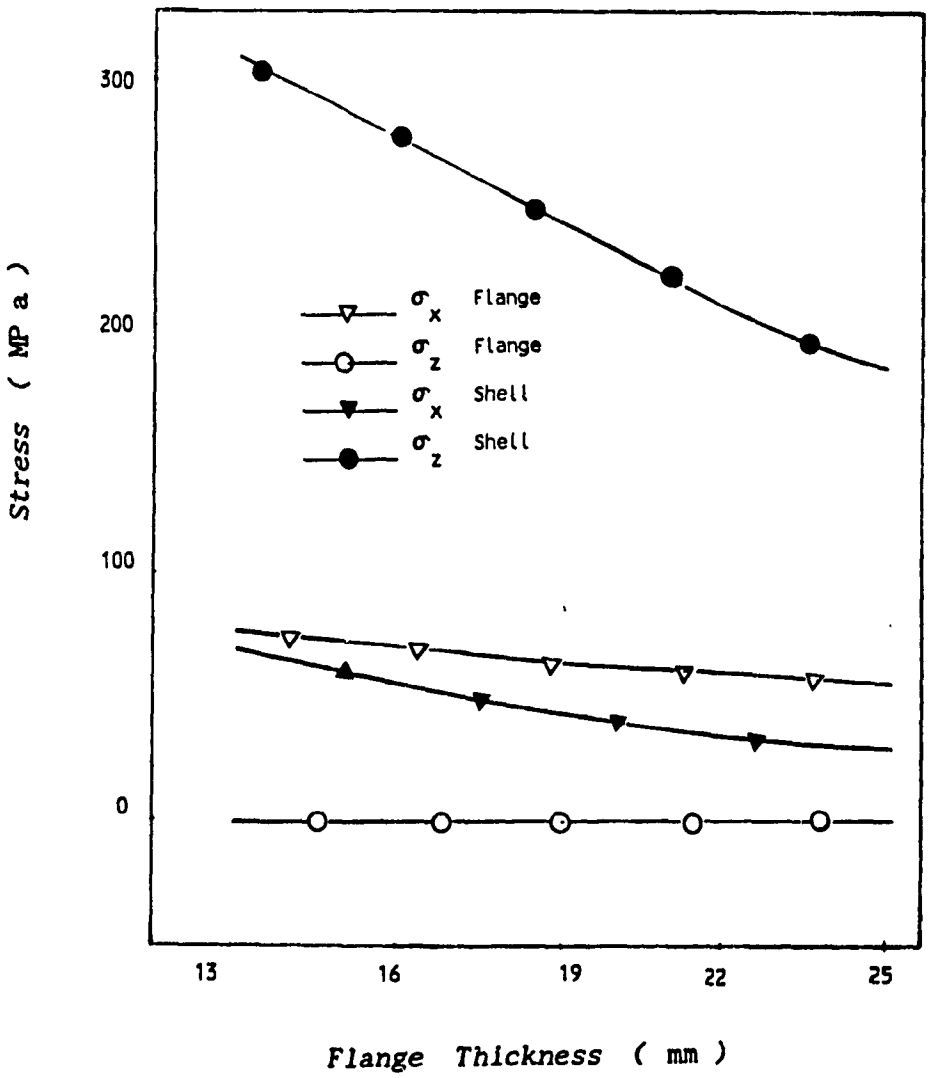

Figure 3.22 Maximum Stress of Bolted Flange on Rib-reinforced Vessel with Strip Gasket due to Flange Thickness Variation

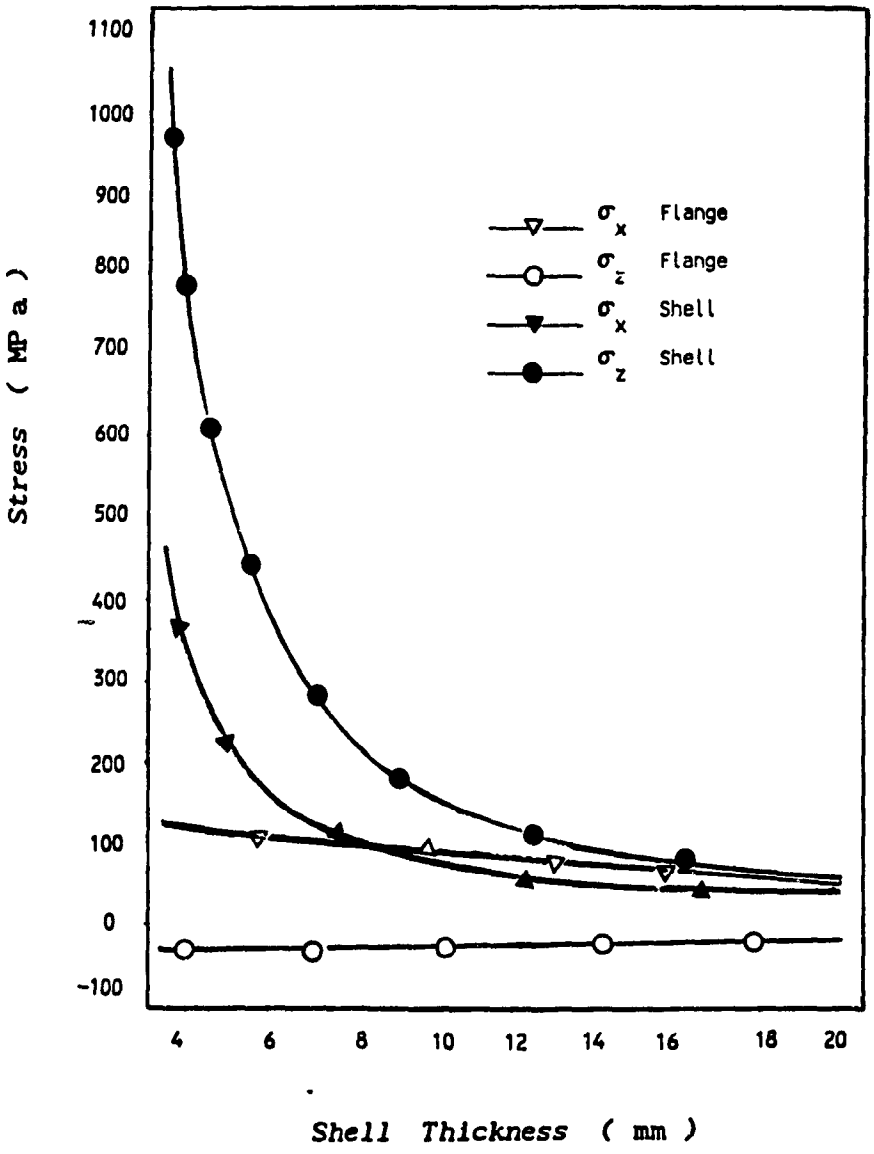

Figure 3.23 Maximum Stress of Bolted Flange on Thick Walled Vessel with Full Face Gasket due to Vessel Thickness Variation

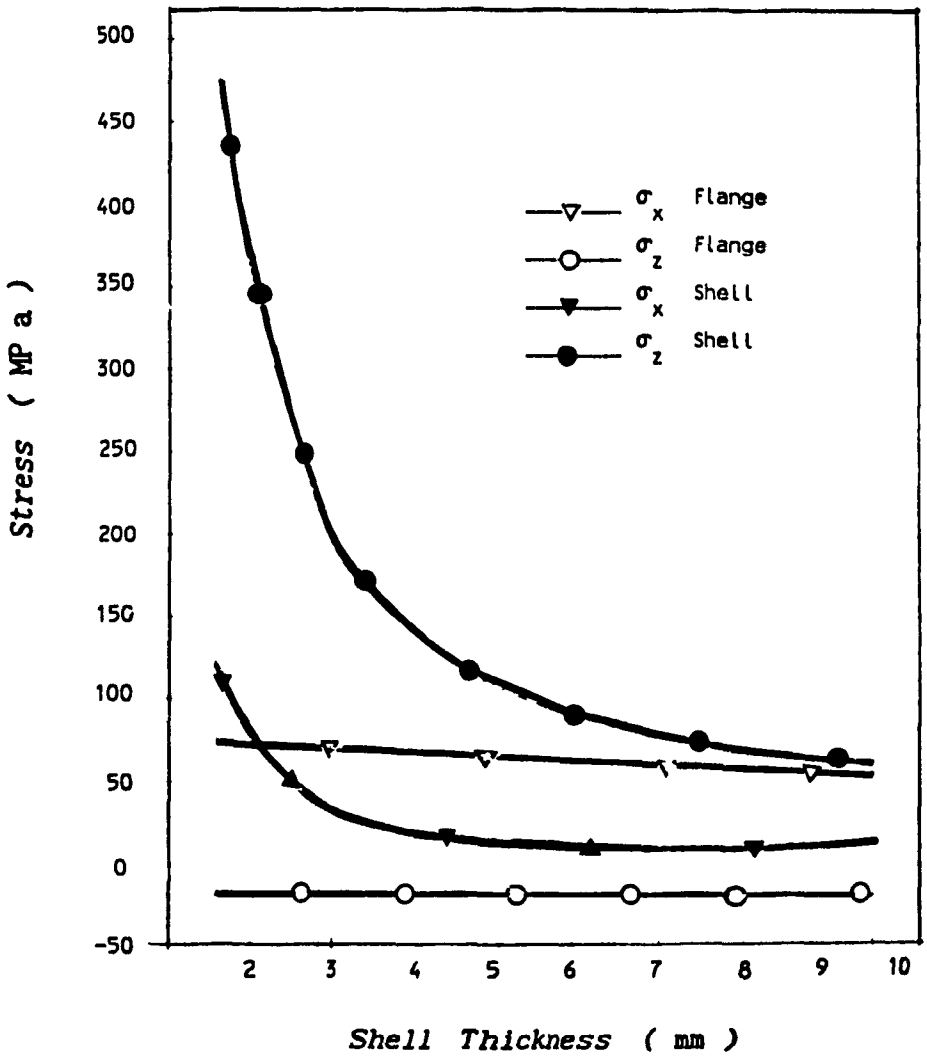

Figure 3.24 Maximum Stress of Bolted Flange on Rib-reinforced Vessel with Full Face Gasket due to Vessel Thickness Variation

failure of the vessel.

3.4.3 Influence Due to Reinforcement Parameters

The parameters presented in this section include the influence of the size of rib reinforcement and the distance between ribs on the maximum stresses of the reinforced thin wall vessel structure.

3.4.3.1 Rib Size

Figure 3.25 shows the change of the maximum stresses in the bolted flanged structure due to the change in rib size. The height of the rib is fixed while the width of the rib is varied with respect to the original size, from the ratio of 1/3 to 2. It is observed that when the rib width value is relatively small, the maximum stress level in the thin wall vessel is lower; when rib width is increased the maximum stress level also increases, which can be explained in the way that when the rib reinforcement stiffness is compatible with the wall stiffness, then the maximum stress level will be lower. When the rib reinforcement is too stiff as compared with the wall stiffness, there will be a large deflection within a small area of the thin wall, a higher stress level is therefore generated.

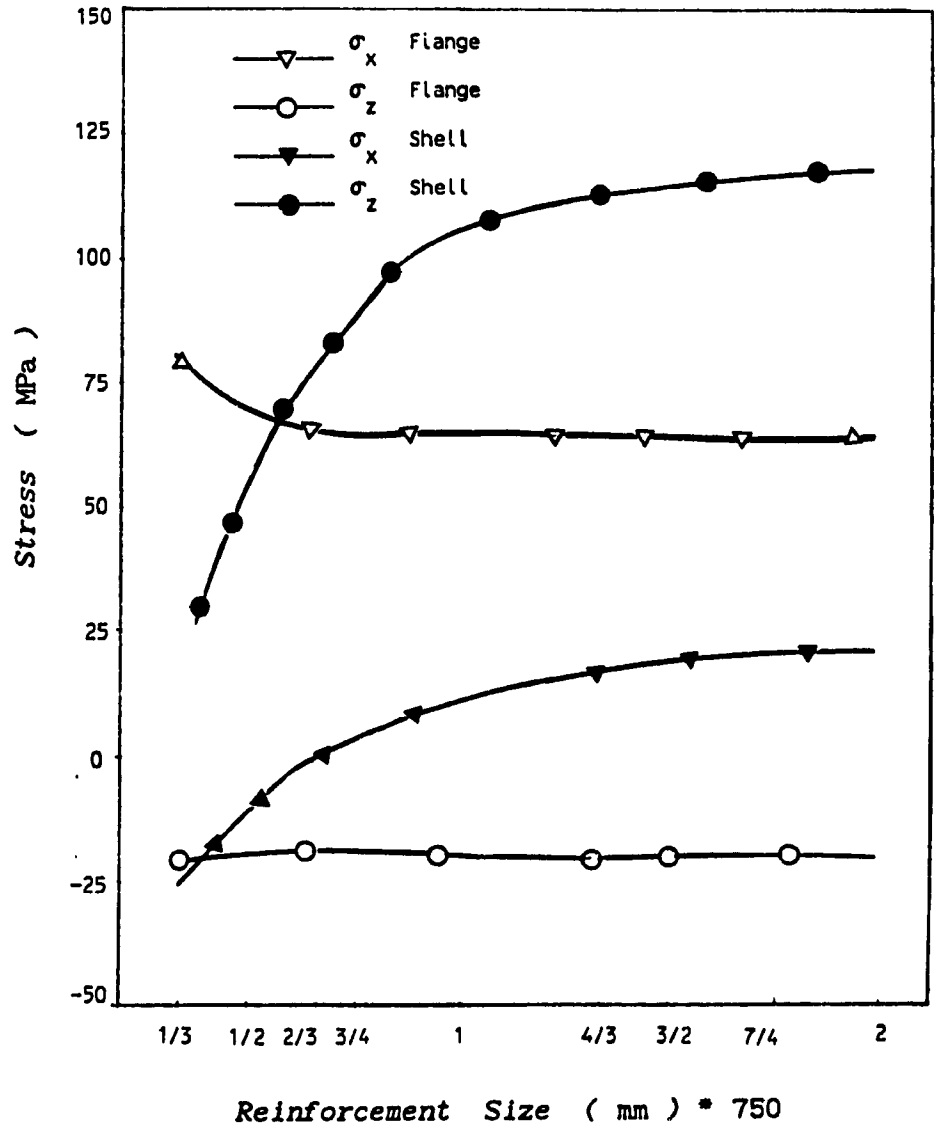

Figure 3.25 Maximum Stress of Bolted Flange on Rib-reinforced Vessel due to Variation in Size of the Reinforcements

3.4.3.2 Distance Between Reinforcement

The change of maximum stress in the rectangular flanged structure due to distance variation between reinforcements is shown in Figure 3.26. The distance varied is the distance of the first rib with respect to the flange. It can be seen that the maximum stresses in the reinforced thin wall structure are increased when the distance between the reinforcing ribs is increased. It can be also seen that the longitudinal stress σ_z is more sensitive to the distance change than the tangential stress σ_x.

3.4.4 Bolt Preload Influence

As shown in sections 3.2 and 3.3, the strip gasket structure is much more sensitive to the bolt preload than the O-ring gasket and full face gasket cases. The change of maximum stresses in the flanged vessel with strip gasket due to a change in bolt preload is shown in Figure 3.27. The preload force value varies from 4/7 of F_1 (F_1= 62.3 KN) to F_2 (F_2= 89.0 KN). It can be seen that the longitudinal stress σ_z is very much sensitive to a bolt preload increase. When the preload reaches the value of F_2 , the maximum longitudinal stress σ_z due to bolt preload alone will be very close to the allowable stress of the material.

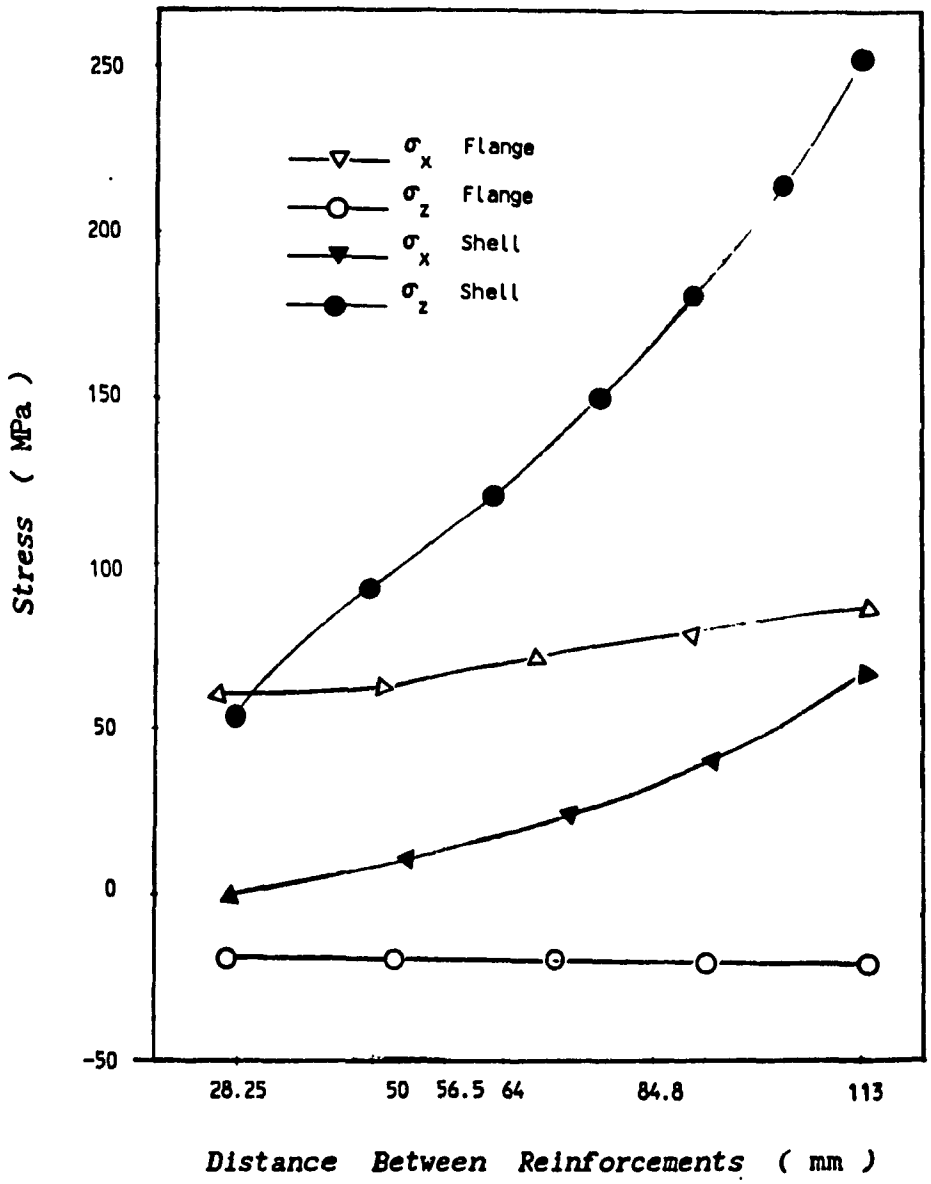

Figure 3.26 Maximum Stress of Bolted Flange on Rib-reinforced Vessel due to Variation in Distance Between Reinforcements

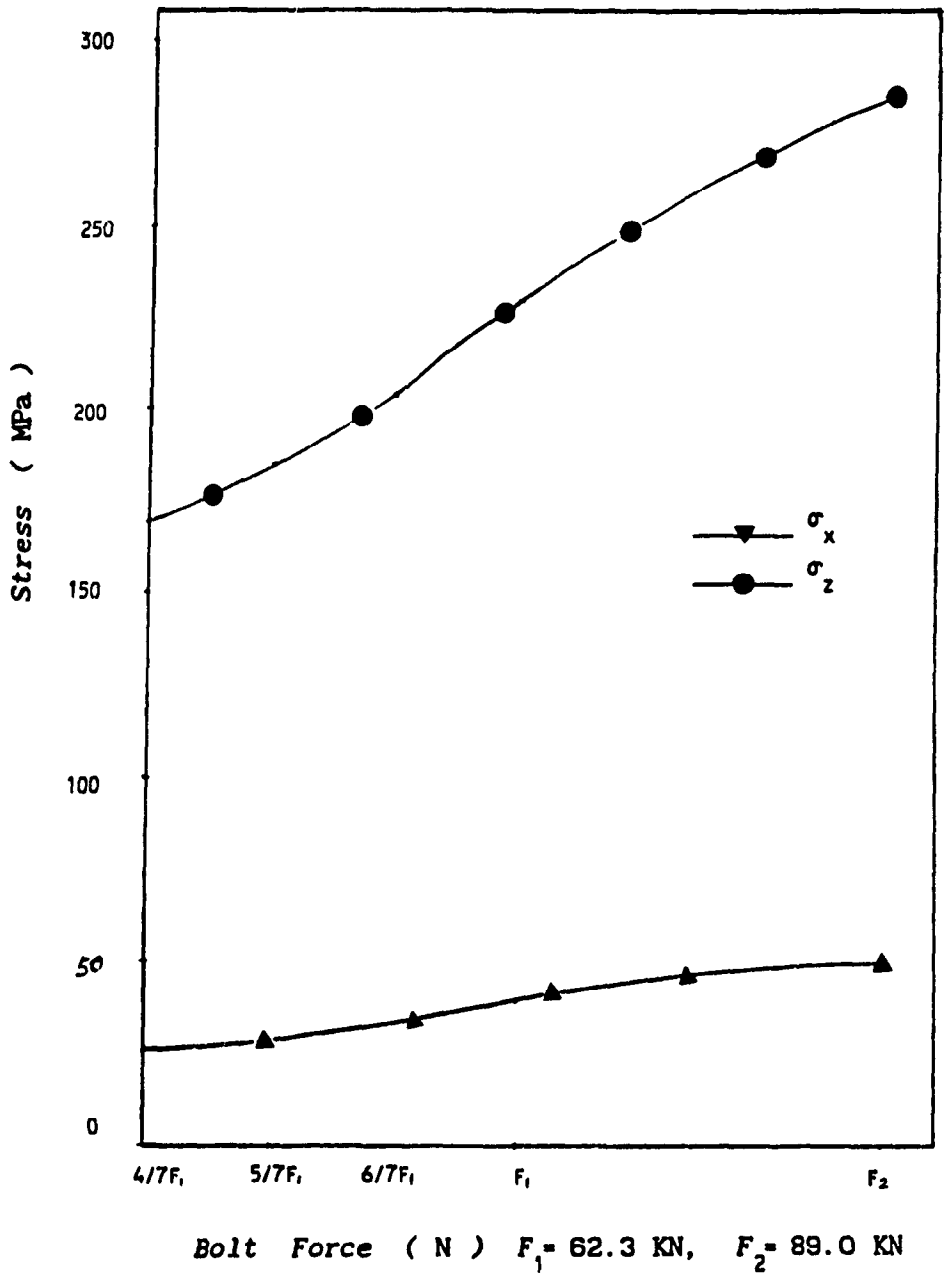

Figure 3.27 Maximum Stress of Bolted Flanged Connections with Strip Gasket due to Bolt Preload Variation

3.5 Summary

The rectangular bolted flanged connection structures are numerically analyzed by employing the finite element method. The stiffness and strength characteristics of both thick wall and reinforced thin wall flanged structures are evaluated in terms of deflection and stress profiles. Three types of gaskets are incorporated in the analysis. A brief parametric study of the bolted flanged structure is also carried out to identify the relative influence of the design parameters.

The numerical results show that the rectangular flanged structure with strip gasket is very sensitive to the bolt preload value. It is also observed that a too stiff reinforcement and too thin vessel wall will result in a high stress level in the shell of the structure.

CHAPTER 4

COMPARISON OF RESULTS WITH ANALYTICAL APPROXIMATE METHODS AND EXPERIMENTAL WORK

4.1 General

The ASME Code contains extensive rules for the design of pressure vessels and pressure vessel components, including rules for non-circular pressure vessels. There are, however, no rules for non-circular bolted flanged connections. In order to evaluate such non-circular bolted flanged connections, approximate design methods, and sometimes experimental analysis are used by pressure vessel designers.

In this chapter, some of the approximate design methods presently used by pressure vessel designers are critically reviewed and compared with strain gage measurements of rectangular bolted flanged connections. The results of both, approximate methods and experimental work, are then compared with the finite element method. The relative merits and limitations of the different methods are also discussed, based on above comparison.

4.2 Analytical Approximate Methods

There are several analytical approximate design methods which can be used in the design of non-circular bolted flanged connections. Two of these methods, preferred by pressure vessel designers, are reviewed

in this chapter. One of the methods is based on an equivalent circular flange approximation, in the case of square or nearly square flanges. The other one uses a combination of frame analysis for the flange to retain its rectangular shape, and of bending of an infinitely long flanged section in a perpendicular plain with respect to the frame. The analysis results of the rectangular bolted flanged structure by using the approximate methods are obtained and then compared with that of the finite element analysis.

4.2.1 Equivalent Circular Flange Method

The equivalent circular flange method is essentially similar in approach to the procedure presented in the ASME Code, Section VIII, Division 1, Article UG-34 [1], for the design of non-circular flat covers. In the code, a factor Z is introduced to relate a flat cover of rectangular shape to a circular one. The factor Z is defined as:

$$Z = 3.4 - \frac{2.4\ b}{a} \qquad (4.1)$$

with the limitation that Z does not need to be larger than two and a half, ($Z \leq 2.5$), and where a and b are length and width of the rectangular shape, respectively. The square root of the factor Z is used as a multiplier of the small side of the rectangular cover to obtain an equivalent diameter B to be used in the formula for the cover thickness.

$$B = b\sqrt{Z} \qquad (4.2)$$

It can be seen, by comparing square and rectangular cover stress

factors with equivalent circular cover factor, that for a welded flat cover, this approach yields a cover thickness on the safe side. In the case of a rectangular cover with little fixation at the rim (thin vessel, thick cover), from Roark and Young [26], the factor β in the stress equation of the cover

$$\sigma = \beta \, p \left[\frac{b}{t}\right]^2 \tag{4.3}$$

is 0.287 for a square plate and approaches 0.750 for a long rectangular plate with length-to-width ratio $a/b > 4$. Using the Code formula for rectangular plates, a comparison can be made with the factors given in equation (4.3). Equating the stresses from both formulas given by [1] and [26] yields,

$$\sigma = \beta \, p \left[\frac{b}{t}\right]^2 = c \, Z \, p \left[\frac{b}{t}\right]^2 \tag{4.4}$$

It can be seen that the factors β and cZ should have the same values. In fact, using the Code constant $c = .33$ and the appropriate values for Z, the product cZ is always numerically larger than β, hence the Code formulas yield results on the safe side.

In the equivalent circular flange method, the square root of factor Z is used as a multiplier for the small side of the rectangular pressure vessel and thus an equivalent circular shape is obtained. Any obround or rectangular flange can then simply be designed and analyzed as equivalent circular flange, and all flange design Code rules per Appendix 2 or Appendix Y of the ASME Code [1] are applicable without modification.

In the case of full face gaskets, often used with rectangular flanges, no ASME Code rules exist at present. References [33] by Blach et al. and [36] present flange design methods for the full face gasketed bolted flanged connection.

The application of the equivalent circular flange method a the rectangular flange of 200 × 300 mm (8 × 12 inch) is illustrated in Figure 4.1. The equivalent circular flange is superimposed over the rectangular one. The factor Z of the rectangular shape is obtained per equation (4.1),

$$Z = 3.4 - \frac{(2.4)(200)}{300} = 1.8 \qquad (4.5)$$

The equivalent inside diameter of the circular flange is then calculated per equation (4.2),

$$B = (200)\sqrt{1.8} = 268 \text{ mm} \qquad (4.6)$$

The bolt circle and outside diameters are then obtained by adding of the actual bolt location distance and the flange width to the equivalent inside diameter, respectively, as shown in figure 4.1.

This method, which apparently has never been verified, seems to yield a safely designed rectangular flange if the length to width ratio is close to unity, that is, for "almost square" rectangular geometry. For long rectangular flanges with length to width ratios of over two (2), however, there is no more resemblance in the behaviour of the rectangular flange when compared with a circular flange. This fact is acknowledged by designers, and length to width ratio limit of

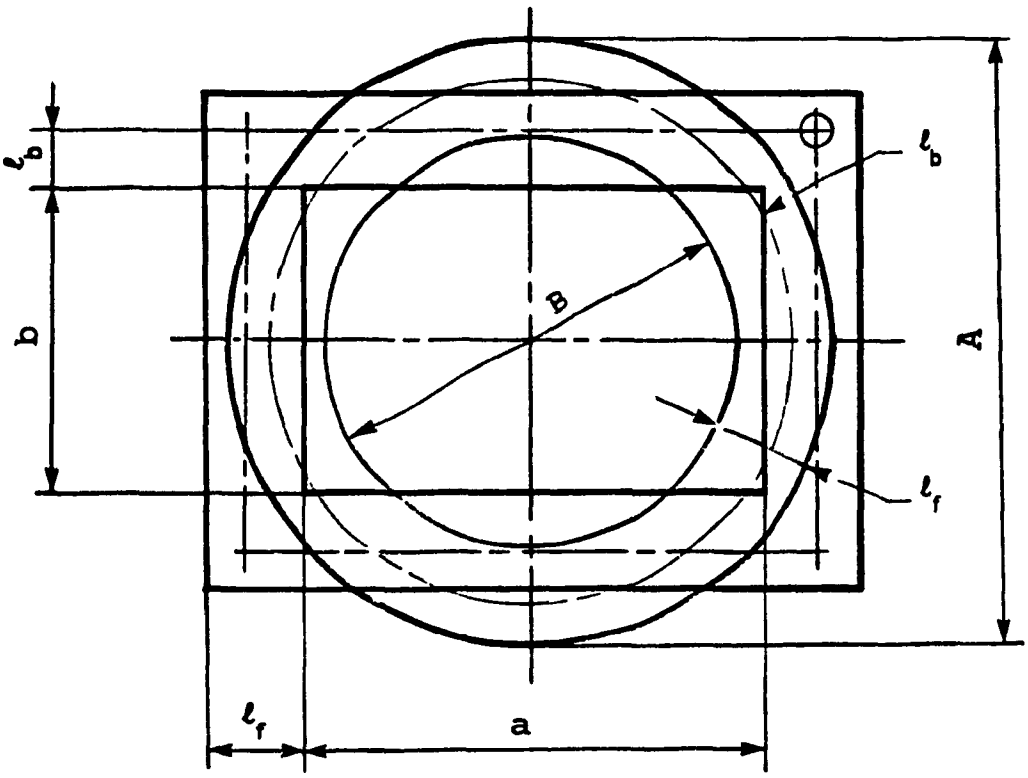

Figure 4.1 An Equivalent Circular Flange

1.6 is usually applied.

For rib-reinforced rectangular vessels, however, this method does not seem to properly account for frame bending stresses present in such flanges. In unreinforced rectangular vessels frame bending stresses are absorbed in the vessel walls.

4.2.2 Frame Bending Flange Design Method

The equivalent circular flange method discussed in section 4.2.1, in addition to limitations on length-to-width ratio, is applicable only for unreinforced non-circular pressure vessels where the frame bending stresses are fully absorbed by the pressure vessel side plates. A large percentage of non-circular pressure vessels, however, are of reinforced type as shown in Figure 4.2. In this case, the flange must also act as stiffener for the vessel side plates, as well as to provide a tight seal between components. Such flanges thus have to resist, in addition to flange bending stresses in planes parallel to the vessel axis, the frame bending stresses in a plane perpendicular to this axis.

The two bending stresses of the reinforced rectangular flange, that is, the frame bending and flange bending stresses, are obviously the result of biaxial loading and should, therefore, not really be separated. Most designers, however, add these two stresses in order to compute a safe flange thickness. This procedure is thus considered to yield a flange design on the safe side.

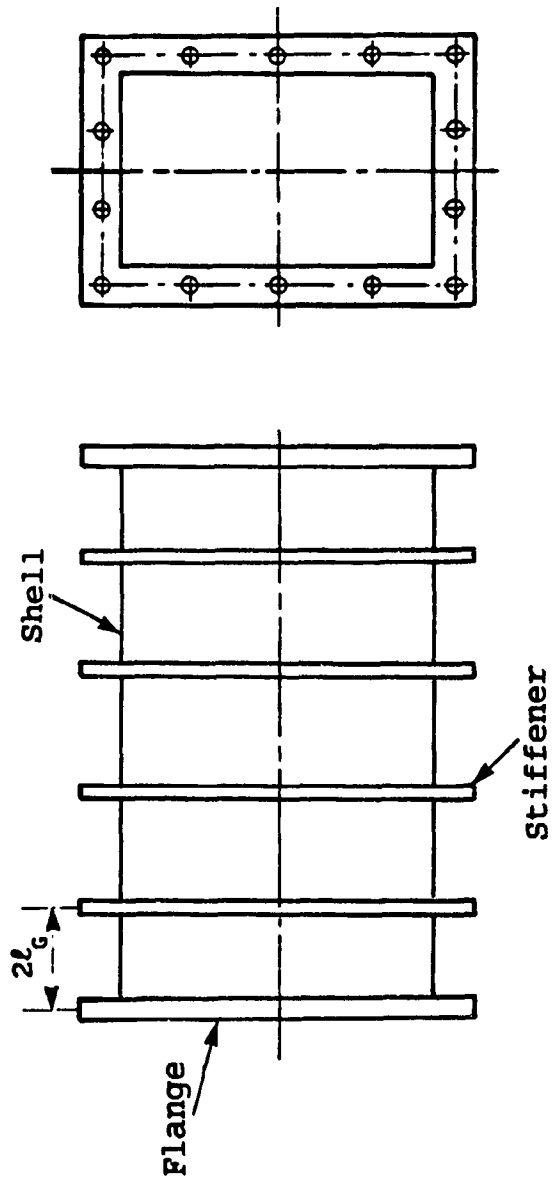

Figure 4.2 Reinforced Non-circular Pressure Vessel

Frame Bending Stresses

The frame bending stresses of a rectangular flange of uniform thickness can be found by structural analysis. For rectangular frames of uniform cross section, that is, flanges with uniform width, the corner moment M_A, due to uniformly distributed loading w, is given by

$$M_A = \frac{w}{12} \frac{\ell_1^3 + \ell_2^3}{\ell_1 + \ell_2} \tag{4.7}$$

And the bending moment M_B, at the center of the long span of the frame are expressed as

$$M_B = \frac{w\ \ell_1^2}{8} - M_A \tag{4.8}$$

Owhere ℓ_1 and ℓ_2 are the length dimensions taken between the centroid of the flange sections, or of the flange shell junction if part of the connecting shell is included in the calculation, as illustrated in Figure 4.3. When flanges are of unequal width, a stiffness factor must be included in equation (4.7), which may be obtained using the "three moment equation".

The maximum frame bending stress σ_f, with respect to the elastic section modulus S of the flange, can then be calculated by

$$\sigma_f = \frac{M}{S} \tag{4.9}$$

Flange Bending Stresses

The flange bending stresses due to bolt-up and operating pressure for a long rectangular flange (a/b > 2) can be approximated by considering a unit width of flange at the center of the longer side.

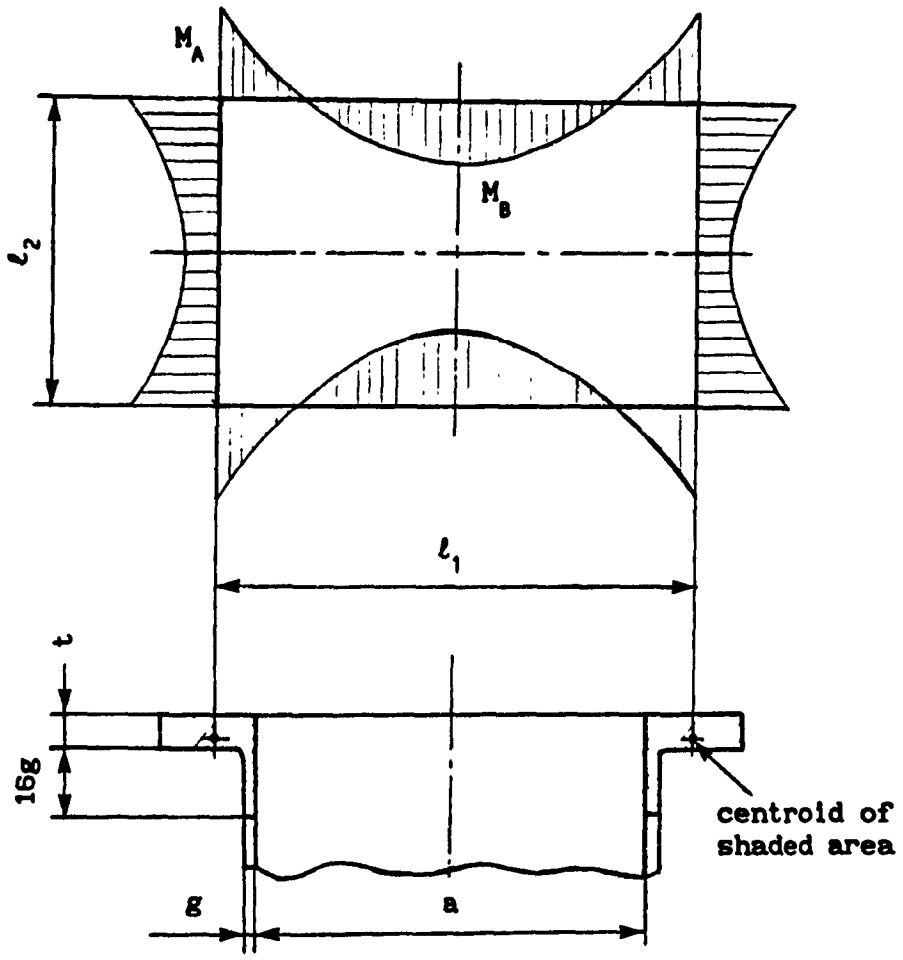

Figure 4.3 Frame Bending Moments and Stresses

Though the pressure distribution in such a flange is not uniform, the maximum stress is known to occur at this point.

To calculate the stress at the center of the longer side, it is convenient to introduce a factor β which can be taken from the stress distribution of a rectangular plate with fixed end conditions, as presented in [26] and other books on structural analysis. This factor β varies numerically from 0.308 for a/b = 1 to 0.500 for a/b > 2.

For flanges used with strip gaskets which are fully inside the flange bolts, as shown in Figure 4.4, the flange bending moment per unit length is given by

$$M_o = H_D\, h_D + H_G\, h_G + H_T\, h_T \qquad (4.10a)$$

or

$$M_o = \beta\, b\, P\, h_D + 2\, \ell\, m\, P\, h_G + (g - b)\, P\, h_T \qquad (4.10b)$$

For flanges used with full face gaskets, as shown in Figure 4.5, the gasket compression on the outside of the flanges provides some resistance against rotation. This resistance has been included in the flange bending moment by using the flange design method described in [33]. The flange bending moment per unit length for full face gasket can be then given by

$$M_o = \frac{\alpha}{1 + \alpha} \left[H_D\, h_D + H_T\, h_T \right] \qquad (4.11a)$$

or

$$M_o = \frac{\alpha}{1 + \alpha} \left[\beta\, b\, P\, h_D + \frac{1}{2} \left[c - b - d \right] h_T \right] \qquad (4.11b)$$

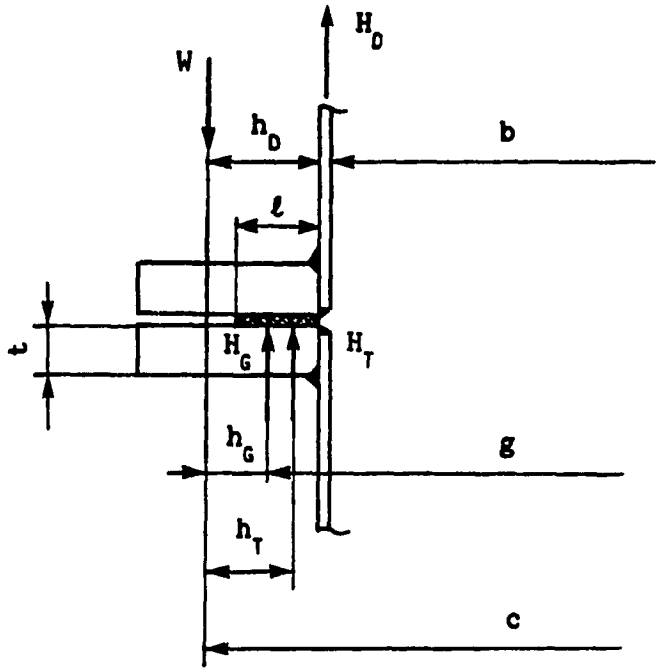

Figure 4.4 Flange Bending with Strip Gasket

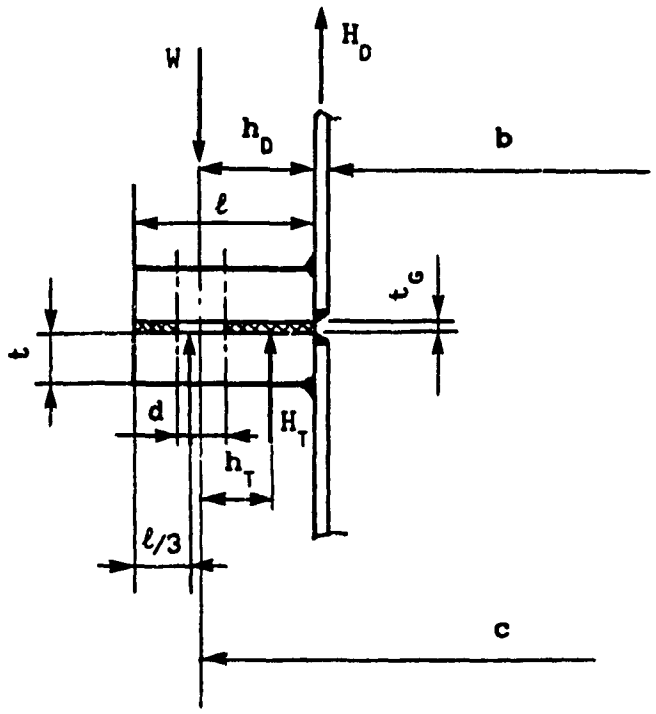

Figure 4.5 Flange Bending with Full Face Gasket

where

$$\alpha = \frac{E\, t^3\, t_G}{8\, E_G\, \ell^4} \tag{4.12}$$

E is the elasticity modulus of flange material, E_G is the elasticity modulus of the gasket. The moments in equations (4.10) and (4.11) must be resisted by a unit width of the flange, assuming that the connecting strip of shell plate is in direct tension only. This assumption is based on the fact that the shell plate attached to a rectangular flange is usually much thinner and thus more flexible than the flange. The same reasoning is made by the ASME Code in the case of the "loose optional flange", where the contributions of connecting shell in resisting bending are neglected.

The section modulus of a rectangular section of unit width can be expressed as

$$S_u = \frac{t^2}{6} \tag{4.13}$$

The flange bending stress in the rectangular flange can thus be calculated by

$$\sigma_b = \frac{6\, M_o}{t^2} \tag{4.14}$$

For a safe design, stresses due to frame bending are usually combined with stresses due to flange bending. At the center of the long side of the flange, the frame bending stresses at the inside of the flange are compressive. For flanges with strip gaskets, the frame bending stresses should thus be added to flange bending stresses

occurring at the same location. While for flanges with full face gaskets, flange bending stresses should be added to frame bending stresses at both inside and outside of the flange.

It may be argued that flange and frame bending stresses occur in different planes and need not be simply added together. In a safe design method, however, it is often suggested that these stresses be added to ensure a flat and undistorted flange surface for easy sealing of the flanged joint.

When flanges are used with non-reinforced rectangular pressure vessels, the connecting shell plate is usually of considerable thickness. The frame bending stresses on the flange, in this case, are relatively small and need not be included in the computation.

4.2.3 Numerical Results

The rectangular bolted flanged connection structures, described in Chapter 2, are analyzed by employing the two approximate design methods presented in the previous two sections. A design pressure of 2070 kPa is used, the same as was actually employed for the experimental work. A 3.2 mm compressed mineral fiber gasket is used. The gasket constants are m = 2, y = 11 MPa, E_G = 55 MPa.

Equivalent Circular Flange Method

The inside diameter of the equivalent circular flange corresponding to the rectangular bolted flange was obtained per equation (4.6) in section 4.2.1, as B = 268 mm. The other dimensions of the equivalent circular flange are presented in Figure 4.1.

The method presented in [33] is used in analysis of the equivalent circular flange with full face gaskets, for the unreinforced pressure vessel flange. The ratio of the outside to inside diameter, K, of the equivalent circular flange is obtained as

$$K = \frac{A}{B} = \frac{396}{268} = 1.478 \qquad (4.15)$$

The flange parameter, Y of the ASME Code is then given by

$$Y = \frac{3}{\pi\,(K - 1)} \left[\left[1 - \nu\right] + 2 \left[1 + \nu\right] \frac{K^2 \ln K}{K^2 - 1} \right] \qquad (4.16)$$

$$= 5.144$$

where ν is the Poisson's ratio of the flange material. The hydrostatic end force on the circular flange is computed as

$$H_D = \frac{\pi}{4} B^2 P \qquad (4.17)$$

$$= \frac{\pi}{4} \left[268^2\right] \left[2.07\right] = 116770 \text{ N}$$

The moment arm, h_D for the hydrostatic end force is obtained as

$$h_D = \frac{1}{2} \left[C - B\right] \qquad (4.18)$$

$$= \frac{1}{2} \left[344 - 268\right] = 38 \text{ mm}$$

The hydrostatic force under the gasket, H_T is given by

$$H_T = \frac{\pi}{4}\left[\left(C - D\right)^2 - B^2\right] P \qquad (4.19)$$

$$= \frac{\pi}{4}\left[\left(344 - 22\right)^2 - 268^2\right]\left(2.07\right) = 51880 \text{ N}$$

The moment arm, h_T for hydrostatic force under the gasket is

$$h_T = \frac{1}{4}\left(C - B + D\right) \qquad (4.20)$$

$$= \frac{1}{4}\left(344 - 268 + 22\right) = 24.5 \text{ mm}$$

The gasket compression coefficient, α is computed by

$$\alpha = \frac{2\, E\, t^3\, t_G}{Y\, \pi\, E_G\, l^4} \qquad (4.21)$$

$$= \frac{2\,(200000)\,(25)^3\,(3.2)}{(5.144)\,\pi\,(55)\,(64)^4} = 1.34$$

The external flange bending moment, M_o is obtained as

$$M_o = \frac{\alpha}{1 + \alpha}\left(H_D\, h_D + H_T\, h_T\right) \qquad (4.22)$$

$$= \frac{1.34}{2.34}\left[\left(116770\right)\left(38\right) - \left(51880\right)\left(24.5\right)\right] = 3267700 \quad \text{N mm}$$

The flange stress, σ_T is then computed by

$$\sigma_T = \frac{Y\, M_o}{t^2\, B} \qquad (4.23)$$

$$= \frac{(5.144)\,(3267700)}{(25)^2\,(268)} = 100.3 \quad \text{MPa}$$

Frame Bending Flange Design Method

For the reinforced pressure vessel, shown in Figure 4.2, the flange stresses are calculated by using the equations presented in section 4.2.2. This method calculates two stresses due to the frame bending moment and flange bending moment, respectively.

1) **Frame Bending Stress**

The uniformly distributed load per unit length of the flange in the frame plane, W is

$$W = \ell_g P = \left[44\right]\left[2.07\right] = 91 \quad N/mm \tag{4.24}$$

where ℓ_g is half the distance between the flange and the first reinforcing rib. The corner moment M_A, is given per equation (4.7)

$$M_A = \frac{91}{12}\,\frac{364^3 + 264^3}{364 + 264} = 804560 \quad N\cdot mm \tag{4.25}$$

The frame bending moment M_B, at the center of the span is computed per equation (4.8) as

$$M_B = \frac{(91)(364)^2}{8} - 804560 = 702580 \quad N\cdot mm \tag{4.26}$$

The elastic section modulus S of the flange is

$$S = \frac{t\ \ell^2}{6} = \frac{(25)(64)^2}{6} = 17070 \quad mm^3 \tag{4.27}$$

The maximum frame bending stress σ_f, can then be calculated by

$$\sigma_f = \frac{M_B}{S} = \frac{702580}{17070} = 41.2 \quad MPa \tag{4.28}$$

2) **Flange Bending Stress**

The length-to-width ratio of the rectangular flange is

$$\frac{a}{b} = \frac{300}{200} = 1.5 \tag{4.29}$$

The factor β is then found from [26] to be $\beta = 0.45$.

The hydrostatic end force H_D, per unit length is computed as

$$H_D = \beta\ b\ P = (.45)(200)(2.07) = 186 \quad N/mm \tag{4.30}$$

The hydrostatic force under gasket, H_T is found to be

$$H_T = \frac{1}{2}\left[c - b - d\right] P \qquad (4.31)$$

$$= \frac{1}{2}\left[276 - 200 - 22\right]\left[2.07\right] = 56 \quad N/mm$$

The moment arms for the hydrostatic end force and for the force under the gasket are

obtained as $h_D = 38$ mm and $h_T = 24.5$ mm, respectively. The gasket compression coefficient, α is calculated per equation (4.12)

$$\alpha = \frac{E\, t^3\, t_G}{8\, E_G\, \ell^4} = \frac{(200000)(25)^3(3.2)}{(8)(55)(64)^4} = 1.35 \qquad (4.32)$$

The external flange moment M_o is then obtained per (4.11)

$$M_o = \frac{1.35}{2.35}\left[(186)(38) + (56)(24.5)\right] = 4848 \quad N \qquad (4.33)$$

The flange bending stress σ_b in the rectangular flange can thus be calculated per (4.14)

$$\sigma_b = \frac{6\, M_o}{t^2} = \frac{(6)(4848)}{25^2} = 46.5 \quad MPa \qquad (4.34)$$

The total stress of the rectangular flange is obtained by simply adding of the flange and frame bending stresses.

$$\sigma = \sigma_f + \sigma_b = 41.2 + 46.5 = 87.7 \quad MPa \qquad (4.35)$$

This stress is then compared with the allowable stress. If it exceeds the allowable stress, a thicker flange is assumed and the calculations are repeated.

4.3 Experimental Work

The experimental set-up described in [22] and used in the comparison of results, is shown in Figures 4.6 and 4.7. It consists of two rectangular pressure vessel structures, 200x300 mm in cross section. One of the vessel is unreinforced with relatively heavy wall thickness; the other is thin walled and rib-reinforced. Both vessels have identical flange dimensions, to permit bolting them together. Furthermore, the flanges of both vessels were welded with full penetration welds to permit machining down the flange thicknesses in successive steps for a series of strain gage measurements.

Five different flange thicknesses from 25 to 13 mm were tested, in 3 mm decrements, all with strip and full face gaskets, using two gasket materials in two different thicknesses. The vessels were used in series of bolt-up and pressurization tests. Some of the bolts were instrumented to ensure a correlation between bolt torques and induced bolt stresses.

The two gasket materials used in the tests were the following: 1.6 mm and 3.2 mm thick compressed mineral fiber composition and synthetic rubber with 75 durometer hardness. Both materials and thicknesses are extensively used in process industries.

Strain gages were mounted along the center of the long side of both pressure vessels, as shown in Figures 4.6 and 4.7. Biaxial strain gages were used.

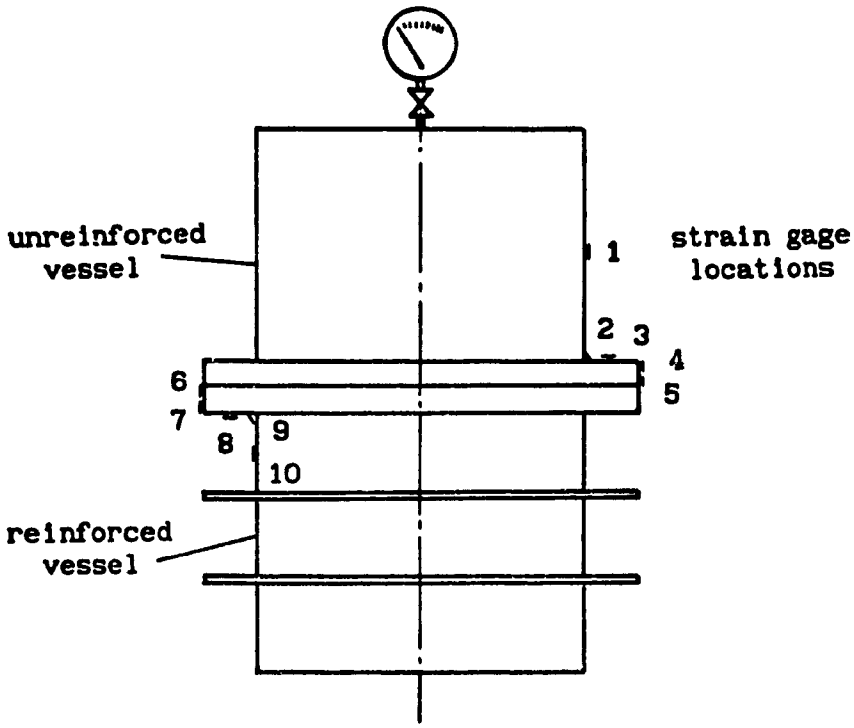

Figure 4.6 A Schematic View of the Experimental Set-up

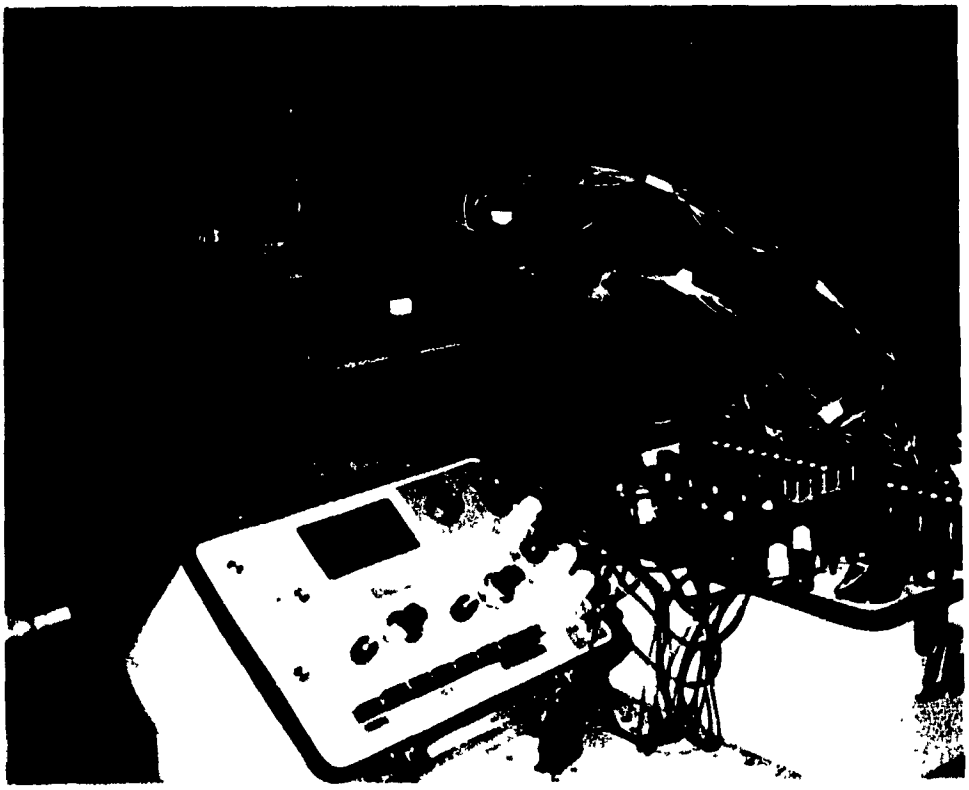

Figure 4.7 Strain Gages and Strain Gage Analyser

4.4 Comparison of Results

The results of the finite element analysis are compared with the results from experimental strain gage measurements, and with numerical results by using the analytic approximate methods.

The numerical examples considered use the same dimensions as the test pressure vessels, that is, unreinforced and rib-reinforced vessels with both strip and full face gaskets. However, no metal-to-metal contact calculations are included. The design pressure assumed was 2070 kPa, the maximum test pressure used in the experiments. For the comparison, a 3.2 mm compressed mineral fiber gasket was assumed.

The finite element analysis permits the calculation of principal and surface stresses. In the comparison, principal stresses are used. Local surface stresses, in particular stresses at bolt locations, are often appreciably higher than principal stresses. Such stresses, in accordance with the philosophy of the ASME Code [1], are considered safe if they do not exceed the yield strength of the material (see [1], paragraph UG-23(c)). All stresses are compared along a section through the center of the long side of the rectangular pressure vessels.

The comparative values due to the three approaches have been plotted in Figures 4.8 and 4.9, for various flange thicknesses. A logarithmic scale is used for the flange thickness in order to better

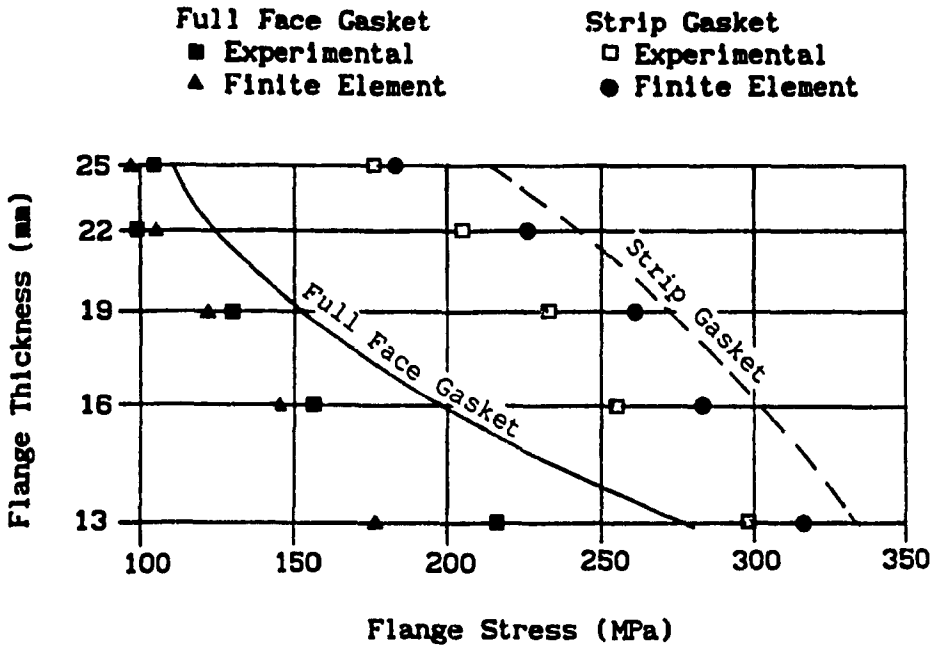

Figure 4.8 Stresses in Unreinforced Vessel Flanges

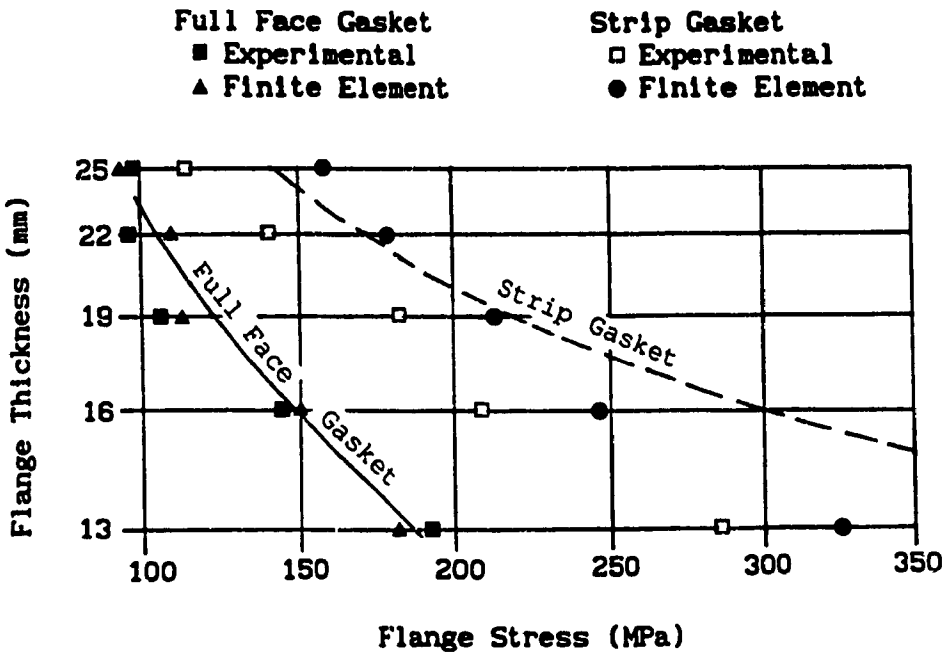

Figure 4.9 Stresses in Rib-reinforced Vessel Flange

describe the behavior of the flange stress as the flange thickness is reduced. The results shown in Figure 4.8 are stresses in the unreinforced pressure vessel due the three methods, while Figure 4.9 presents the comparative stress results for the rib-reinforced pressure vessel.

Comparing the numerical values from the finite element analysis with the calculated values by using the analytic design methods, and with experimental data, it can be seen that a good correlation is obtained with the experiments. For calculated values using the analytic design methods, it appears that the results are on the safe side and conservative, as required for simplified design methods.

4.5 Summary

Two approximate design methods presently used by pressure vessel designers are reviewed and used to calculate the stresses in the rectangular bolted flanges. Strain gage measurements on the rectangular flanged structure are also employed to provide comparison data with analytical methods. The results of both approximate methods and experimental work are compared with the numerical results using the finite element method. It is concluded that a good correlation between the results from the three different approaches has been observed. The analytic approximate design methods yield results on the conservative side.

CHAPTER 5

CONCLUSIONS AND RECOMMENDATIONS

5.1 Highlights of the Work and Conclusions

Non-circular bolted flanged connections on pressure vessels are employed extensively in industry. Due to the complexity of the rectangular bolted flange connections, it is often necessary to carry out stress analysis of non-circular flanges to determine their acceptability for a specific application. The ASME Boiler and Pressure Vessel Code contains rules for non-circular pressure vessels of unreinforced and reinforced construction. These rules cover the sides, reinforcing ribs, and end plates of such vessels. For bolted flanged connections of such non-circular pressure vessels, however, no design rules are presently included in the Code.

In this thesis, the finite element method is utilized to model and analyze rectangular bolted flanged connections employed in pressure vessels. The results are compared with experimental values from the strain gauge measurements, and with analysis data derived by approximate analytical methods presently used by pressure vessel designers. Two types of rectangular bolted flanged connections, thick walled vessels and on reinforced thin wall vessels, are discussed for three kinds of flange gaskets: O-ring gasket, strip gasket and full face gasket.

A modified structural model meshing scheme is proposed to fully make use of the limited space of the pre-wave front matrix used in the frontal method of the ANSYS program. The best possible numerical results that can be offered by the program employed is then obtained.

A parameter analysis of the rectangular bolted flanged connections is also carried out via the convenient finite element method. The influence of design parameters on the bolted flanged connections, and on their stiffness and strength characteristics are thus established. Design guidelines are also given.

Based upon comparison of the results by using the approximate methods, the experimental work, and the finite element analysis, it is concluded that a good correlation between the results from the three different approaches has been observed. The analytical approximate methods yield results on the conservative side. The finite element analysis gives a complete picture of mechanical behavior of the flange structures.

The analysis results show that the rectangular flanged structure with strip gasket is very sensitive to the bolt preload value. It is also observed that the stiffness of the reinforcement should be properly designed with respect to the wall stiffness. A too stiff reinforcement and too thin vessel wall will results in a high stress level of the structure.

It has been shown from the work that to obtain the best design for these non-circular bolted flanged connections, a large number of parametric variation and analyses have to be carried out. The finite element method, which utilizes a discretized structural model and computer numerical technique, is the most accurate and efficient approach out of the three methods presented, to obtain design sensitivity and guide-line without costly experiments.

5.2 Recommendations for Future Work

The work presented in this thesis, with respect to the analysis and design of non-circular bolted flanged connections, is by no means complete. Recommendations for the future work are given below.

1) The gaskets used in flanged connections are usually non-linear materials and subjected to large deformation under preloading and operating pressure. In order to predict the influence of rectangular gaskets, under both frame and flange bending moments, on the deformation and stress distribution, sealing characteristics and connection performance, the plastic material behavior should be accounted for in the analysis.

2) The fatigue strength of the rectangular bolted connections subject to cyclic thermal and pressure loadings could be studied by using the finite element method.

3) Dynamic analysis of the rectangular bolted flanged structures

could be carried out to predict natural frequencies and dynamic characteristics of the structures in dynamic loading environments.

4) A more complete parametric study for different design variables should be carried out to determine the sensitivity of the rectangular bolted flanged connection to each variable. The optimal design technique could be employed to obtain the optimized flange design with respect to strength and weight.

REFERENCES

1. "ASME Boiler and Pressure Vessel Code, Section VIII, division 1, Pressure Vessels," The American Society of Mechanical Engineering, New York, NY, 1986 Edition.

2. Desalvo, G. J. and R. W. Gorman, "ANSYS Engineering Analysis System User's Manual," Swanson Analysis Systems INC, Houston, Pennsylvania, U.S.A., June 1, 1987.

3. Bach, C.,"Versuche über die Widerstandsfähigkeit ebener Platten", Springer Verlag, Berlin, Germany, 1891, 104 pages.

4. Westphal, M., "Berechnung der Festigkeit loser und fester Flansche", VDI-Z, Vol.41, No.36, Sept., 1897, pp.1036-1042.

5. Waters, E.O. and J. H. Taylor, "The Strength of Pipe Flanges", Mech.Eng. Vol.49, No.5a, May 1927, pp.531-542.

6. Timoshenko, S.,"Flat Ring and Hubbed Flanges", Contribution to discussion of [6]. Mech.Eng. Vol.49, No.12, Dec., 1927, pp.1343-1345.

7. Holmberg, E.O. and K. Axelson, "Analysis of Stresses in Circular Plates and Rings" (With Application to Rigidly Attached Flat Heads and Flanges), ASME Trans. J. Appl.Mech. Vol.54, No.2, Jan., 1932, pp.13-32.

8. Waters, E.O., D. B. Wesstrom and F.S.G. Williams + others, "Formulas for Stresses in Bolted Flanged Connections", ASME Trans, Vol.59, 1937, pp.161-169. Discussion: Vol.60, Apr 1938, pp.267-278.

9. Waters, E.O., D.B. Wesstrom and F.S.G. Williams + others, "Development of General Formulas for Bolted Flanges", Taylor Forge & Pipe Works, Chicago, 1937 (printed 1949).

10. Huang, C. Y.,"Techniques of Measurmant and Experiment in Mechanical Engineering", Machine Building Press, Beijing, China 1981.

11. Thum, A.,"Feindehnmessungen und Dauerprüfungen an Flanschen als Grundlage fur eine Flanschberechnung" (Strain Measurements as a Basis for a Flange Design Method), Maschinenelemente Tagung Düsseldorf 1938 Proc., VDI-Verlag, Berlin, 1940, pp.1-6.

12. Andreosso, S. and B. Flesch, "Parameters Governing Mechanical and Thermal Behaviour of the Bolted Flange-Simplified Method", 1986, unpublished.

13. Mckenzie, H.W.,D. J. White and C. Snell, "Design of Steam-Turbine Flanges: A Two-Dimensional Photoelastic Study", Jour. Strain Anal., Vol.5, No.1, Jan., 1970, pp.1-13.

14. Spaas, H.A.C.M., D.G.H. Latzko and A. Bakker, "High-Pressure Vessel Flange Behaviour Under Transient Thermal Loadings", 3rd Int. Conf. Press. Vessel Techn., 1977, Proc., Vol.1, pp.293-309.

15. Boissenot, J.M. and J. C. Lachat, "Elastoplastic Flange Design", 3rd Int. Conf. Press. Vessel Techn. 1977, Proc., Vol.1, pp.215-222.

16. Zienkiewicz, O. C., "The Finite Element Method", third edition, McGraw-Hill, New York, NY., 1977.

17. Irons, B.M., "A Frontal Solution Program for Finite Element Analysis", International Journal for Numerical Methods in Engineering, 1970, Vol.2, pp.5-32.

18. Gould, H.H. and B. B. Mikic, "Areas of Contact and Pressure Distribution in Bolted Joints", ASME Trans., Ser.B, Vol.94, No.3, Aug., 1972, pp.864-870.

19. Nerli, G. and G. Bertoni, "Calculation and Experimental Determination of the Deformation of the Supporting Surface of the Gasket in a Series of High Pressure Flanges", Meccanica, Vol.9, No.2, Jun., 1974, pp.130-142.

20. Cassidy, L.M. and T. J. Kim, "Literature Search and Interpretive Study on the Design of Bolted Flanges with External Loads and Non-Circular Flanges", unpublished report, PVRC, Sept., 1979, 57 pages.

21. Blach, A. E. and A. Bazergui, "Methods of Analysis of Bolted Flanged Connections - A Review", WRC Bulletin, No.271, Oct., 1981, pp.1-15.

22. Blach, A.E., "Bolted Flanged Connections For Non-Circular Pressure Vessels," Proceedings of 6th International Conference on Pressure Vessel Technology, Beijing, China, September, 1988, pp. 267-280.

23. Mickesell, W.R. and R. T. Brown, "Application of Primary Sealing Criteria to a Self Energized Gasket", ASME Trans., Ser.B, Vol.91, No.3, Aug., 1969, pp.553-562.

24. Smoley, E.M., "Initial Gasket Stresses in Flanged Joints", Rubber Vol.100, No.11, Nov., 1969, pp.73-75.

25. Hamada, K., H. Ukaji and T. Hayashi, "Stress Analysis of Bolted Flanges for Pressure Vessels", First Int. Conf. Press. Vessel Techn., 1969 Proc., Vol.1, pp.513-529.

26. Roark, R.J. and W. C. Young, "Formulas for Stress and Strain", McGraw-Hill, New York, NY, Fifth ed., 1975.

27. Nishioka, K.,Y. Morita and H. Kowashima, "Strength of Integral Pipe Flanges", JSME Bul., Vol.22, No.174, Dec., 1979, pp.1707-1718.

28. Cheung, Y. K. and Ya., M. F., "A Practical Introduction to Finite Element Analysis," Pitman Publishing Limited, London, 1979.

29. Irons, B. and Ahmad, S., "Techniques of Finite Elements," Ellis Horwood Limited,England, 1980.

30. Pina, H.L.G., "An Algorithm for Frontwith Reduction", International Journal for Numerical Methods in Engineering, Vol.17, 1981, pp.1539-1546.

31. Singh, K.P. and A. L. Soler, "Mechanical Design of Heat Exchangers and Pressure Vessel Components", Arcturus Publishers, Inc. P.O. Box 666, New Jersey, Cherry Hill, 1984.

32. Blach, A. E., "Bolted Flanged Connections with Full Face Gaskets" A Thesis for the Degree of Doctoé of Philosophy at University of Montreal, Montreal, Quebec, 1983.

33. Blach, A. E., Bazergui, A. and Baldur, R., "Bolted Flanged Connections with Full Face Gaskets," WRC Bulletin, 314, May, 1986, pp.1-13.

34. Sawa, T., T. Morhoshi and K. Yamameto, "The Characteristics of Bolted Joits Subjected to External Bending Moments", JSME Int. J. Vol.30, No.270, Dec., 1987, pp.2018-2026.

35. Brown, S.J. and T. J. Brown, "A Computer Simulation of A Bolted Flange with A Spiral Wound Gasket in A Tee Shell", ASME PVP Vol.185, Nashville, Tennessee, June 17, 1990.

36. Anonymous, "Design of Flanges for Full-Face Gaskets", Taylor Forge, Inc., Eng.Dept., Bulletin No.45, Chicago, 1951.

37. Englesson, G., "Analysis of Stress in Flanges of Turbine Pipelines", Water Power, Vol.3, No.9, Sept. 1951, pp.335-340.

38. Gu Qinhua, "Experimental Stress Analysis", Machine Industry Publisher, Beijing, 1982.

39. Shigley, J. E. and L. D. Mitchell, "Mechanical Engineering Design," Fourth Ed., McGraw-Hill Book Company, New York, NY, 1983.

40. Blach, A. E. and Lihua Xue, "Rectangular Bolted Flanged Connections Finite Element Analysis and Test Results," Proce. ASME Pressure Vessels and Piping Conference, Nashville, Tennessee, PVP Vol.185, June 17-21, 1990, pp.29-35.

APPENDIX A

STIFFNESS MATRIX OF ISOPARAMETRIC ELEMENT

For a 3-D isoparametric element shown in Figure 2.5, the displacement function in the local coordinate system (ξ, η, ζ) can be expressed as:

$$u = \sum_{i=1}^{8} N_i(\xi, \eta, \zeta)\, u_i \qquad (A.1)$$

where,

u = displacement function of the element

u_i = displacement of the ith node (i=1,2,...,8)

N_i = shape function of the element

For linear element, the shape function $N_i(\xi, \eta, \zeta)$ can be given as:

$$N_i(\xi, \eta, \zeta) = \frac{1}{8}(1 + \xi_i\xi)(1 + \eta_i\eta)(1 + \zeta_i\zeta) \qquad (A.2)$$

$$(i = 1, 2, \ldots, 8)$$

where ξ_i, η_i and ζ_i are the coordinate values of node i.

The global coordinates x, y and z inside the element domain can be described in a similar way by

$$x = \sum_{i=1}^{8} N_i(\xi, \eta, \zeta)\, x_i \qquad (A.3)$$

$$y = \sum_{i=1}^{8} N_i(\xi, \eta, \zeta)\, y_i \qquad (A.4)$$

$$z = \sum_{i=1}^{8} N_i(\xi, \eta, \zeta)\, z_i \qquad (A.5)$$

where x_i, y_i and z_i are the global coordinate values of node i.

The strains of a three dimensional element are expressed as [28]:

$$\{ \varepsilon \} = \begin{Bmatrix} \varepsilon_x \\ \varepsilon_y \\ \varepsilon_z \\ \gamma_{xy} \\ \gamma_{yz} \\ \gamma_{zx} \end{Bmatrix} = \begin{Bmatrix} \frac{\partial u}{\partial x} \\ \frac{\partial v}{\partial y} \\ \frac{\partial w}{\partial z} \\ \frac{\partial u}{\partial y} + \frac{\partial v}{\partial x} \\ \frac{\partial v}{\partial z} + \frac{\partial w}{\partial y} \\ \frac{\partial u}{\partial z} + \frac{\partial w}{\partial x} \end{Bmatrix} \tag{A.6}$$

Since from equation (A.1)

$$\begin{Bmatrix} u \\ v \\ w \end{Bmatrix} = \sum_{i=1}^{8} N_i(\xi, \eta, \zeta) \begin{Bmatrix} u_i \\ v_i \\ w_i \end{Bmatrix} \tag{A.7}$$

The strains are, therefore, obtained as:

$$\{ \varepsilon \} = [B] \{ q \} = [B_1 \; B_2 \; \ldots \; B_8] \{ q \} \tag{A.8}$$

where

$$\{ q \} = [u_1 \; v_1 \; w_1 \; u_2 \; v_2 \; w_2 \; \ldots \; u_8 \; v_8 \; w_8]^T \tag{A.9}$$

and

$$[\,B_i\,] = \begin{bmatrix} \frac{\partial N_i}{\partial x} & 0 & 0 \\ 0 & \frac{\partial N_i}{\partial y} & 0 \\ 0 & 0 & \frac{\partial N_i}{\partial z} \\ \frac{\partial N_i}{\partial y} & \frac{\partial N_i}{\partial x} & 0 \\ 0 & \frac{\partial N_i}{\partial z} & \frac{\partial N_i}{\partial y} \\ \frac{\partial N_i}{\partial z} & 0 & \frac{\partial N_i}{\partial x} \end{bmatrix} \qquad (A.10)$$

The shape functions of isoparametric elements are defined with respect to the curvilinear coordinates ξ, η and ζ. The relationship between the derivatives of the two sets of coordinates (ξ, η, ζ) and (x, y, z) can be obtained by:

$$\begin{Bmatrix} \frac{\partial N_i}{\partial \xi} \\ \frac{\partial N_i}{\partial \eta} \\ \frac{\partial N_i}{\partial \zeta} \end{Bmatrix} = \begin{bmatrix} \frac{\partial x}{\partial \xi} & \frac{\partial y}{\partial \xi} & \frac{\partial z}{\partial \xi} \\ \frac{\partial x}{\partial \eta} & \frac{\partial y}{\partial \eta} & \frac{\partial z}{\partial \eta} \\ \frac{\partial x}{\partial \zeta} & \frac{\partial y}{\partial \zeta} & \frac{\partial z}{\partial \zeta} \end{bmatrix} \begin{Bmatrix} \frac{\partial N_i}{\partial x} \\ \frac{\partial N_i}{\partial y} \\ \frac{\partial N_i}{\partial z} \end{Bmatrix} = [\,J\,] \begin{Bmatrix} \frac{\partial N_i}{\partial x} \\ \frac{\partial N_i}{\partial y} \\ \frac{\partial N_i}{\partial z} \end{Bmatrix} \qquad (A.11)$$

where matrix [J] is the Jacobian matrix. In order to obtain the Jacobian matrix, substituting equations (A.3) to (A.5) into [J] yields the following expression:

$$[\,J\,] = \begin{bmatrix} \sum_{i=1}^{8} \frac{\partial N_i}{\partial \xi} x_i & \sum_{i=1}^{8} \frac{\partial N_i}{\partial \xi} y_i & \sum_{i=1}^{8} \frac{\partial N_i}{\partial \xi} z_i \\ \sum_{i=1}^{8} \frac{\partial N_i}{\partial \eta} x_i & \sum_{i=1}^{8} \frac{\partial N_i}{\partial \eta} y_i & \sum_{i=1}^{8} \frac{\partial N_i}{\partial \eta} z_i \\ \sum_{i=1}^{8} \frac{\partial N_i}{\partial \zeta} x_i & \sum_{i=1}^{8} \frac{\partial N_i}{\partial \zeta} y_i & \sum_{i=1}^{8} \frac{\partial N_i}{\partial \zeta} z_i \end{bmatrix} \qquad (A.12)$$

After substituting the derivatives of the shape function with respect to the local coordinates ξ, η and ζ into equation (A.12), the Jacobian matrix [J] is obtained. With [J] determined it is a straightforward matter to express the derivatives of the shape function with respect to global coordinates x, y and z through the inverse matrix of [J]:

$$\begin{Bmatrix} \frac{\partial N_i}{\partial x} \\ \frac{\partial N_i}{\partial y} \\ \frac{\partial N_i}{\partial z} \end{Bmatrix} = [\,J\,]^{-1} \begin{Bmatrix} \frac{\partial N_i}{\partial \xi} \\ \frac{\partial N_i}{\partial \eta} \\ \frac{\partial N_i}{\partial \zeta} \end{Bmatrix} \qquad (A.13)$$

The general form of element stiffness matrix is given as:

$$[\,k\,] = \int_V [\,B_i\,]^T [\,D\,] [\,B_i\,]\, dV \qquad (A.14)$$

where the strain matrix [B_i] is given in equation (A.10). Matrix [D] is the elasticity matrix,

$$\{ \sigma \} = [D] \{ \varepsilon \} \tag{A.15}$$

where $\{ \sigma \}$ is the stress vector. For a 3-D element with isotropic properties,

$$[D] = \frac{E(1-\mu)}{(1+\mu)(1-2\mu)} \begin{bmatrix} 1 & \frac{\mu}{1-\mu} & \frac{\mu}{1-\mu} & 0 & 0 & 0 \\ \frac{\mu}{1-\mu} & 1 & \frac{\mu}{1-\mu} & 0 & 0 & 0 \\ \frac{\mu}{1-\mu} & \frac{\mu}{1-\mu} & 1 & 0 & 0 & 0 \\ 0 & 0 & 0 & \frac{1-2\mu}{2(1-\mu)} & 0 & 0 \\ 0 & 0 & 0 & 0 & \frac{1-2\mu}{2(1-\mu)} & 0 \\ 0 & 0 & 0 & 0 & 0 & \frac{1-2\mu}{2(1-\mu)} \end{bmatrix} \tag{A.16}$$

where E is the Young's modulus and μ is the Poisson's ratio. The dV can be expressed in terms of the local coordinates,

$$dV = | J | \, d\xi \, d\eta \, d\zeta \tag{A.17}$$

The stiffness matrix of the hexahedron isoparametric element is, therefore, obtained from equations (A.14) to (A.17):

$$[k] = \int_{-1}^{1} \int_{-1}^{1} \int_{-1}^{1} [B_i]^T [D] [B_i] | J | \, d\xi \, d\eta \, d\zeta \tag{A.18}$$

The integration range for equation (A.18) is a cubic body. The stiffness coefficients can be calculated through numerical integration, such as Gaussian quadrature.